COARSE BED-MATERIAL TRANSPORTATION

## A GEOMORPHOLOGICAL APPROACH TO COARSE BED-MATERIAL MOVEMENT IN ALLUVIAL CHANNELS, WITH SPECIAL REFERENCE TO A SMALL APPALACHIAN STREAM

Jonathan B. Laronne

### ABSTRACT

The bedload literature is examined and found to rely too often on assumptions unsupported by field evidence. Certain hypotheses are also shown to be invalid for most natural channels and specifically for coarse-bedded ones.

Channel configuration, cross-sectional shape and longitudinal bed gradient change continuously and abruptly in a 600 m long reach of Seale's Brook, a part of a coarse-bedded channel studied during two years. The surficial bed-material, which has been found to be altogether coarser than, and depleted in fines, relative to the underlying material, shows a definite trend for particle calibre to decrease downstream and towards the channel flanks. The surface material is, moreover, characterized by definite, systematic bed relief, textural associations and structural arrangements, all of which are interdependent. These characteristics are also shown to result from the non-uniform composition of the bed and from several bed-material transport mechanisms.

The distance of transport of coarse labelled bed-material is found to depend only partly on particle and flow parameters. In light of this and other results, it is concluded that the transport of coarse particles is a function of hydraulics but also, and possibly to the same extent, of bed stability.

M.Sc. Thesis
Department of Geography
McGill University
Montreal, Quebec

# A GEOMORPHOLOGICAL APPROACH TO COARSE BED-MATERIAL MOVEMENT IN ALLUVIAL CHANNELS, WITH SPECIAL REFERENCE TO A SMALL APPALACHIAN STREAM

Jonathan B. Laronne

A thesis submitted to the Faculty of Graduate

Studies and Research in partial fulfillment of

the requirements for the degree of Master of

Science.

Department of Geography

McGill University

Montreal, Quebec

August, 1973

#### **PREFACE**

This study forms part of a larger project being conducted by graduate students in the Department of Geography at McGill University, under the supervision of Professor M.A. Carson. The project is aimed at investigating the response of the Eaton River basin in southeastern Quebec to different hydrologic events during the year; it includes studies of the dissolved and the suspended load as well as the movement of bed-material.

The financial assistance of research grants from the

National Research Council of Canada and the Ministère des Richesses

Naturelles du Québec is gratefully acknowledged.

Appreciation is extended to the Lydiatt family for allowing me to carry out the research on their land and for offering me their hospitality and cooperation. To Mr. L. McCallum and the United Church of Canada, I thank for permission to use the church at Randboro as a field base. I also wish to thank Mr. E.C. McCallum and their respective families for the help and hospitality offered to me during my stay at Randboro.

Special thanks are extended to the following friends and colleagues who helped with field work: M. Carson, P. Clément,

J. Chyurlia, B. Grey, C. McCallum, R. Hout, S. Tam and C. Taylor. I would also like to extend my thanks to my wife, N. Laronne, who consistently helped with most of the field work.

The pleasant discussions and the sincere advice from the following friends and colleagues is much appreciated: M. Carson, P. Clément, J. Chyurlia, T. Dunne, B. Grey, A. Sen and C. Taylor.

Finally, I would like to thank Sharon Hirtle and Janine Vasseur for typing the thesis.

## TABLE OF CONTENTS

	•	Page
PREFACE	•	1
TABLE OF CO	NTENTS	iii
LIST OF FIG	URFS	v
LIST OF TAB	LES	ix
GLOSSARY OF	SYMBOLS	×
Chapter	•	
I	INTRODUCTION	1
11	BEDLOAD PROBLEMS: MEASUREMENT, THEORY AND FACT	6
2.1 2.2 2.3 2.4	Instruments and Procedures for Measuring Bedload  Bedload Theories	7 15 15 26 39 42 50
111	THE COARSE-BEDDED CHANNEL OF SEALE'S BROOK	
3.1 3.2	General Description	56 59 59
	b) Cross-Sectional Profiles and the Thalweg	59 66
3.3	Micromorphology of the Channel Bed  a) Bed Relief	70 72 77 86
ıv .	OBSERVATIONS ON BED-MATERIAL MOVEMENT IN SEALE'S BROOK	
4.1 4.2 4.3	Collection and Preparation of Material  Disposition of Coloured Particles	101 102
	Spring 1972	105

Chapter  4.4 Distance of Transport of Labelled Bed- Material	,	•	Page
Material	Chapter		
4.5 Structure and Form as Indicative of Particle Velocities and Transport Mechanisms	4.4		
Velocities and Transport Mechanisms		Material	117
4.6 Dynamic Competence and Bedload Movement	4.5	Structure and Form as Indicative of Particle	
4.6 Dynamic Competence and Bedload Movement		Velocities and Transport Mechanisms	131
a) Downstream Particle Size Diminution	4.6		
b) Classical Competence			
c) Dynamic Competence		· ·	
REFERENCES		•	
· · · · · · · · · · · · · · · · · · ·	v	CONCLUSIONS	149
APPENDICES 161	REFERENCES	5	152
APPENDICES 161			
	APPENDICES	, 3 - , , , , , , , , , , , , , , , , , ,	161

## LIST OF FIGURES

( (

	e''	Page
1.1	Location of the Eaton and Seale's Brook drainage basins	3
2.1	Moments on a submerged sand particle resting on a horiz- ontal flat bed at the threshold of movement according to White, 1940	21
2.2a	Shield's diagram relating the entrainment function to bed roughness under conditions of a plane bed surface, (from Carson, 1971)	21
2.2b	Shield's diagram relating the entrainment function to the Reynold's number under conditions of a plane bed surface (from Henderson, 1966)	21
2.3	The regime approach, as exemplified by a width versus discharge graph, after Kellerhals, 1967	41
2.4	The entrainment function with bedload material of diameter d, after Ippen and Verma, 1953	41
2.5	Particle size - competent velocity relationship, after Mavis and Laushey, 1949	45
2.6	Mean velocities and depth-slope products at which particles of different sizes begin to move on a stream bed, after Rubey, 1937	. 45
2.7	Relations of sediment transport rates to power, shear (γDs), mean velocity and shear (γRs) for varying depths of flow, after Williams, 1967	. 47
2.8	Effect of depth of flow on the relationship between mean velocity and empirically-determined discharges of bed-material (0.3 mm median diameter) at 60° F, after Colby, 1961	49
2.9	Relationship of particle size to belocity, after Fahnestock, 1961	. 51
2.10	Bedload discharge rating curves, Elbow River at Bragg Creek, after Hollingshead, 1971	
2.11	Comparison of results from different methods of computing bed-material discharge, after Jordan, 1965	. 5 <b>3</b>
2.12	Sediment rating curves and observed values in the Colorado River (from Henderson, 1966)	54

## LIST OF FIGURES (continued)

		Page
3.1a	The 1972 spring flood hydrograph	57
3.1b	The 1973 spring flood hydrograph	58
3.2	Map of studied reach showing the location and colour of recovered particles	60
3.3	Longitudinal profile of the lower (1500 m) Seale's Brook channel	62
3.4	Longitudinal profile of the studied reach	64
3.5	Transverse ribs in the right-hand channel, Seale's Brook	65
3.6	Five cross-sectional profiles of the upper right-hand channel	67
3.7	Discharge rating curve for the gauging station, Seale's Brook	69
3.8	Miniature longitudinal bar	73
3.9	Boulder shadow and flat deposits	75
3.10	Structure and texture in the bed of the uppermost part of the studied reach	76
3.11	Schematic longitudinal section of the bed, Seale's Brook	78
3.12	Cumulative graphs and histograms of particle sizes on the surface of the bed: point bar versus further downstream	79
3.13	Cumulative graphs and histograms of particle sizes on the surface of the bed: random areal sample versus thalweg sample	81
3.14	Stoss side and steep flank deposits	82
3.15	Gradual decrease of particle size on a low-angle flank	84
3.16	Abrupt change to boulder shadow and low-angle flank deposits	85
3.17	Low and high-angle flank deposits of a side channel	87
3.18	Flat deposits and open structures	88

## LIST OF FIGURES (continued)

		Page ·
3.19	Closed structures and partial infilling of interparticle voids	90
3.20	Tight, incompletely-filled structures	. 91
3.21	The role of gravel particles in increasing the stability (or interlocking) in tight, vertically-infilled structures	93
3.22	Well-developed and partly-developed imbrication	94
3.23	Well-developed imbrication	96
3.24	Augmentation of friction in imbricate structures (from Lane and Carlson, 1954)	99
4.1	Zingg diagram depicting shapes of 100 particles of the surface layer of the reach immediately upstream of the divergence	104
4.2	Zingg diagrams depicting the shapes of the 242 recovered particles	108
4.3	Transport distance of coarse particles as a function of particle weight, after Leopold et al, 1966	112
4.4	Particle size - particle velocity relations, normal (4.4a) and rectangular (4.4b) $\phi$ distributions, after Meland and Norrman, 1969	114
4.5	Particle diameter - particle weight relationship for the 242 recovered particles	116
4.6	Longitudinal profile showing location and weight of recovered particles	121
4.7	Transport distance of particles as a function of particle weight, yellow particles	125
4.8	Transport distance of particles as a function of particle weight, red particles	126
4.9	Transport distance of particles as a function of particle weight, green particles	127
4.10	Transport distance of particles as a function of particle weight, blue particles	128

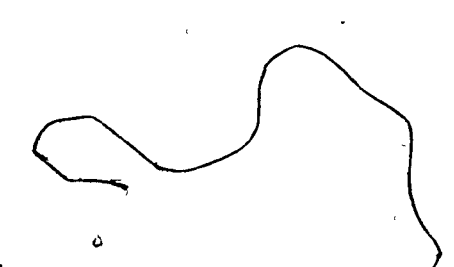
## LIST OF FIGURES (continued)

	` :·	rage
4.11	Schematic diagram showing transport mechanisms and transport distances of particles as a function of particle weight for the May 4 - 5th flood of 1972, Seale's Brook	130
4.12	Cumulative graphs of particle sizes: downstream diminution in calibre of surficial bed-material	136
4.13	The effect of spacing on percentage of rocks moving for a given discharge and particle size, after Leopold et al, 1966	141
4.14	Cumulative graphs and histograms of particle sizes: surface layer versus underlying material	144
4.15	Hjulström's (1936) curves for erosion and deposition of a uniform material	146
4.16	Map showing locations of 7 yellow cobbles on April 15 and April 23, 1972	147
A.1	Cross-sectional profiles of the lower part of the studied reach	161
A.2	Cross-sectional profiles of the upper part of the studied reach	162

## LIST OF TABLES

Q a

,		Page
3.1	Increase and rates of increase of width, average velocity and average depth with increase in discharge, Seale's Brook, spring 1973	71
3.2	Comparison between the force needed to move a particle and its submerged weight	, 98
4.1	Number of labelled particles placed on the bed, number recovered and recovery rates for each colour group, Seale's Brook, 1972	106
4.2	Results from linear regression analysis on distance of transport of labelled bed-material: correlation matrix	119
4.3	Results from linear regression analysis on distance of transport of labelled bed-material: correlation matrix, after Keller, 1970	123
A.1	Axes data of 100 particles randomly picked from the bed above the divergence, Seale's Brook, fall 1972	163
A.2	Transport distance, cross-sectional location, particle and slope data of recovered labelled bed-material, Seale's Brook, 1972	166
Ā.3	Particle size distribution data for the surface layer and the underlying layers; Seale's Brook	183



## GLOSSARY OF SYMBOLS

SYMBOL	-DESCRIPTION	DIMENSION
a	long axis of particle	λL
ъ	intermediate axis of particle	L
c	short axis of particle or	L
c	sediment parameter	
đ	depth of flow	L
e	base of natural logarithms (=2.718)	
e <sub>b</sub>	bedload efficiency	
e <sub>c</sub>	'carpet' efficiency (=1/3 for turbulent flow)	•
. e <sub>g</sub> ,	efficiency of individual particles.	
8	acceleration due to gravity	LT <sup>-2</sup>
8 <sub>b</sub>	bedload discharge per unit width	$MT^{-3}$
g'	submerged bedload discharge per unit width	MT <sup>-3</sup>
1	angle of inclination of channel bed	/
i <sub>b</sub>	fraction of bed-material in a specific size range	
i <sub>B</sub>	fraction of bedload in a specific size range	,
k	coefficient	
n	Manning's roughness coefficient	L-1/3 <sub>T</sub>
p	probability of a particle being dislodged in saltation in unit time	т-1
t	time	T ,
ū	average velocity of flow	LT <sup>-1</sup>
<b>u</b> b .	bottom velocity of flow	LT <sup>-1</sup>
u <sub>ber</sub>	critical bottom velocity of flow	LT <sup>-1</sup>
W	width of flow	L

SYMBOL	DESCRIPTION	DIMENSION
A <sub>*</sub>	constant .	,
B <sub>★</sub>	constant	
c <sub>b</sub>	sediment parameter	
D	particle diameter	L
D <sub>50</sub>	particle diameter of which 50% is finer	L
E	dam efficiency	
F <sub>d</sub>	drag or tractive force on a single particle	MLT <sup>-2</sup>
F <sub>D</sub>	total drag or tractive force	MLT <sup>-2</sup>
$\mathbf{F}_{\mathbf{L}}$	lift force acting on a particle	MLT <sup>-2</sup>
C	particle-Reynolds number	
G <sub>P</sub>	bedload discharge	MLT <sup>-3</sup>
$\mathbf{G}_{\mathbf{r}}$ .	sediment weight	MLT <sup>-2</sup>
G <sub>81</sub>	input discharge of suspended sediment	MLT <sup>-3</sup>
G <sub>s2</sub>	output discharge of suspended sediment	MLT <sup>-3</sup>
<b>K</b> ,	sediment parameter	
L	channel length	L .
N	number of particles	
P	disperssive stress	$ML^{-1}T^{-2}$
P <sub>w</sub>	wetted perimeter	L .
R	hydraulic radius	L
R'B	hydraulic radius of the bed pertaining to individual particle roughness	L
Re	Reynold's number	
S	water surface slope	,
S <sub>e</sub>	slope of the energy gradient	-

SYMBOL	DESCRIPTION	DIMENSIONS
T	dynamic friction or frictional resistance offered by particles	$ML^{-1}T^{-2}$
W	Weight of particle	MLT <sup>-2</sup>
w'	submerged weight of particle	MLT <sup>-2</sup>
α	angle for which tand is the dynamic equivalent of the friction coefficient	
β ,	coefficient	
<b>y</b>	unit weight of water	$ML^{-2}T^{-2}$
δο	thickness of laminar sublayer	L
ρ <sub>f</sub>	mass density of fluid	$ML^{-3}$
ρ s	mass density of particle	$ML^{-3}$
ρ'	submerged mass density of particle $(=\rho_8 - \rho_f)$	ML <sup>-3</sup>
η	packing coefficient (=ND <sup>2</sup> )	
η <sub>o</sub>	root mean square value of the variability factor of the lift force	
μ	coefficient of friction or	
μ	dynamic or absolute viscosity	$ML^{-1}T^{-1}$
ξ	hiding factor	
το	boundary shear stress	$\mathrm{ML}^{-1}\mathrm{T}^{-2}$
$\bar{\tau}_{o}$	average boundary shear stress	$ML^{-1}T^{-2}$
τ <sub>c</sub>	critical unit tractive force	$ML^{-1}T^{-2}$
τt	stress form of the energy dissipated in transporting bedload	ML <sup>-1</sup> T <sup>-2</sup>
π	constant (3.14)	•
ф	angle of interlock among particles $(\phi = \tan^{-1} \mu)$ or	
•	scale for particle sizes (= -log <sub>2</sub> D)	

SYMBOL	DESCRIPTION	DIMENSION
ω	mean available power of a stream per unit width	$\mathrm{ML}^{-1}\mathrm{T}^{-2}$
λ	ratio of D to the average free distance between adjacent particles	ι
	dimensionless parameter of flow intensity $ \left(=\frac{\rho'}{\rho_f} \frac{D}{R_B' S_e}\right) $	
Ф	dimensionless parameter of sediment discharge	

## CHAPTER I

### INTRODUCTION

This study deals with the transportation of bedload in alluvial channels, a topic long-recognized to be of prime importance to fluvial geomorphology (Gilbert, 1914), but one in which most of the research has been undertaken by civil engineers, rather than by geographers or geologists. Therefore, a considerable portion of the thesis (Chapter II) is devoted to a review of this literature. Particular attention is drawn to the often problematic application of hydraulic formulae, derived from controlled flume experiments, to bedload transportation in Nature, where rather different conditions prevail, and to the problems and the possible invalidity of applying many simplifying assumptions made in theoretical hydraulic approaches. Fieldwork was undertaken in the spring and summer of 1972 and in the spring of 1973 on a reach of a small tributary of the North (Eaton) River, in the Quebec Appalachians, in an attempt to investigate several of these problems. The data from the work are examined in Chapter III and IV and, in light of these observations, the problems of developing workable, but theoretically sound models for the movement of coarse bed material are summarized in the final chapter.

Bedload projects are related to geomorphology from several aspects. Comparable to other landscape features, the channel bed is small in area, but it plays a major role in the evolution of landforms. The theory of the cycle of erosion strongly hinges on base level and on the graded channel bed (Davis, 1902), i.e., on its four-dimensional

)

stability (in time and in space), which, in turn, is partly dependent on the capacity and competence of the stream. The transportation of channel bed-materials is the underlying mechanism in the denudation of fluvially-controlled landscapes: it exerts a strong control on the rapidity and mode of valley side evolution as well as on the morphology of the valley bottom and the stream channel itself.

The importance of coarse material movement can be exemplified in either transport or in weathering limiting situations. In the former, if competent conditions prevail such that the stream is capable of transporting its coarsest armour, and if its capacity exceeds incoming sediment discharge, the stream will eventually cut down into its bed and a new, weathering and/or corrading-limiting situation will predominate. If, on the other hand, the incoming sediment discharge then becomes greater than the capacity, aggradation will necessarily occur, with a concurrent change in slope.

Coarse material transportation is so important a process in the development of most landscapes that it has lately become one of the most active research fields in geomorphology. In view of its importance, studies undertaken to analyze river materials and their behaviour, both invaluable aspects of the dynamics of river mechanics, are needed to understand the processes involved with the entrainment, transportation and deposition of bedload. Pertinent hydraulic data also help to provide an essential understanding of these processes.

It seems, however, that a deductive approach has rarely been preferred to induction. The basic description of the relevant processes and of the bed itself is part of the role of geographers in describing

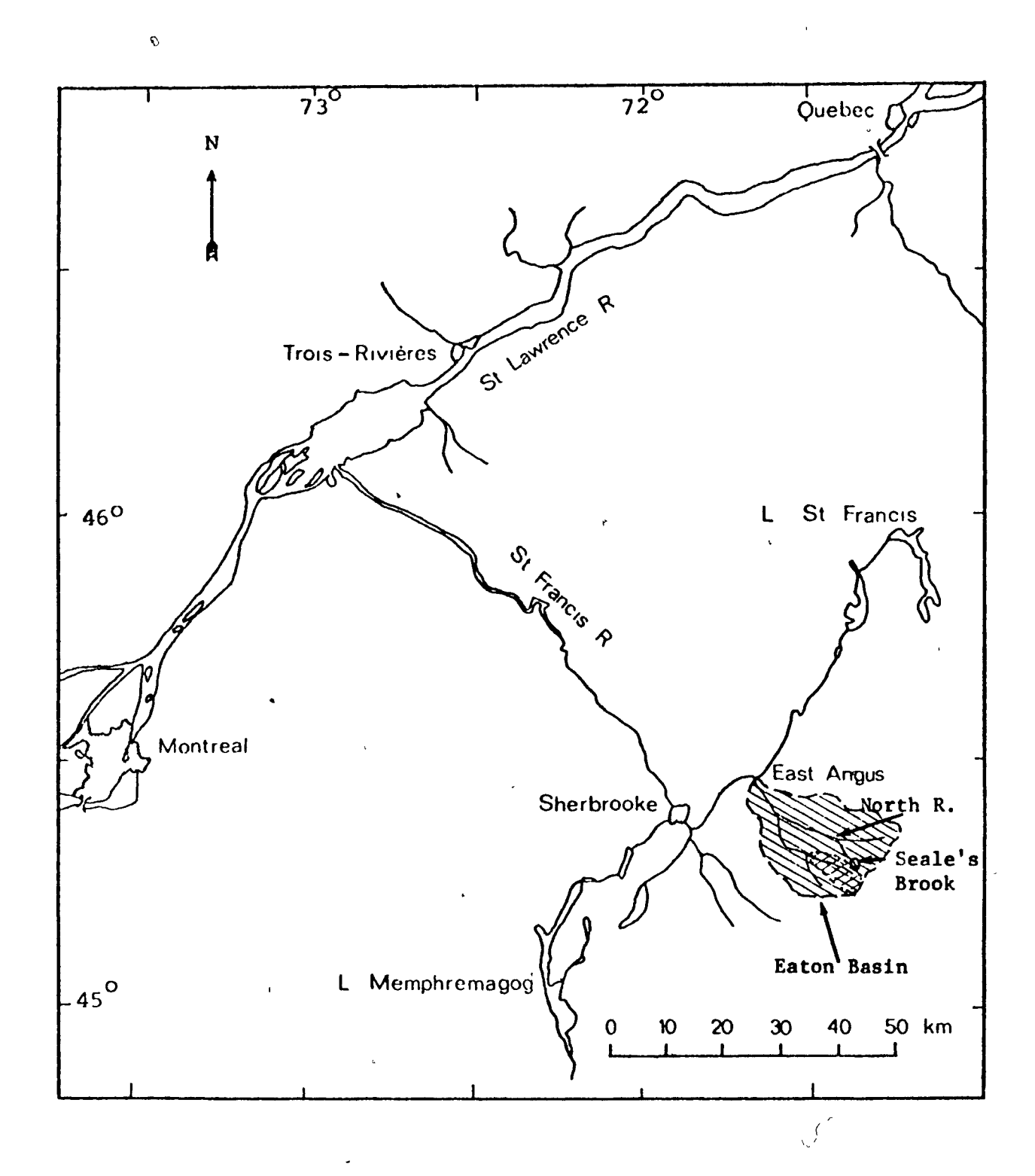


Figure 1.1: Location of the Eaton River basin, the North River and Seale's Brook. (Source: Ministère des Richesses Naturelles du Québec, 1967).

٧

المد سيهير

process and form. Thus, descriptive bedload studies are in great need.

In addition to its relevance to geomorphology, bedload research is useful in geology in the interpretation of certain fluvial deposits, in engineering and in environmental studies. To date, only partial and usually costly solutions have been found to such problems as stabilization of irrigation and diversion canals, aggradation above and degradation below man-made dams and in highly urbanized areas, all with specific ecological systems of modified habitats, which invariably cause certain drastic effects on aquatic life.

Bedload movement was examined in the field along a 600 m stretch of a small tributary of the North River in the IHD Representative basin of the Eaton River, about 35 km east of Sherbrooke, Quebec (Figure 1.1). The Eaton Basin has previously been described by Cartier and Leclerc (1964). Simard (1970) and Clément (1972) and has been the location of a number of research projects by the Department of Geography at McGill University in recent years (e.g., Taylor, 1972, and Grey, 1972). The particular Seale's Brook tributary was chosen because it is small enough to allow detailed observation of the movement of individual bed fragments, but large enough to have boulder sized particles in its bed, and also because of its relative isolation from human interference. It was also hoped that bedload could be examined through the use of a removable trap, but this has not yet been proven successful. A detailed description of the Seale's Brook channel is provided in Chapter III. At a more general scale, the physical geography of this part of the Eastern Townships of Quebec has been described by Cann and Lajoie (1942) (with special reference to the soils), by Cooke (1950) (the geology of the area), by McDonald (Pleistocene

deposits) (1969), by Bird (1970) (major land-forming units) and the climate by Gagnon et al (1970).

Before this fieldwork is described, a lengthy review of the previous literature is provided in order to emphasize the difficulties and dangers involved in attempting to apply established hydraulics formulae to the movement of coarse bed-material in natural channels.

### CHAPTER II

## BEDLOAD PROBLEMS - MEASUREMENT, THEORY AND FACT

Engineers and geologists have devised different types of bedload measuring equipment, but they all suffer from low, variable and
unreliable sampler efficiencies. The calculation of bedload discharge
via sedimentation processes is more reliable, but this method, with the
present accuracy of river bed sounding at high stages, is only applicable
to long term estimates. Other questions at issue are that none of the
bedload theories is widely accepted, results from flume experiments are
sometimes contradictory and are probably inapplicable to natural rivers,
and only very few field studies have been undertaken. These abovementioned problems, dealt with in this chapter, are being inspected in
studies throughout the world; but without their solution, the future
status of bedload research will forever remain in disorder and partial
darkness, by which it has been characterized for too long.

It is necessary, first, to deal with the concept of bedload movement before attempting to describe and analyze other problems.

According to Gilbert (1914), "Some particles of the bedload slide, many roll, the multitude make short skips and leaps, the process being called saltation." This definition of bedload movement agrees well with most of the literature. In a different approach to bedload, Bagnold's (1966) physical reasoning guided him to define it as "that part of the [sediment] load, which is supported wholly by a solid transmitted stress."

Although true, this latter definition is abstract and statistical in nature,

and it can only be of use in theoretical studies.

An important characteristic of bedload movement is that it may take many forms, depending on particle shape and calibre, and on hydraulic conditions. Moreover, bedload movement is the mode of transportation of the coarser, and not just the coarse, fraction of the bed-material. While during low or intermediate flows particles in the sand and pebble size ranges may very likely move as bedload, at sufficiently high stages they can move as suspended load. Moreover, disk-shaped particles will tend to slide rather than roll at conditions of incipient motion, and particles af any shape, if large enough, will not move by saltation unless highly competent conditions prevail. Consequently, bedload theories which rely only on saltation as a mode of transportation of coarse particles (e.g., Yalin, 1963) should be treated as irrelevant to the transportation of very coarse materials (> 2 mm), with which this study is concerned.

## 2.1 Instruments and Procedures for Measuring Bedload

Most of the information contained in this section is derived from Hubbell (1964). Samplers used before 1940 were chiefly direct measuring ones, and they are described in detail in Report 2 of the Federal Inter-Agency River Basin Committee (1940).

Every direct measuring bedload sampler has an intrinsic efficiency, or rather, range of efficiencies. Sampler efficiency is defined as the ratio of bedload weight trapped in a sampler to the weight of bedload which would have been transported through the width of channel occupied by the sampler, during the same time, if the sampler had not been there.

Sampler efficiencies vary considerably with sampling time, with water

depth and velocity, as well as with bedload size distribution, bedload discharge, degree of sampler filling and the size of its mesh (if any) and with bed configuration. Obviously, the efficiency also varies with every basic type of sampler.

Because direct measuring bedload samplers, excluding the pittype, have efficiencies which do not approximate 100 percent, and because bedload discharge and consequently, measured bedload discharge, vary tremendously with time (Samide, 1971), determinations of sampler efficiency are merely a very rough approximation. This is especially so because most sampler efficiencies are determined in flumes, where conditions are much simplified. Even an efficiency determined in the field involves approximations and inaccuracies (Hollingshead, 1968 and Charlton, 1972) which are not only the cause for the wide ranges of efficiencies, but also for different reported estimates of these ranges.

Box or basket samplers operate by causing deposition of sediment in the sampler due to screening of the flow or due to reduction in flow velocity. Basket samplers are open but screened on all sides except the front and sometimes the bottom, while box samplers are open only at the front and top. As an example, Schick (1967) used a small basket-type sampler on the dry channel bed of Nachal Yael, a representative basin of the IHD in Eilath, Israel. Its efficiency is unknown, but it seems to be low mainly because of its small capacity and also due to the clogging of the wire mesh (Schick, pers. comm., 1971).

Basket efficiencies vary considerably, but average about 45 percent (Hubbell, 1964). Field-tested 1 and 1 (screen opening) basket

efficiencies have been reported to increase with competent discharges from zero to 45 and to 60 percent respectively (Samide, 1971). In this instance, incipient motion of bedload began at about 23 m<sup>3</sup>/sec (800 ft<sup>3</sup>/sec). but the basket efficiency remained unchanged at zero until water discharge increased to 37 m<sup>3</sup>/sec (1300 ft<sup>3</sup>/sec). The inoperability of these and other kinds of direct-measuring bedload samplers at low but competent conditions is a big disadvantage to geomorphologists, particularly due to the often dominating effects of events of moderate magnitude and frequency (Wolman and Miller, 1960). Because basket samplers usually have a large capacity (i.e., volume), they are adopted for measuring transport rates of coarse and even cobble-sized materials. As the mesh size is decreased, so is the sampler suitable to trap smaller and even suspended particles, although this necessamily diminishes the efficiency by causing a greater obstruction to the flow with a consequent decrease in velocity, shear stress and available stream power immediately upstream of the sampler opening.

Pan or tray samplers operate by maintaining the sediment that drops into a slot or slots after it has moved over an entrance ramp or straight into an entrance. Their average efficiency is about 45 percent, but the range is large and the efficiency decreases rapidly in streams having high velocities and high bedload discharges. This reduction in efficiency is possibly the result of the suspension of particles above or inside the samplers. Due to their small capacity, the relatively small cross sectional area of the opening and in some cases, due to the upstream dip of the entrance ramp, these samplers are best suited for sand-bed streams.

Pressure-difference samplers, especially improved models of the early types, have relatively high efficiencies averaging 65 percent and varying from 45 to 80 percent. Actually, their efficiency at low rates of bedload discharge is zero. These samplers are designed so that stream and entrance velocity tend to be the same by creating a pressure drop at the sampler exit. This is accomplished by constructing the sampler walls so that they diverge toward the rear. The VUV (Novak, 1957) is a widely-accepted pressure-difference sampler which, excluding the basket type, is at present most commonly used. Its great advantage is that it has a hydraulic efficiency of 101 percent (where hydraulic efficiency is comparable to sampler efficiency but concerns water instead of sediment). The VUV, which is an improvement of the Karolyi sampler, is designed for use with particle sizes up to 100 mm. Novak determined its efficiency in a flume at 70 percent, while Samide (1971) field-tested the VUV and maintains that its efficiency is 30 percent. Samide also compared basket and VUV samplers and found that there is practically no difference in the particle size distributions of bedload samples taken with these samplers. It is, however, apparent that the VUV is more complex to handle and the time between two consecutive sampling periods is twice longer than the one associated with basket sampling.

Slot or pit samplers are placed in the stream bed and catch bedload particles as they move over the bed. Their efficiency is very high because they do not obstruct the flow of water, but their disadvantage is that they cannot be emptied except by digging or pumping, and they must be placed in the stream bed. Pit samplers are usually very large and are thus suitable to trap all the material transported as bedload. One exception

is a fraction of the saltating particles whose leap length is greater than the dimension of the pit in the flow direction.

Despite their high efficiency, especially as regards the coarser fractions of the bedload, two recently-developed pit samplers seem to be inoperable. Leopold installed equipment in a small channel in Wyoming; it comprises a hauling system which moves several top-open boxes in a pit dug in the stream bed. When pulled out of the water, each box drains the bedload which had accumulated in it while passing in the pit and then continues moving in a chain series with the rest of the boxes to the other bank; at this point it re-enters the pit and the cycle continues. This type of sampling is similar to the one with the portable pit sampler suggested by Hubbell (1964) in that it fulfills similar functions. In its present condition, the Wyoming installation had been repeatedly blocked by sand, but recent changes may prove to be effective in solving this problem. Moreover, the modified installation includes photographic equipment designed to deal with the problem of long saltation leaps. A different type of pit sampler has been developed at the hydraulic laboratory of the Technion, Israel. Sand accumulates on a tray placed on a balance connected to a recording device. The value of this installation is questioned because of problems of scour upflume of the pit and due to problematic emptying of the tray.

Bedload measuring samplers developed in the last three decades may be extremely sophisticated, are often quite expensive and, in many cases, provide only indirect measurements of bedload rates. A pumping sampler and a magnetic sampler, both of the direct-measuring type, have

been suggested (but are not in use) by Hiranandi and by Kennedy respectively (Hubbell, 1964). Recently developed indirect-measuring instruments are acoustic, ultrasonic, tiltmeter-type, photgraphic and pressure-transducer samplers. These devices do not measure the actual bedload discharge, but only the relative bedload discharge. Acoustic instrumentation is used to record sound generated by interparticle and in some cases by particleinstrument collisions. For example, Hollingshead (1968 and 1971) used a directional crystal transducer as a hydrophone in order to detect the active width of bedload movement in gravel streams. A device that records impacts of bedload particles on a receiving plate of an electrically operated pressure transducer, placed near the stream bed facing upstream, is described by Solov'yev (1966). The validity of the unit in its present use is doubted because knowledge of particle velocities is needed in order to compute bedload discharges. Solov'yev assumes that particle velocity is equal to the flow velocity near the bed, an assumption which is contrary to flume investigations (Gilbert, 1914, Fahnestock and Haushild, 1962 and Meland and Norrman, 1966 and 1969).

Bedload concentration has been measured with high frequency (ultrasonic) sound waves. When different amounts of transmitted acoustic energy are absorbed by mediums of different sediment concentrations, a graph relating these two variables can be plotted and unknown bedload concentrations can be determined in this manner. The method cannot, however, be applied without knowledge of the size distribution of the load. Ultrasonic sounding has also been used in tracking dune movement (Richardson, Simons and Posakony, 1961). In addition, the discharge of large (100 mm) particles might be

determined by a system of ultrasonic depth sounders; such an installation has not been tested so far.

A tiltmeter sampler has been developed by Taniguchi (Hubbell, 1964) to measure the variations in ground-tilt near the channel that result from the passage of different weights of water and sediment. So far, however, it has not proved to be very accurate. Photographic installations have also failed to be useful, the main reasons being the high costs of film and optical equipment and problems of visibility and motion reduction.

There are two additional categories of bedload discharge determinations apart from those using direct or indirect-measuring bedload samplers: those by sedimentation processes and those by empirical and/or theoretical relations.

As an example of the sedimentation method, Østrom (1972) described a bedload trapping procedure in a glacier-fed Norwegian stream. A wire fence was erected from bank to bank causing deposition of coarse material upstream of the fence, which could be measured by levelling. Unfortunately, the fence was damaged by a flood wave. A similar procedure attempting to determine long-term bedload accumulation behind weirs and dams has long been used and is widely accepted (Kunkle and Comer, 1972, Brown, Hansen and Champagne, 1970 and McPherson, 1971). Knowledge of the density and the porosity of the sediment enables calculation of its weight (G<sub>r</sub>). If the total suspended sediment discharge transported into the reservoir (G<sub>s1</sub>) is known, and if the efficiency of the dam or the weir (E) in terms of total load rather than suspended sediment load is calculated (Brune,

1953 or Fair and Geyer, 1954), or if the total suspended sediment discharge out of the reservoir is known  $(G_{s2})$ , then the bedload discharge throughout that same period of time  $(G_b)$  into the reservoir would be:

$$G_{b} = \frac{G_{r}}{E} - G_{g1}$$
 (2.1)

or 
$$G_b = G_r - G_{s1} + G_{s2}$$
 (2.1a)

respectively. It seems, however, that such and other similar calculations (Nanson, 1972) may underestimate bedload discharges, because too often no consideration is made to the effect of bedload deposition upstream of the reservoir. Another complexity is that proper care must be taken inusing a Brune-type efficiency, which is usually considered only as a rough approximation of an average value. Moreover, it is also important to interpret correctly the deposits in the reservoir. Even if it is assumed that part of the suspended sediment in the reservoir water is carried out of it through an overfall or through a sluice gate with a wire fence in front of it, it is obvious that the damming causes most of the suspended sediment to be settled. This is particularly so in regards to the coarser fractions of the suspended matter (Kunkle and Comer, 1972). Consequently, it may be deduced that although sedimentation procedures are helpful in evaluating total long-term sediment yields, and even shorter-term ones (Milhous and Klingeman, 1971, cited by Nanson, 1972), they have not yet solved the basic problems of measuring bedload discharges and evaluating bedload/suspended load ratios in the channel proper.

## 2.2 Bedload Theories

Bedload formulae (i.e., equations for the prediction of bedload discharge) are usually based on the principle of excess shear stress, excess velocity or excess discharge (e.g., Du Boys, 1879, Schoklitsch, 1934). These equations state that the capacity of a stream to transport bedload at any given time varies directly with the difference between the critical values of shear stress, velocity or discharge and the value prevailing at that time. Accordingly, an outline on theories of the initiation of motion of particles resting on a stream bed, that is, the critical condition, will precede the review of bedload formulae.

The following section, as well as the rest of the thesis, concerns only cohesionless particles lying on and in the stream bed.

A review of the literature on cohesive bed and bank materials and their relationship to bedload transportation was presented by the A.S.C.E.

Task Committee (1966) and in discussions related to that particular paper.

## a) Initiation of Motion: Competence

An equation relating flow velocity to the initiation of motion of particles on a stream bed was formulated by Brahms (cited by Leliavsky, 1966) as early as 1753. It states that

$$u_{bcr} = k(W^{i})^{1/6}$$
 (2.2)

in which u is the critical 'bottom velocity' of the water, k is a coefficient and W' the submerged weight of the particle.

The equation was derived theoretically by equating the force of water acting on the particle (the product of the bottom velocity and the mass of the water that pushes the particle in unit time) with the force resisting movement (the product of the submerged weight of the particle and  $\mu$ , the coefficient of friction). The mass of water acting on a particle per unit time equals the product of the bottom velocity of the flow  $(u_b)$ , its mass density  $(\rho_f)$  and its cross-sectional area. Assuming a spherical particle, this cross-sectional area equals  $\pi(D/2)^2$ , where D is particle diameter. At threshold conditions  $(u_b = u_{bcr})$  these forces are equal and

$$u_{\rm bcr} \rho_{\rm f} \pi (D/2)^2 u_{\rm bcr} = (4/3) \pi (D/2)^3 (\rho_{\rm g} - \rho_{\rm f}) g \mu$$
 (2.3)  
volume submerged friction unit coeffiweight cient

in which  $\rho_{_{\bf S}}$  is the mass density of the particle and g is the acceleration due to gravity. Reducing equation 2.3 leads to

$$\frac{D}{2} = \frac{3}{4} \frac{\rho_f g(u_{bcr})^2}{\rho_g - \rho_f}$$
 (2.3a)

Because the weight of the particle (W) is proportional to the cube of its radius, the general conclusion is that

$$D/2 \propto W^{1/3} \propto (u_{bcr})^2$$
 (2.4)

or 
$$W \propto (u_{bcr})^6$$
 (2.4a)

However, if it is assumed that  $u_b \propto \overline{u}$ , where  $\overline{u}$  denotes the average velocity in the cross-section, then

$$W \propto (\bar{u}_{cr})^6 \tag{2.4b}$$

This latter equation, commonly known as the 'sixth power law', was arrived at independently by Airy (1834, cited by Leliavsky, 1966) in a similar manner. It constitutes the approach to the problem of initiation of motion based on the pushing effect of the impact of water on the particle. Rubey (1937) and White (1940), who used the tractive force approach, presented a more sophisticated form of the equation, wherein the slope angle up which the component force of the water tends to move the particle was taken into consideration, while the cross-sectional area of the particle which the water hits was taken as  $\beta\pi(D/2)^2$ , where  $\beta$  is a coefficient that depends partly on the portion of the particle that is exposed to the current and partly on the proportion of the total force of the impinging water that is actually expended on the particle (see the discussion on flow resistance).

All these equations are hindered in that they incorporate the simplifying assumption that a general initiation of motion of the bed-material depends solely on average stream velocity (or on u<sub>b</sub>, the bottom velocity), average weight of a particle of average diameter D lying on the stream bed, average bed slope and in some way on particle shape. A more

comprehensive approach is presented by Helley (1969), who also considers particle shape and orientation.

p

A somewhat different approach to the problem incorporates the concept of a critical unit tractive force  $(\tau_c)$ . This latter approach is not completely different from the 'sixth power law' because there is an obvious interdependency between average flow velocity  $(\bar{u})$  and average boundary shear stress  $(\bar{\tau}_c)$  in a cross section. As a matter of fact, it can be shown that the 'sixth power law' can be deduced from  $\tau_c \propto D$ .

The total tractive force  $(F_D)$  that acts along the boundaries (bed and banks, or the wetted perimeter,  $P_w$ ) of a stream over a length L is equal to

$$F_{D} = \tau_{O} P_{W} L \qquad (2.5)$$

which, for the simple case of a rectangular channel, becomes

$$F_{\rm D} = \tau_{\rm O}(2d + w) L$$
 (2.5a)

where  $\bar{\tau}_0$  is the average boundary shear stress along the bed and the banks, and d and w are the depth and width of flow respectively. In the case of steady, uniform flow, this force is equal to the downstream component of the weight of water whose volume is wdL. That is,

$$\rho_f g d w L sini = \bar{\tau}_0 (2d + w) L$$
 (2.6)

or 
$$\bar{\tau}_{o} = \rho_{f} g \frac{dw}{2d + w} \sin i = \gamma RS$$
 (2.6a)

the 'Du Boys equation', where i denotes the angle of inclination of the bed,  $\gamma$  is the unit weight of water,  $R(=dw/P_w)$  is the hydraulic radius and S is the water surface slope. For small angles  $\sin i = \tan i = S$  (in radian measure).

It should be stressed that the 'Du Boys equation' considers only an average value of the tractive force, a fact that has been ignored by several enthusiasts of this approach (e.g., Schoklitsch, in Shulits, 1935). In natural streams, and particularly in coarse bedded channels with wide ranges in calibre of bed-material and with relatively narrow widths (high ratios of d/w) such as Seale's Brook, there is an enormous variability of shear stresses along different parts of the boundary in any cross-section. Moreover, the velocities at the center of such channels during high flows, and in the thalweg during low flows, are much greater than in the vicinity of the banks (Nanson, 1972, see also Chapter III). It is thus obvious that, at least in such channels,  $\bar{\tau}_0$  is meaningless in respect to incipient motion.

White (1949) showed that theoretical considerations lead to the conclusion that at a critical value of the unit tractive force (equal to but opposite in direction to the boundary shear stress) particles of a specific size would be at a condition of instability, i.e., at incipient motion. He considered a flat horizontal bed (a sloping bed was considered separately) covered with N particles of diameter D, per unit area. The

total tractive force on each such ideal particle is thus  $F_d = \tau_o/N$ . Introducing  $\eta = ND^2$ , a dimensionless measure of the packing of the particles on the bed, the tractive force may be rewritten as  $F_d = \frac{D^2}{\eta}$ . Assuming that rough boundary conditions prevail, the tractive force on each particle passes through its centre of gravity. Assuming that all the drag on the bed is offered solely by the individual particles, he then considered the moments acting on any particle about its downstream contact point (Figure 2.1). At threshold conditions  $\tau_o = \tau_c$  and

$$\frac{4}{3} \pi \left(\frac{D}{2}\right)^3 \rho' g \frac{D}{2} \sin \phi = \frac{\tau_c D^2}{n} \frac{D}{2} \cos \phi \qquad (2.7)$$

where  $\rho' = (\rho_s - \rho_f)$  is the submerged mass density of the particle. Reducing equation 2.7 and transposing  $\tau_c$  yields

$$\tau_{c} = \eta \frac{\pi}{6} \rho^{\dagger} g D \tan \phi \qquad (2.7a)$$

White took into consideration that flow in natural channels is almost invariably turbulent with consequent shear fluctuations. From his experiments he concluded that  $\tau_{\rm C}$  was, in fact, about half the value predicted from equation 2.7a. This is a confirmation that in turbulent flow, the ratio of the maximum to average velocities or shear stresses is 2. White also incorporated the effect of viscous flow (when most of the drag on the particles is skin friction drag, rather than form drag) by adding a dimensionless coefficient, the aforementioned  $\beta$ . However, a serious disadvantage of this kind of approach is that it contains the generalizations

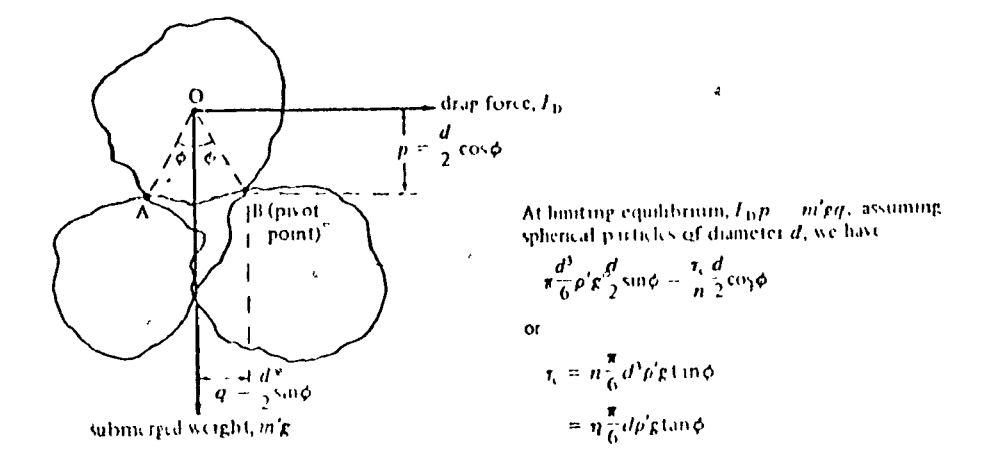


Figure 2.1 Moments on a submerged sand particle resting on a horizontal flat bed at the threshold of motion according to White, 1940.

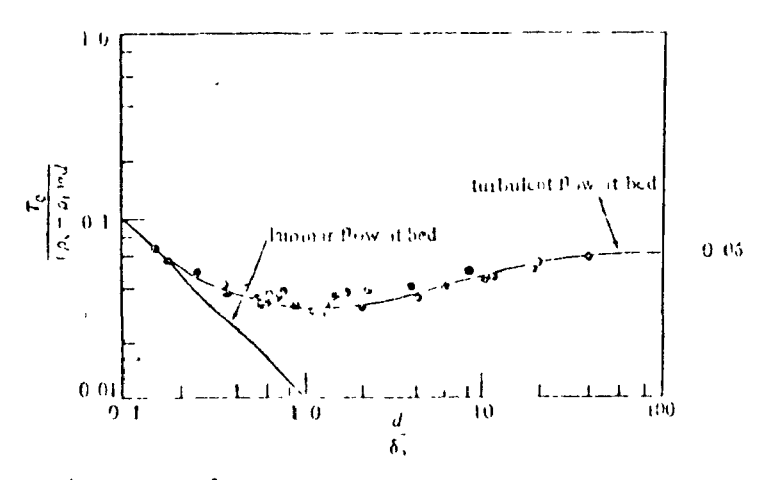


Figure 2.2a Shield's diagram relating the entrainment function to bed roughness under conditions of a plane bed surface, (from Carson, 1971).

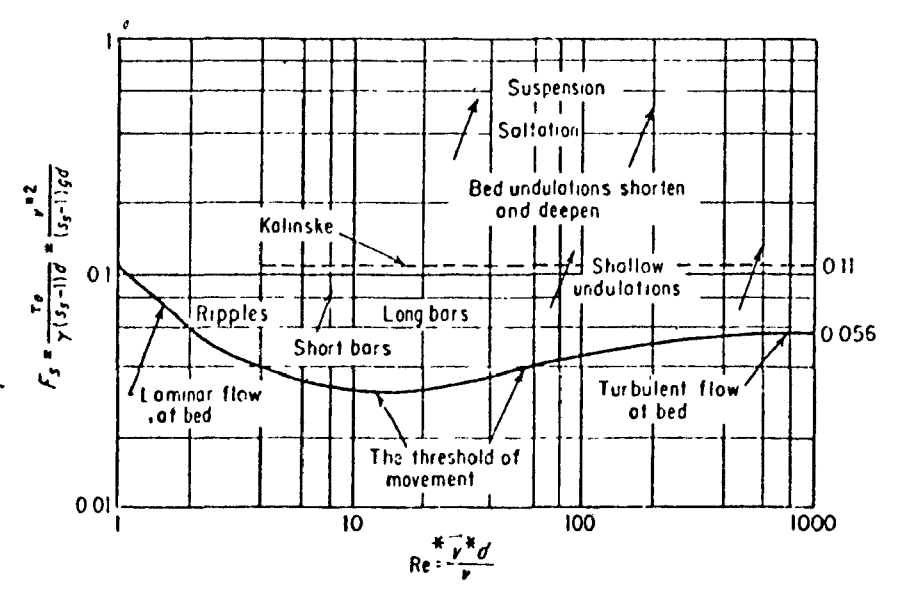


Figure 2.2b: Shield's diagram relating the entrainment function to the Reynold's number under conditions of a plane bed surface, (from Henderson, 1966).

and simplifications of the former one — the 'sixth power law'. For example, the angle  $\phi$  (Figure 2.1) may vary from particle to particle to a great extent, expecially in bed-materials with a wide range in calibre (see Figure 3.11); moreover, AB (Figure 2.1) will not be parallel to the drag force vector for every particle. Another meaningless simplification is the concept of  $\eta$  in any but uniform, usually sandy, stream beds. A similar remark is also valid in relation to the existence of a downstream contact point, which in actual fact is usually replaced by a number of points or by a whole contact surface. This point is discussed more fully, in the context of the Seale's Brook study, in Chapter III.

Shields (1936, cited by Leliavsky, 1966) is probably the first to have approached the bedload topic from what is presently known as the principle of dimensionless hydraulic parameters. Based on flume experiments with sands, he presented a diagram (Figure 2.2a) of the well known Shields entrainment function plotted against the ratio  $D/\delta_0$ , where  $\delta_0$  is the depth of the laminar sublayer. It can be seen that for plane bed conditions the function approaches a constant value of 0.056 as  $D/\delta_0$  increases above unity, or as the Reynolds number (Re in Figure 2.2b) increases above the range of values corresponding to transitional flow conditions (i.e., between fully developed laminar flow and fully developed turbulence), which also corresponds to the transition between hydraulically smooth and rough conditions. The decrease in the entrainment function with increase of  $D/\delta_0$  (for  $D/\delta_0 < 1$ ) was explained by White as the result of higher drag forces in viscous flow acting on a higher point in the particle than its centre of gravity. The important aspect of Figures

2.2a-2.2b is that, for plane bed conditions,  $\tau_c = \rho^*$  g D 0.056, and that for every size of bedload material, the critical tractive stress can be evaluated. However, the entrainment function is not a constant for varying bed conditions and for rippled or other rougher surfaces it increases and becomes an unknown variable.

The tractive force approach, in its various forms, is particularly deficient in its neglect of the lift forces acting upon particles on a stream bed. On the other hand, it can be shown that both the drag and the lift forces increase with the second power of the bottom velocity, so that in actual fact, an equation predicting incipient movement and based on the existence of drag forces is still valid when lift forces are not considered, although its coefficient, and thus its numerical value, will be changed.

The significance of the lift force was pointed out by Jeffreys (1929, cited by Leliavsky, 1966), who deduced his theory from the Bernoulli equation. From this equation it is apparent that as velocity decreases with nearness to the stream bed, the pressure increases. The immediate corollary is that any particle lying on a stream bed, whether or not protruding from the laminar sublayer, experiences an upward force in excess of the buoyant force in static water. It is customary to consider the velocity at the 'surface' of the bed as zero. With increase of discharge of water there is a concurrent increase in water velocity at every point in a vertical (except at the bed surface) and a consequent increase of the buoyant (or lift) forces. Eventually, when these latter forces are large enough, they will lift the particles, which will be rolled,



slid or they may skip (saltate) downstream.

Although lift forces do occur, this approach is again very simplified. Incipient motion in natural channels is not a sharply defined process. At the bed of the channel, where particles are characterized by different sizes, shapes and stabilities, and where velocity fluctuations are high due to turbulence, it is more conceivable that the development of a strong enough buoyant force, acting on an unstable and small enough particle (or, rather, particle structure), will cause local incipient motion. It is quite well known in soil mechanics that the greater the variability in particle calibre, the greater the interlocking and the more stable will the bed structures be (see also Chapter III); stability of the bed material will also increase as particles on the bed are less equant-shaped and, obviously, as particle sizes increase. lift force approach does not consider the relative importance of lift forces in relation to drag forces. For instance, it is common knowledge (Lane and Carlson, 1954 and Helley, 1969) that farticles on gravelly stream beds usually dip upstream. The pressure of water impinging on such particles presses them against underlying particles, thus causing resistance to lift forces in addition to the resistance offered by the weight of the particle, by the weight of parts of overlying particles, and by the resultant friction between the particle and neighbouring ones.

The approach of Helley (1969) to incipient motion is more complete than others, and it is therefore very likely that it is more applicable to threshold conditions in natural streams. Unlike the rest of the literature on this topic, Helley's report contains actual field measurements. Critical conditions for motion of bedload particles can be analyzed in terms of forces

or in terms of moments. Unlike White (1940), the approach adopted by Helley (1969) visualizes incipient motion as an equality of the resultant turning moments of drag and lift and the oppositely directed resistance moment of the submerged particle weight. From this theory, which takes into consideration a typical, though somewhat simplified, posture of coarse particles in a natural stream bed, and which incorporates several concepts and coefficients derived from previous flume investigations, an equation linking critical bed velocity and particle parameters is developed. The equation, which has the form of the 'sixth power law', includes the following particle parameters: size, density, inclination and shape. Helley assumes, however, that bed slope and its influence on incipient motion are insignificant.

Helley's approach has merit in that it attempts to explain and predict threshold conditions with the aid of field measurements and field observations, the latter being as important, if not more so, than the former. As previously mentioned, the theory does incorporate what seem to be invalid generalizations. For instance, the coarse material placed on the bed and whose incipient motion was observed is not typical of the bed-material characterizing the measured reach (Helley, 1969). In fact, the large bed particles were brought from another reach of the same channel. Although the large particles were placed on the bed with inclinations like those characterizing the rest of the material, they were placed on the bed and not in it. Accordingly, it is maintained in the theory that coarse particles lie on the bed. Although this may be true for a small number of individual particles, it does not apply to most coarse bed-materials in natural channels. Thus although sand-sized

particles do lie on the bed, observations undertaken in Seale's Brook (Chapter III) show that most of the surface material of gravelly and of coarser-grained beds is positioned between and partly under neighbouring This is also true for coarse particles in sand bed channels (Fahnestock and Haushild, 1962). It follows that all the foregoing theories on incipient motion do not sufficiently take into account the influence of the mixed composition of bed-materials. Although some workers (Rubey, 1937, White, 1940, and Helley, 1969) have pointed out that not all the particle area is being acted upon by the impinging water, they have solved this question by using an unexplained or an empirically-derived coefficient, instead of simply measuring the degree of insertion of different particles in a natural stream bed. Other complexities arising from the mixed composition of bed-materials (e.g., low pressures developed underneath coarse particles that are being lifted from a finer matrix (Reynolds, cited by Lane and Carlson, 1954), friction between every particle and its 'neighbours', expecially when there is a very close-fitting structure of the bed-material (Chapter III), or the adverse effect on incipient motion of particles almost invariably being partly overlain by other particles) seem to have escaped the attention of workers studying incipient motion.

#### b) Bedload Formulae: Capacity

The literature on bedload formulae is so vast, it is scattered in so many publications and, as Bagnold (1966) wrote "... has been discussed from so many viewpoints that it is doubtful whether any one person has read it all, let alone digested it sufficiently to appreciate all the implications

of each [approach]." Accordingly, only the better known formulae will be discussed, and that mainly in order to be analyzed from a standpoint of their applicability to natural channels.

The principle of excess tractive force is the basic idea which underlies many bedload equations. Whether be it excess shear stress (Du Boys), excess discharge (Schoklitch) or excess velocity (Bagnold, 1954a, concerning the aeolian transportation of sand), these forces depend on a critical value, that of incipient motion.

Du Boys (1879, cited by Chien, 1956) presented the first formula of this kind. He assumed that sliding layers of bed-material, each over-riding the lower, are propelled by the tractive force of the moving water, a force that was assumed to decrease with increase of depth in the bed.

O'Brien and Rindlaub (1934) maintained, however, that a decrease of shear stress with depth in the stream bed would result in a continuous acceleration of bedload discharge, because the bed is actually in dynamic equilibrium.

The classical Du Boys formula

$$g_b = C_b \tau_o (\tau_o - \tau_c)$$
 (2.8)

(where  $\mathbf{g}_{\mathbf{b}}$  is bedload discharge measured in weight per unit width and time, and  $\mathbf{C}_{\mathbf{b}}$  is a sediment parameter) was consequently replaced by their own equation

$$g_b = K (\tau_o - \tau_c)^c \qquad (2.9)$$

where K and c are sediment parameters. O'Brien and Rindlaub accepted the idea of overriding bed layers, but maintained that the velocity (rather than the shear stress) of these layers decreases with increased depth in the bed. Similar types of formulae have been presented by Shields (1936, cited by Chien, 1956) and Schoklitsch (1926 and 1934, in Shulits, 1935).

In order to evaluate any of these excess forces, a preliminary knowledge of threshold conditions is a prerequisite. It has already been mentioned that there are no reliable equations or procedures by which threshold conditions can be determined in the field (Chapters 2.1 and 2.2a) and that the efficiency of all but pit-type bedload samplers is low and variable enough to render the determination of incipient motion to a considerable error (Samide, 1971). However, this is merely a technical impediment which should eventually be overcome.

A more serious question at issue concerns the assumed sole dependency of average values of incipient motion conditions and rates of bedload discharge on average values of shear stress, water discharge or velocity. This is not only a simplification, but also a misconception of the various processes operating in natural alluvial channels (Maddock, 1969). Every bedload formula is dependent on empirically determined constants which are drawn from flume experiments. These flume runs are systems with constraints (uniform supply of water or of sediment, uniform grain size, maximum allowable width, etc.) which rarely occur in Nature, and, therefore, it is not surprising that rules governing sediment transportation in flumes are different, and in extreme cases completely unlike, those operating in Nature. The importance of inde-

terminate hydraulics is also mentioned later in this chapter.

The general validity of every bedload formula depends on the various interrelationships between all the variables associated with the dynamics of alluvial channels, but more specifically on theories which claim to be capable of determining both the resistance to flow and the rate of transportation of sediment (whether bedload and/or suspended load). Most of the stream energy in any channel is dissipated in turbulent friction and is not available for bedlbad transportation (Rubey, 1933). The energy which is dissipated in transporting bedload, in form of stress, is herein denoted  $\tau_{\text{t}}$ . Part of  $\tau_{\text{t}}$  is the result of the dissipation of energy due to the resistance to flow offered sensu stricto by the particles (e.g., Einstein, 1950), but some of  $\tau_{\rm t}$  is the result of the dissipation of energy offered by bank and bedforms protruding into the flow. Although  $\tau_{t}$  may be a function of  $\bar{\tau}_{0}$ , this relationship is certainly unknown, it may very likely change with time due to changes in bedforms, suspended sediment concentrations etc., and  $\tau_{r}$  is difficult to determine (Colby, 1964c). This is precisely why Einstein (1942) and Meyer-Peter and Müller (1948) emphasize the importance of separating the hydraulic radius and the slope of the energy gradient respectively into various components. By doing this they could supposedly determine the actual resistance to flow and the problem simplifies to evaluating bedload discharge rates.

In 1942 Einstein presented a different bedload formula from those previously mentioned, which referred solely to bed-material of uniform calibre. The later (Einstein, 1950) extension to bed-material of mixed calibre is reviewed and discussed in the following paragraphs.

The approach is statistical in nature, and contains both rational and empirical elements. First, Einstein considers the number of particles of a specific diameter deposited on a bed area of unit width and length equal to the average length of steps taken by these particles. The probability (p) that a particle will be lifted from such a unit bed area per unit time is then expressed as the probability that the lift force (F<sub>L</sub>) acting on the particle to its submerged weight (W') is greater than unity. At equilibrium conditions, the values attributed to these two rates (deposition and erosion) are equal, and the final bedload formula, for the specific particle diameter, is obtained

$$p = 1 - \frac{1}{\pi^{\frac{1}{2}}} \int_{-B_{\star}}^{B_{\star}} \frac{\psi_{\star} - 1/\eta_{o}}{dt} = \frac{A_{\star} \Phi i_{B}/i_{b}}{1 - A_{\star} \Phi i_{B}/i_{b}} = \frac{A_{\star} \Phi_{\star}}{1 - A_{\star} \Phi_{\star}}$$
(2.10)

where  $\psi = \frac{\rho_B - \rho_f}{\rho_f} \frac{D_{35}}{R_B^i S_e}$ 

is a dimensionless parameter of flow intensity,

$$\Phi = \frac{g_b}{\rho_g g} \left( \frac{\rho_f}{\rho_s - \rho_f} \right)^{\frac{1}{2}} \left( \frac{1}{gD^3} \right)^{\frac{1}{2}}$$
 is a dimensionless parameter of sediment discharge,

 $S_e$  is the slope of the energy gradient,  $R_B^{\bullet}$  is the hydraulic radius of the bed pertaining to individual particle roughness,  $n_o$ ,  $A_{\star}$  and  $B_{\star}$  are constants

such that equation 2.10 may be described by a single curve of  $\Phi_{\star}$  against  $\psi_{\star}$ , t is time, e is the base of natural logarithms and  $i_B$  and  $i_b$  are the respective fractions of the bedload and the bed-material in the specific size range. Equation 2.10 is then recalculated for each size range transported as bedload and, ultimately, the formula is extended to include the suspended sediment fraction and thus becomes a bed-material formula. Certain difficulties in applying the Einstein formula to field conditions are discussed below. The discussion may also be applied to two other but similar formulae (Kalinske, 1947, and Meyer Peter and Müller, 1948).

Einstein (1942) maintains that lift forces are alone responsible for the entrainment of individual particles. He then argues that from flume investigations (Einstein and El Samni, 1949), using plastic spherical balls of one calibre glued to the sides as roughness elements, one may obtain an equation describing the average lift force acting on particles at rest on the bed. Lift forces may be all important in sand-bed streams. In fact, numerous investigations have shown that when sand-sized particles the initial portion of their paths is characterized move by saltation, by vertical leaps. This also confirms Chepil's (1961) demonstration that lift forces are as strong as drag forces very close to the bed. However, most if not all the particles on a coarse, usually mixed-sized, natural river bed are partly underlain by and partly overlie other neighbouring particles (Chapter III, see also Einstein, 1942). Consequently, even if interparticle friction is ignored, a lift force that actually lifts such particles is greater than the submerged weight of each individual. Put in another way, a dislocation of one particle would, under most circumstances, necessitate moving, if not completely dislodging, several other particles. According

to their size and shape, and the manner in which they are embedded in their surroundings, a tractive force, rather than a lift force or, more logically, a certain combination of the two, would dislodge and subsequently entrain the particles. Such particles are usually partly buried in their surroundings (i.e., in the bed) and partly hide and/or are hidden by other particles. Although the effectiveness of lift forces to entrain the smaller particles of sediment mixtures is taken into consideration by introducing an empirical "hiding factor" ( $\xi$ ), the latter is assumed to depend only on  $D_{65}$  and on transitional conditions of flow. Neither the complete size distributions of the bed material and the material lying on the bed surface, nor particle shape are taken into consideration. Thus, Chien (1956) emphasizes that  $\xi$ , amongst other factors, "should by no means be considered as a final solution". Because lift forces are not totally effective nor solely responsible (Chepil, 1961 and Helley, 1969) for initiation of motion, especially not in coarse beds of mixed calibre, it is erroneous to generalize that p may be expressed as the probability that  $F_{\tau}/W' > 1.$ 

In another assumption concerned with the entrainment and subsequent transportation of particles, Einstein maintains that i<sub>b</sub>, the fraction of the bed-material of a specific size range, also represents the fraction of the bed area covered by these particles. If this were indeed so in natural stream beds, it would mean that once general incipient motion has started (i.e., most of the surface material has been entrained), then the same forces would also be capable of entraining the lower layers of the bed-material. It would also mean that the same forces are needed to entrain either the surface layer or deeper lying layers. However, a number of studies

(Kellerhals, 1967, Leopold, Emmett and Myrick, 1966, Milhous, 1972 and this study, Chapter III) have demonstrated that the size distribution of sediment lying on the bed of an alluvial stream is different from that of the underlying materials, with the surface material being appreciably coarser. Therefore, Einstein's assumption may be somewhat restricted when applied to natural streams with wide ranges in sediment size.

Einstein's theory largely depends on equilibrium conditions. The concept of equilibrium (where amount of sediment deposited is equal to amount eroded) in a given river reach should, however, be designated to units of time in the order of months or years rather than minutes or seconds, because it is a well established fact that alluvial rivers tend to scour and fill their beds locally during the passage of a flood wave (Brooks, 1958, and Leopold amd Maddock, 1952, cited by Colby, 1964-b). Lack of equilibrium in sediment transportation in local areas of river beds over a period of time equivalent to the duration of a flood wave, and over any unit time thereof, is also exemplified by channel shifting and floodplain construction or by the process of braiding. Although it is not maintained here that bedload entrainment and deposition rates are always different in magnitude, it is obvious that any portion of a stream bed characterized by change in elevation with time is, in fact, in temporary disequilibrium. Thus, nonuniformity (change downstream) is not a prerequisite to bedload transportation, but it is certainly exemplified by several processes. Although this nonuniformity is not widely-accepted (Colby, 1964-b), most researchers are aware that the process of bedload transportation is very unsteady, i.e., changes with time at-a-station. The unsteadiness of bedload transportation is vividly depicted in the

study by Samide (1971, Appendix B, Figure 5-3-B).

A final comment on Einstein's theory necessarily includes an inspection of the determination of flow resistance. It is shown (Einstein, 1942) that the cross-section of a river can be divided into various parts by considering the intrinsic roughness (friction coefficient) of each. This division can be undertaken if the resistance to flow offered by the banks, channel patterns and bedforms, and by the individual particles can be evaluated separately. However, according to Leopold, Wolman and Miller (1964): "the resistance caused by channel alignment and curvature usually cannot be separated from the sum of all resistances computed from data on natural rivers".

The concept of dividing the hydraulic radius or the slope of the energy gradient (Meyer-Peter and Müller, 1948) is based on the assumption that only the resistance to flow of the individual grains is responsible for their movement. The resistance offered by bedforms or channel patterns causes pressure wakes to develop, which are assumed not to contribute to the entrainment, transportation or deposition of bedload particles. If, as Einstein maintains (but Bagnold (1966) denies), no bedload movement can take place in purely laminar flow, then turbulent pulsations originating in or penetrating into the laminar sublayer are alone responsible for bedload movement. In hydraulically rough conditions, which are prevalent in streams, particles protrude into the turbulent zone. Eddies and wakes are generated in this latter zone by various bed and bank irregularities. Some of the particles that rest on the bed or move over it come in contact with these disturbances and are affected by them. In fact, almost any obstruction to the flow causes either local increase or decrease of turbulence and a

consequent increase in scour or fill respectively. This is the reason why there is usually scour around bridge piers, and also the reason why dunes do not grow indefinitely, or why the concave part of meanders is scoured and the convex one becomes buried.

Bagnold's (1956 and 1966) bedload theory is unique in that it relates stream power to bedload discharge. It is, moreover, the first of its kind to incorporate both the dynamic friction (T) and the dispersive stress (P) arising from the solid-to-solid contact of particles in motion. An interesting part of his theory is that, similar to O'Brien and Rindlaub (1934), bedload movement is viewed as the motion of a cloud or carpet of particles, rather than as the motion of individual particles.

The first step in developing the equation is to consider the value of the mean available power of a stream per unit length and width ( $\omega$ ). Flowing water is then viewed as a machine, where the rate at which the machine does work equals the product of its available power and its efficiency ( $e_b$ ). This rate of work is then shown to be equal to the product of the rate of transport of the immersed weight of bedload ( $g_b$ ) and tana, the dynamic solid-liquid equivalent of the coefficient of friction of a mass of solid particles, or the ratio of the tangential to the normal components of grain momentum resulting from particle encounters. Thus

$$g_b' \tan \alpha = e_b \omega$$
 (2.11)

$$g_b^{\dagger} = e_b^{\omega/\tan\alpha}$$
 (2.11a)

The efficiency of the stream to do work  $(e_b)$  depends on the efficiency of the 'carpet' of material moving as bedload  $(e_c)$  and on the efficiency of the individual particles  $(e_g)$  moving in the 'carpet'. That is,

$$e_{b} = e_{c} e_{g}$$
 (2.12)

The carpet efficiency is shown to be 1/3 for turbulent flow, and the grain efficiency is calculated from a graph relating Re (Reynolds number) to the drag coefficient. The rest of the available carpet power per unit area,  $\omega e_c(1-e_g)$ , is maintained to be dissipated due to transfer of stress between particles and the local fluid surrounding them. In order to evaluate tand, Bagnold refers to experiments (Bagnold, 1954b) which have yielded data for which tand equals T/P, where T is the frictional resistance offered by the particles and P is the dispersive stress (a stress normal to and upward from the bed, caused by the shearing of solid particles in motion). T/P is plotted against the second power of a particle-Reynolds number (G), which is given by

$$G^2 = \frac{\rho_g T D^2}{\lambda \mu}$$
 (2.13)

where  $\lambda$  is the ratio of D, particle diameter, to the average free distance between adjacent particles, and  $\mu$  in the absolute (dynamic) viscosity. In using the latter equation, Bagnold chose  $\lambda=14$ , the highest (fluid limit) concentration of the dispersions.

Bagnold's theory is based on assumptions and experimentallyderived coefficients, several of which seem to be inapplicable to natural streams, especially to small, coarse-bedded ones. The concept of a moving 'carpet' is applicable to high rates of bedload transport in sand-bed streams. Mass saltation is obviously prevalent in sand beds where the formation of ripples and dunes is a result of this mechanism of transportation. For much finer grained bed-material (D < 0.2 - 0.062 mm, according to Sundborg, 1967) the only mode of transportation is by suspension, and for much coarser bed-material, mainly by rolling and sliding (Fahnestock and Haushild, 1962). Thus, Kalinske's (1942) view that saltation is an ineffective transport mechanism of particles in water due to the small difference in their respective specific weights is applicable to coarse particles. Although there may be some slight movement of the bed as a whole (Henderson, 1966), especially of a group of particles during incipient motion when stable structures of the bed are dismantled, most of the movement would still be by sliding and rolling of individual particles. Unless exceptional high (and thus, rare) competent conditions prevail, no complete 'carpet' can form on a coarse bed for which the theory is unsuitable.

The problem of resistance to flow arises also in this theory. In an equation which leads to the determination of  $\mathbf{e}_{\mathbf{c}}$  (carpet efficiency), it is postulated that the shear stress due to particle-to particle collisions (T) is equal to the mean boundary shear stress if flow depth is much greater than the saltation height, i.e., the carpet thickness. However, it has already been mentioned that the shear stress associated with the

transportation of bedload particles ( $\tau_{t}$ ) is always smaller than  $\bar{\tau}_{o}$ , the mean boundary shear stress. Another questionable part of the theory is the method by which the numerical value of the efficiency of the stream to do work (eh) is obtained. This value solely depends on  $e_{g}$  (e<sub>c</sub> is constant at 1/3 for turbulent flow), which is evaluated from a graph which Bagnold acknowledges may be in considerable error. The problem is that an average shape factor is used, instead of evaluating in some way the influence of the shape distribution of particles The greater the difference between the average shape of the bed-material in consideration and the shape used in the graph (Heywood, 1938, cited by Bagnold, 1956), and the greater the standard deviation in the shape coefficient (e.g., a Corey or Zingg coefficient) of the bed-material, the less representative will the graph be. Some insight on the effect of particle sphericity, roundness and surface roughness on both settling mode and time, and thus on drag, has been gained from a recent study (Stringham, Simons and Guy, 1969).

Several other bedload formulae and approaches have been introduced into the literature in the last several years. The notable amongst them are those of Laursen (1958), Yalin (1963), Garg, Agrawal and Singh (1971) and Herbertson (1969). Although there are numerous bedload formulae it should be realized that predictions of bedload discharge are inaccurate, to say the least, unless most of the flow and sediment parameters are actually measured. The reason for this lies in the indeterminate nature of hydraulics in general, and bedload transportation in particular, in alluvial channels (Maddock, 1969 and 1970).

That is, the mode of behaviour of alluvial channels is one of tendencies, and it is impossible to predetermine their exact responses to any change. These responses depend on the particular constraints of the variability of each of the variables associated with the system. Because both bed-load discharge and resistance to flow are partly interdependent and partly dependent on each of the other variables associated with the dynamics of alluvial channels, and because little is known about any of these two variables, it seems logical to assume that the best method to understand them as part of the alluvial system is to observe and measure them in the system, i.e., in the field.

## c) Regime Formulae

As far as sediment studies are concerned, there has been a continuous separation between two distinct schools of thought (the Anglo-Indian empirical approach vs the Franco-German-American one) during the past century. This review includes only brief comments on the former regime theory, and most of the space has been devoted to the latter approach. Perhaps the best way to answer for this discrimination is to quote from Leliavsky (1966, p. 193): "... the Regime Theory is not a theory at all, for no one has yet succeeded in producing a specific, strictly mathematical demonstration bridging between pure theoretical mechanics and the 'wilderness' of Indian data on silt-stable canal flow." Most regime canals in India and Pakistan have bed and bank materials predominantly composed of silt and some clay. Thus, most of the sediment is transported in suspension, a process only indirectly relevant to this study.

The true 'regime' concepts are purely empirical. Regime (i.e., silt-stable or equilibrium) canals are defined as such if, on the long run, values of width, depth and slope relations ensure stabilization of their bed and banks. In other words, these relations correspond to below or threshold conditions of particle motion. Each of the equations is given in the form of a function (usually a power) of discharge. However, the data used in the 'theories' are yearly averages, and the periodic phenomena of scour and fill are ignored.

The regime theory remained in its original empirical phase throughout Lacey's (in Leliavsky, 1966) publications. Only later did Lane (1954, cited by Leliavsky, 1966) and Blench (1955) attempt rational, mechanical solutions to the problems of regime canals. The former presented numerous regime diagrams of width/depth ratios and diagrams of  $\tau_0$  plotted against particle size. Presenting other regime formulas, Blench (1955) states they are applicable only if bed-materials are non-cohesive, flow conditions are in the dune phase, banks are smooth and bedload concentrations do not exceed about 100 p.p.m. Obviously many alluvial and non-alluvial streams are thus excluded from (his) regime analysis. A good example of the present regime approach is illustrated by Kellerhals (1967) (see Figure 2.3), a study on stable channels with gravel-paved beds.

A recent analysis of regime canals, viewed as alluvial systems with specific constraints on the variability of several important variables, has been introduced by Maddock (1969 and 1970). The typical constraints of regime canals are that these systems flow over vast and relatively

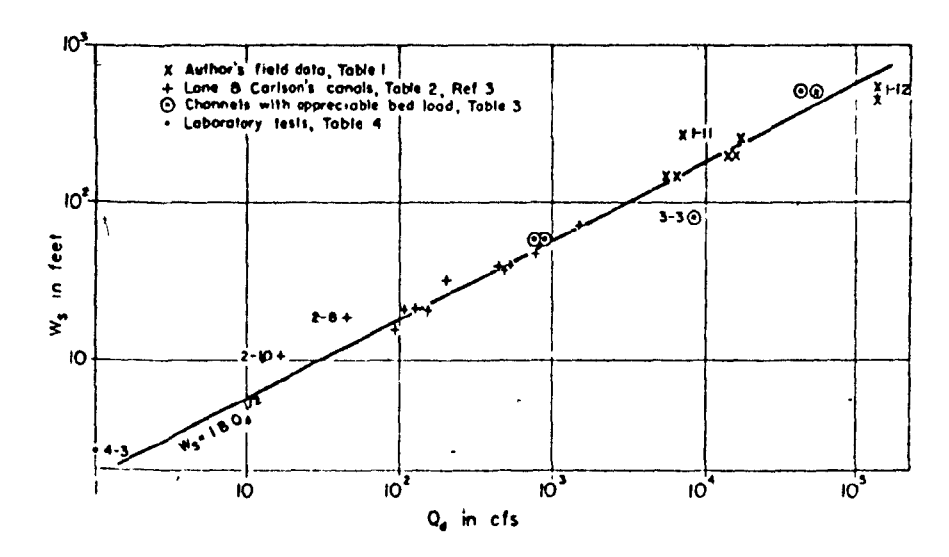


Figure 2.3: The regime approach, as exemplified by a width versus discharge graph, after Kellerhals, 1967.

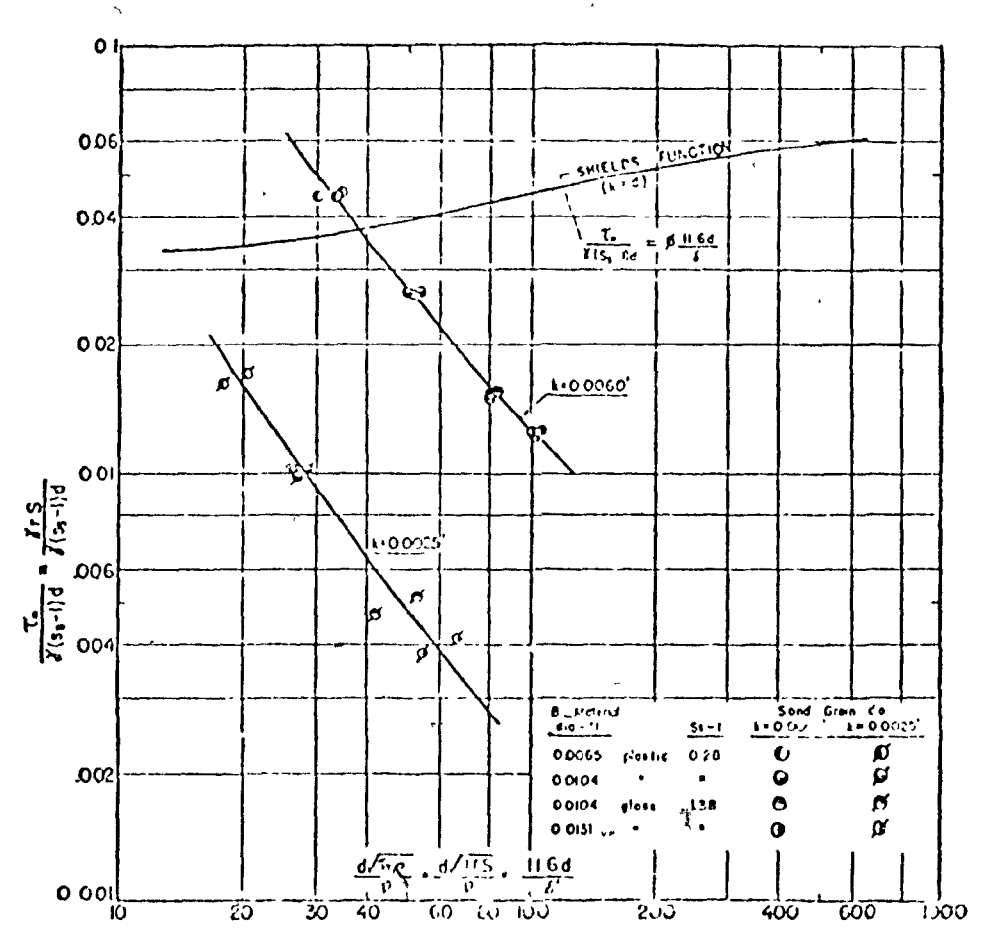


Figure 2.4: The entrainment function with bedload material of diameter d, after Ippen and Verma, 1953.

flat valleys (which imposes a constraint on the variability of the bed slope), they are usually very straight with smooth banks (which imposes a constraint on the variability of bedform changes) and they usually flow over and transport in their waters sediment of a smaller range of sizes than the range associated with natural alluvial systems. All these constraints make the system much simpler to understand, because the tendencies are much stronger than usual. In fact, some of the better known regime equations are shown to follow the same equations for natural alluvial channels wherein the above-mentioned constraints are imposed. This same approach is also maintained to explain the transportation of sediment in flumes, discussed below.

## 2.3 Flume Investigations

Of all the bedload studies mentioned previously, none refrain from comparison with results obtained in flume experiments. Countless such experiments have been undertaken during the last century. Their main purpose is to determine either conditions of incipient motion, or sediment and flow characteristics that correlate well with bedload discharge.

Encouraging as the situation may seem to be, only few of the variety of the conclusions support each other; in addition, few correlate with field data consistently. There are several reasons for this. Some of the discrepancies are due to inaccuracy (e.g., the exact definition of incipient motion). Others are a result of lack of certain data. Bagnold (1966) stated that "... no agreement has yet been reached upon the flow quantity - discharge, mean velocity, tractive force, or rate of energy

Thus, because different transport rates or incipient motion criteria are in use, it is customary to 'transform' data from one study to the criterion used in another, a process by which the accuracy of the data is lowered. For instance, Neil (1967) transforms Sundborg's (1956) mean competent point velocities, and Mavis and Laushey's (1949) competent bottom velocities to mean competent velocities.

The third, and possibly the most critical reason for the discrepancies is the fact that a flume is nothing but a model. If, and only if, there is both a dynamic (geometric) and a kinematic (force ratio or flow pattern) similarity between model and model or between model and stream, can bedload data be compared. This similarity does not have to be completely restrictive (e.g., w/d ratios do not necessarily have to be identical but rather similar in magnitude), but it does impose demands which invalidate comparison between most flume and field data. Supplemented to this demand, and partly dependent on it, is the alluvial constraint character of flume channels. The constraints imposed upon these channels differ from one flume investigation to the other according to the methods by which they are investigated (e.g., constant depth and discharge or constant slope and discharge). Probably the most important dissimilarity between flume and field channels is that the former almost invariably deal with uniform calibre of bed-material. Examples of investigations using natural bed-material with wide ranges in particle size are those by Gilbert (1914), Meyer-Peter and Müller (1948),: Fahnestock and Haushild (1962) and Meland and Norrman (1969). The various differences between flume and field channels, especially regarding their modeldissimilarity, have been discussed by Colby (1964a). In his words:

"Flume investigations can provide much helpful information on sediment transportation, but, until scale effects are understood more completely, flume investigations of the discharge of sands are not model studies of the discharge of sands in field streams." Some of the problems encountered in flume investigations, such as appropriate w/d ratios and high wall drags, are treated by Einstein and Chien (1956), Bagnold (1966) and Henderson (1966).

An additional reason for the different conclusions is due to the need that arose for immediate, rather than general, applicability.

Each flume study merely shows a good correlation between a certain parameter and bedload discharge (G<sub>b</sub>) for specific conditions. Obviously, G<sub>b</sub> increases with increase in mean velocity, shear stress and power. The question arises: How applicable is each predicting variable for all possible combinations of flow and sediment characteristics?

Amongst the earliest experiments concerned with incipient motion are the much quoted results of Shields (1936, cited by Henderson, 1966, and White, 1940), both mentioned previously. Ippen and Verma (1953) investigated flume conditions of initiation of motion of particles of sizes different than those comprising the bed. Figure 2.4 demonstrates their results, showing that Shield's relationship does not hold in such conditions. Their experiments were undertaken in clear water with steady uniform flow. Plastic and glass spheres were transported over plane, sloping beds of two roughnesses (two kinds of sand coatings).

The 'sixth power law' approach is inferred from flume studies by investigators using different types of critical velocities. Mavis and

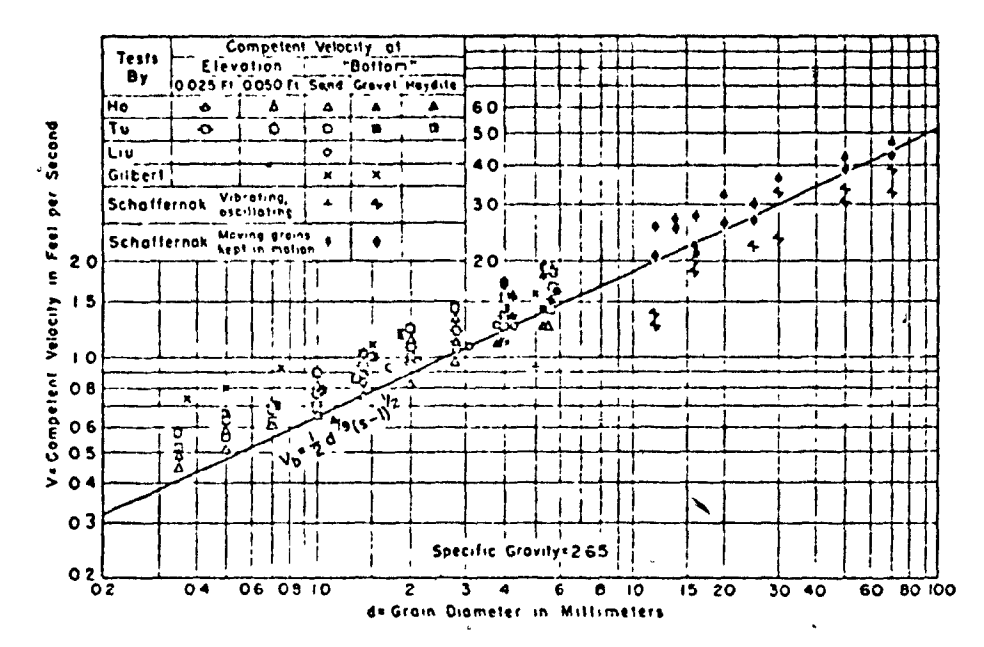


Figure 2.5: Particle size - competent velocity relationship, after Mavis and Laushey, 1949.

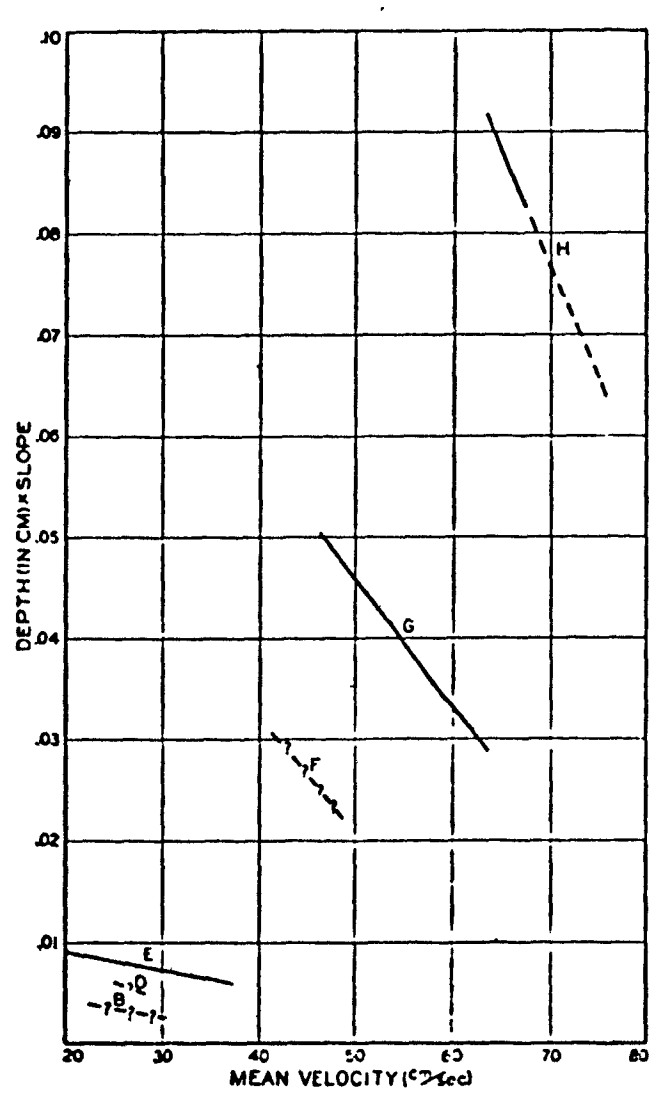


Figure 2.6: Mean velocities and depth-slope products at which particles of different sizes begin to move on a stream bed, after Rubey, 1937.

Laushey (1949) gathered flume data plotted in Figure 2.5. The competent (or critical) mean velocity is shown to correlate well with particle diameter. These experiments were also characterized by plane, level beds in channels of rectangular cross-sectional shape. Cohesionless, uniform material was transported by clear, steady and uniform flows. Similar results were obtained by Neil (1967) for coarse uniform bedmaterial and by Bagnold (1954a) for wind-blown sand. Using Gilbert's (1914) data, Rubey (1937) demonstrated (Figure 2.6) the importance of both shear and velocity (i.e., power) for critical conditions. In fact, Willis' (1967) data support Rubey by showing that available stream power, as compared to velocity or shear, is a better indicator of incipient motion. However, several well-designed experiments (Williams, 1967) with coarse sands indicate (Figure 2.7) that power, shear (YDS) and mean velocity are all bad indicators of incipient motion and of bedload transport rates (Figures 2.7a, 2.7b and 2.7c respectively). Williams shows that each of these is strongly dependent on depth of flow; only shear (YRS, and not YDS nor  $\gamma R_h^{\dagger} S$ ) is shown to be a good predicting variable (Figure 2.7d). These observations are in direct conflict with Colby (1964c), who deduced from laboratory and field investigations that total shear (YRS) "is not considered to be a generally satisfactory or acceptable measure of bedmaterial discharge." Colby concluded that 'for practical purposes' power, mean velocity,  $\gamma R_h^{\dagger} S$  and  $\gamma (RS)_m$ , where the latter is deduced from velocity distributions, can all be used for certain flow conditions to predict bedmaterial discharge. Moreover, the effect of depth of flow on bedload discharge (Figure 2.8) as determined by Colby (1961) is different from the one shown in Figures 2.7a-d.

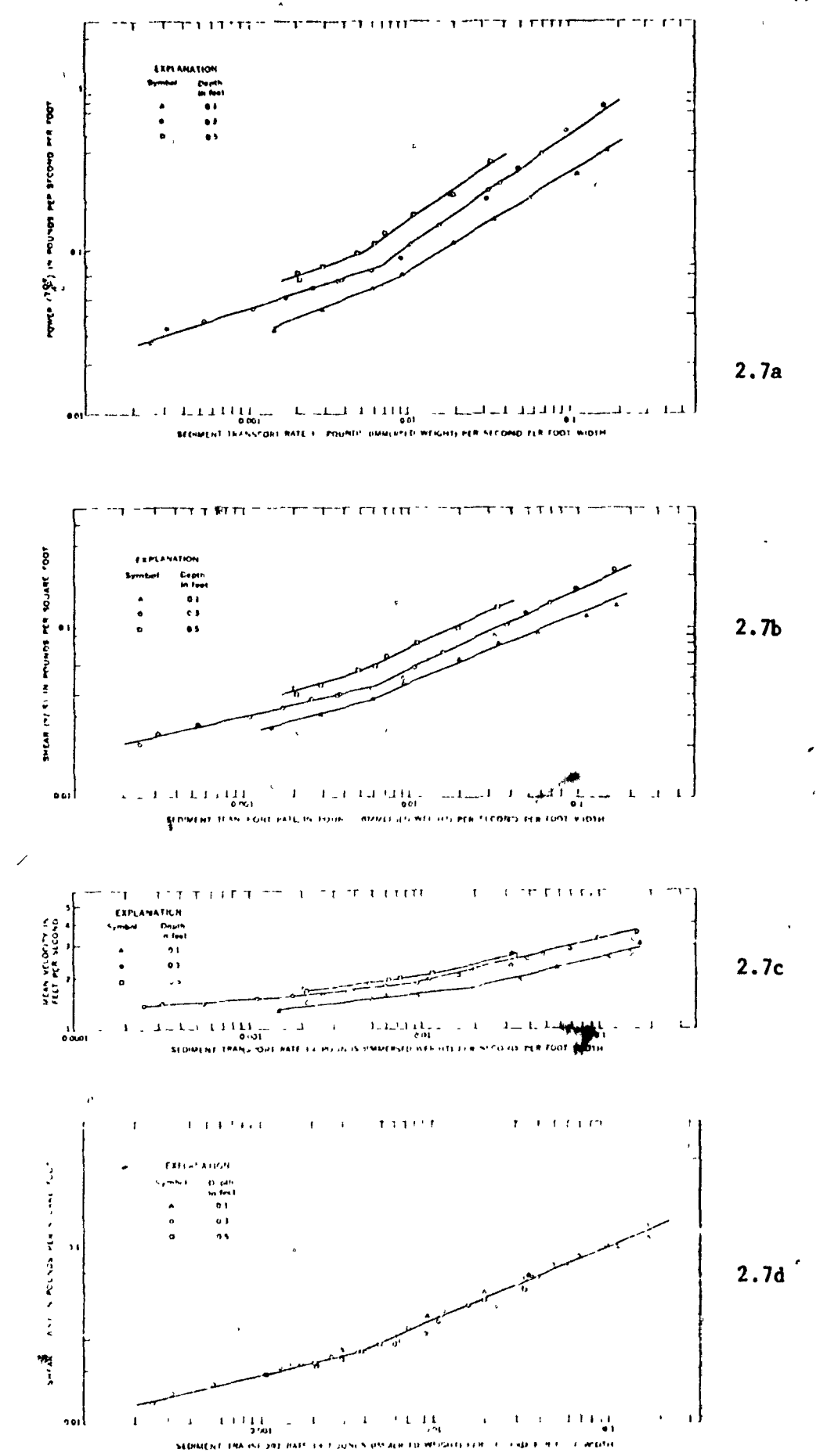


Figure 2.7: Relations of sediment transport rates to power, shear (γDs), mean velocity and shear (γRs) for varying depths of flow, after Williams, 1967.

ή,

The amount of flume data on bedload discharge is so vast that the subject is only treated in general terms. Gilbert's (1914) experiments are a milestone in bedload research. The data are well represented in tables and the experimental conditions are explained in great detail. They have been in continuous use as a basis for various comparisons and even as proof of applicability. For instance, Schoklitsch, Einstein, Meyer-Peter and Müller and Bagnold deduced from their own comparisons that Gilbert's bedload transport rates correlate about equally well with either excess discharge,  $1/\psi_{\bullet}$  or available stream power respectively. What this means is that under restricted experimental and field conditions, the proposed formulae give similar discharge rates. However, it has been shown (see Section 2.4) that river data do not tend to conform to any of these formulae consistently. This incompatibility suggests that some of the important determining factors affecting bedload discharge are not well represented in flume investigations. It should be remembered that most flume runs are invariably characterized by uniform, steady, flow conditions using uniform bed-materials. None of the proposed bedload formulae and very few experimental studies deal with the complexities arising from particle size distributions, areal and depth size distributions of bed-materials, or the structure and morphology of river bed and banks (the latter aspect is mentioned in a general manner in studies of resistance to flow). Ippen and Verma (1953) also suggest to study the effects of particle shape, mutual interference, local boundary changes and secondary currents. Some of these problems have been inspected in the investigations at the Geomorphology Laboratory, Department of Geography, Uppsala, and they have definitely contributed to our knowledge in this

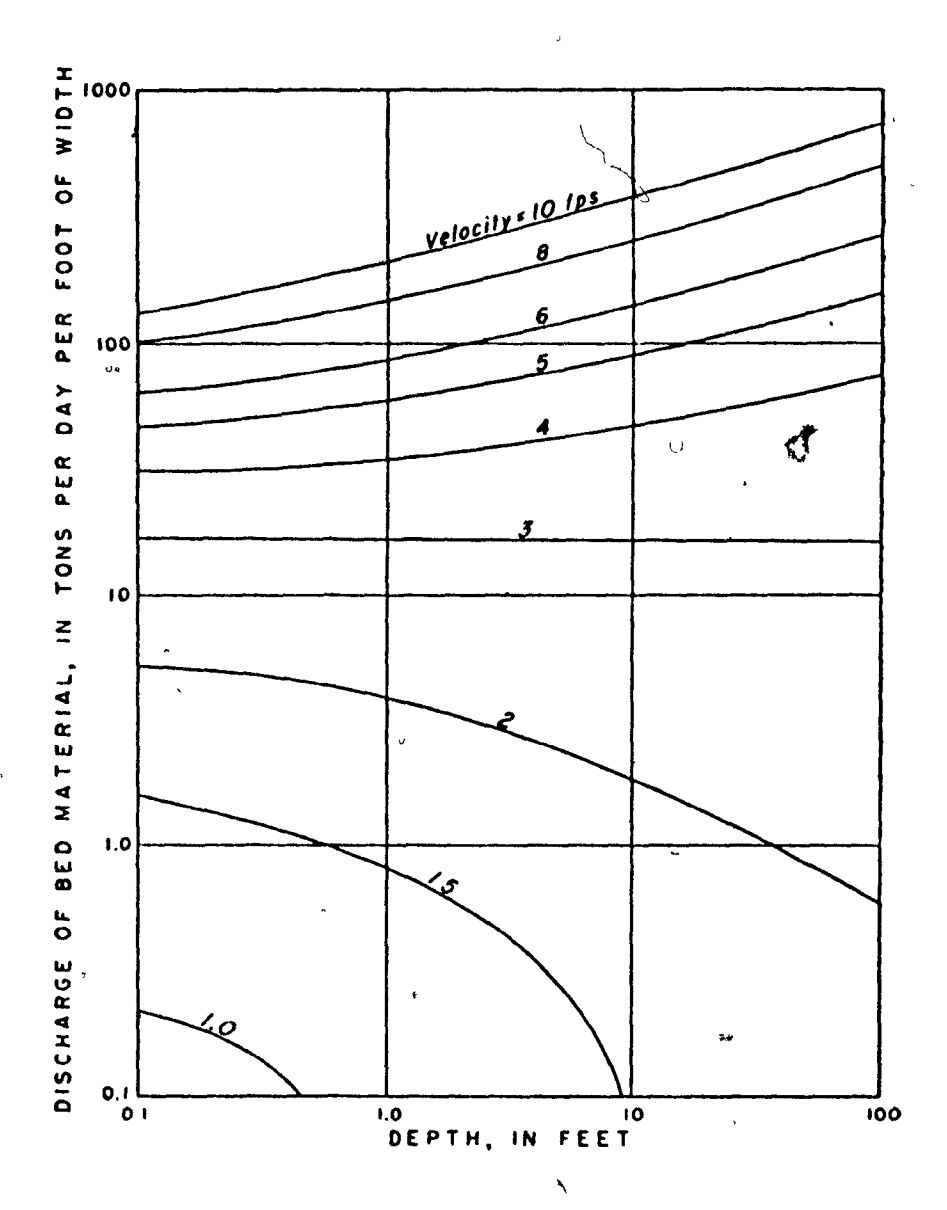


Figure 2.8: Effect of depth of flow on the relationship between mean velocity and empirically-determined discharges of bed-material (0.3 mm median diameter) at 60° F, after Colby, 1961.

complicated field. Results from these and other investigations are mentioned in the next chapter.

# 2.4 Field Studies

As opposed to the literature dedicated to numerou tume investigations, there are only a handful of such field stud. This condition is partly a result of the approach of many engineers, who claim that flumes are a critical means to solve the bedload problem and partly a reflection of the practical difficulties involved in bedload studies in the field.

Fahnestock's (1961 and 1963) excellent study of the morphology and hydrology of the White River, Washington, should serve as an example of a general study that incorporates measurements of many processes - amongst them bedload transportation. The study stresses that large amounts of sediment are transported by the river and brings evidence to this effect by describing changes due to erosion and deposition on the valley train, as well as by giving an indication of the large calibre of material transported as bedload.

An interesting graph (Figure 2.9) which is supplied by the study indicates the kind of scatter that can be expected from field data on incipient motion. The figure indicates that the 'critical traction velocity' (the velocity measured near the bed) is a closer approximation to the effective velocity than Rubey's (1937) bed velocity (defined as the velocity at the transitional zone between the laminar sublayer and the turbulent zone). However, Fahnestock states that his data are for general motion and not for threshold conditions. He indicates that the White River data plot on a line of slope 2.6 (like Nevin's) rather than

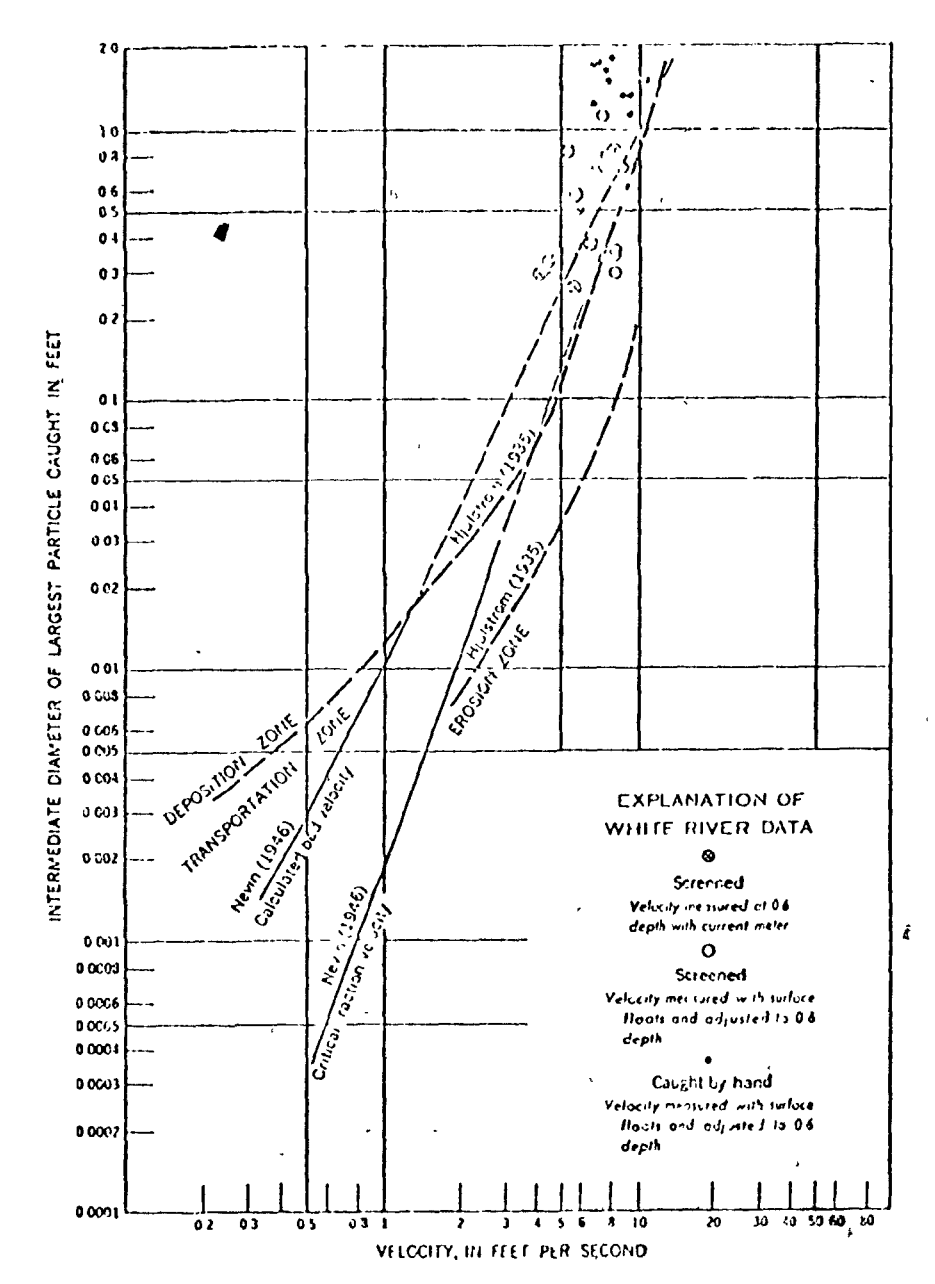


Figure 2.9: Relationship of particle size to velocity, after Fahnestock, 1961.

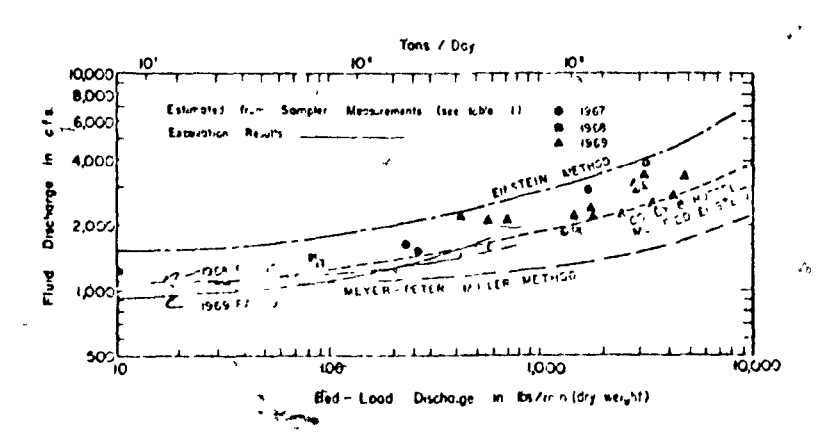


Figure 2.10: Bed-load discharge rating curves, Elbow River at Bragg Creek, after Hollingshead, 1971.

d.

on one with a slope of 2 (the 'sixth power law'). His conclusion is that for materials of D > 30 mm, streams may have greater competence than predicted from the 'sixth power law'.

Two additional studies (Keller, 1970 and Leopold, Emmett and Myrick, 1966) include data on distance of movement of individual particles, as well as on the influence of particle concentrations, particle characteristics and bottom velocity on their movement. The results of these studies are dealt with in Chapter IV.

Hollingshead (1971) measured bedload discharges with basket and VUV samplers in the Elbow River, Alberta. Another method of calculating rates of bedload transportation was used, wherein the rate of filling of a pit dug in the bed was observed. The results of his evaluations (Figure 2.10) clearly demonstrate that the Meyer-Peter and Müller equation underestimates bedload discharges and that Einstein's equation overestimates it. The results of calculations with the modified Einstein procedure (Colby and Hembree, 1955, and Colby and Hubbell, 1961) correlate better with Hollingshead's data. The modified Einstein procedure, which incorporated several field observations, has been successful in some cases (Hubbell and Matejka, 1959) but not in others (Figures 2.11 and 2.12, respectively, taken from Jordan, 1965, and Vanoni et al, 1961, cited by Henderson, 1966). Recent field measurements of bedload discharges with the aid of a basket sampler and a sedimentation method (Nanson, 1972) also show that the equations proposed by Blench, Schoklitsch and Meyer-Peter and Müller and the results obtained from the modified Einstein procedure do not yield reasonable predictions. The studies of Jordan and Vanoni et al were conducted in sand bed rivers while Nanson's study was undertaken in small, coarse-bedded mountain streams in Alberta.

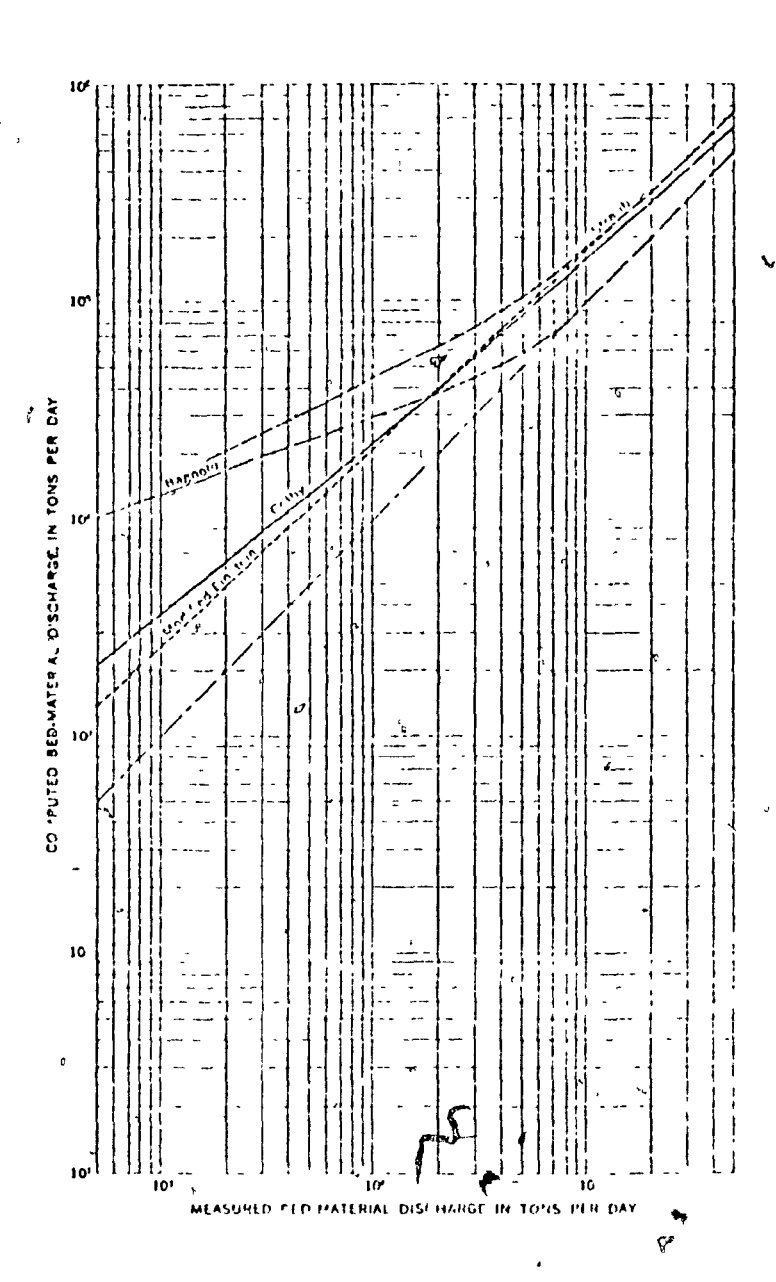


Figure 2.11: Comparison of results from different methods of computing bed-material discharge, after Jordan, 1965.

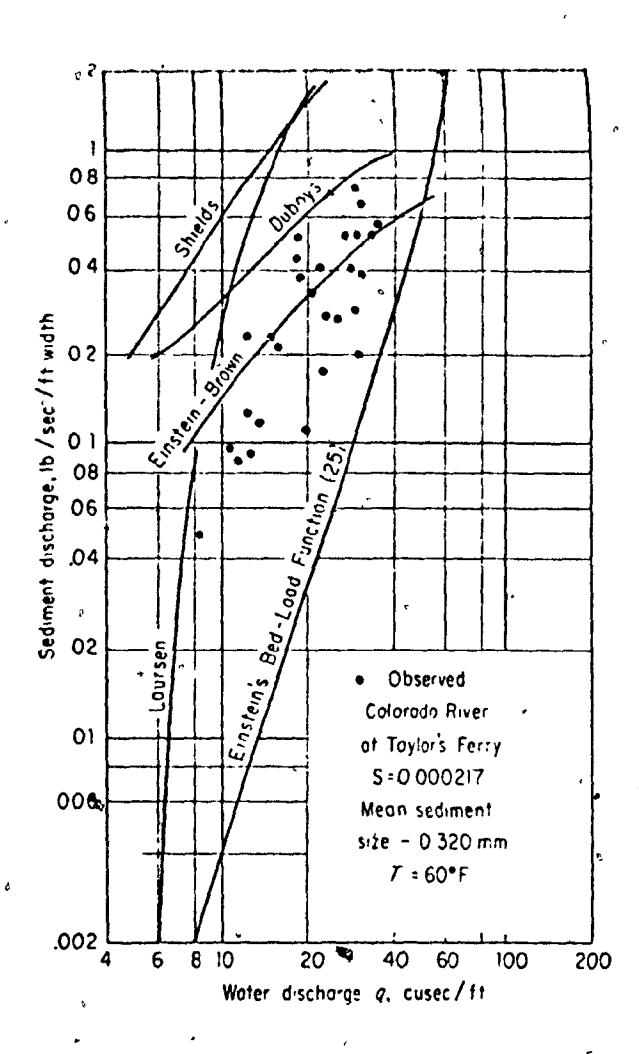


Figure 2.12: Sediment rating curves and observed values in the Colorado River (from Henderson, 1966).

All in all, the review of the literature on bedload movement indicates the scarcity of field data, the need for further studies concerned explicitly with river bed characteristics and specifically with coarse bed-materials, and that bedload studies have remained and will remain defective as long as no solution is found to the problem of bedload samplers and their efficiencies in natural streams. After all, if there are hardly any reliable sources of data on actual bedload transport rates in streams, few if any of the various bedload problems can be solved.

#### CHAPTER III

#### THE COARSE-BEDDED CHANNEL OF SEALE'S BROOK

August 1971 and June 1973, but mainly during the spring thaw periods. At this time of the year high flows are composed of a series of daily flood peaks (Figures 3.1a and 3.1b). It was intended that sediment and flow parameters would be traced throughout periods of rapid stream-flow fluctuations. Data provided by Kunkle and Comer (1972), for a similar basin in nearby Vermont, indicate that about 80 percent of the total annual particulate yield is contributed by the spring runoff period. The data reported in this study were gathered only from the lower (630 m) portion of Seale's Brook as far as its confluence with the North (Eaton) River.

### 3.1 General Description

The main channel of Seale's Brook is approximately 4.5 km (2.8 mi) long; its drainage area is 10.0 km<sup>2</sup> (3.9 mi<sup>2</sup>) with an altitudinal range of 265 m to 510 m (675 ft to 1675 ft). This north-facing drainage basin is mainly underlain by slates, limestones, quartzites and greywackes of the Ordovician St. Francis Group (Cooke, 1950). Most of the channel network is formed in deposits of till, glaciofluvial and rewashed alluvial materials of which a considerable portion is fines (< 2 mm). However, boulders up to 0.6 m in diameter are also common in these deposits. In fact, several boulders of dimensions in the order of lxlx2 m have been measured in the channel bed of Seale's Brook and much larger erratics are scattered throughout the region. A field petrographical analysis of 600 individual particles in six samples of the surface layer of the stream bed shows that about 98 percent of it is

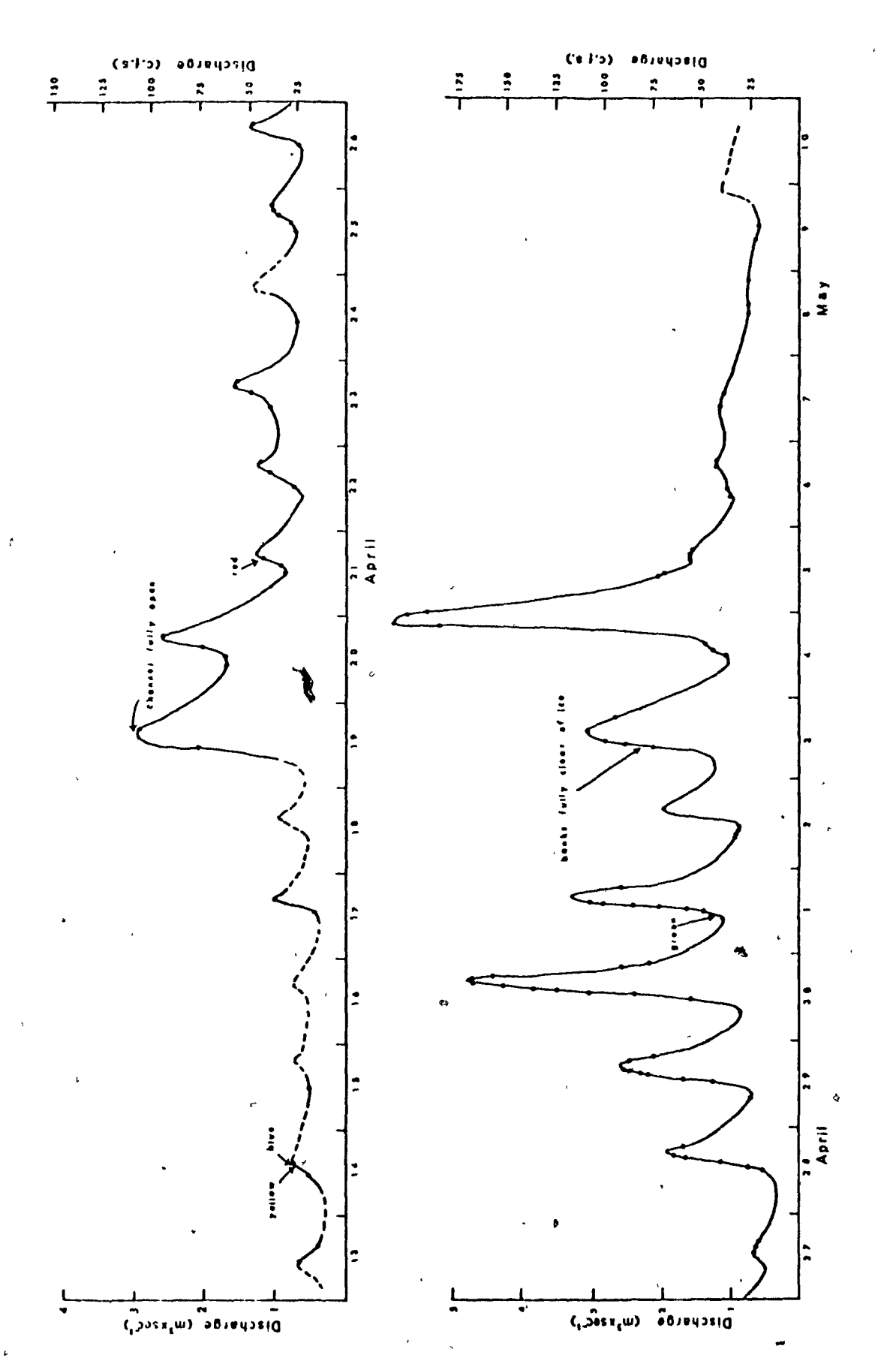


Figure 3.1a The 1972 spring flood hydrograph.

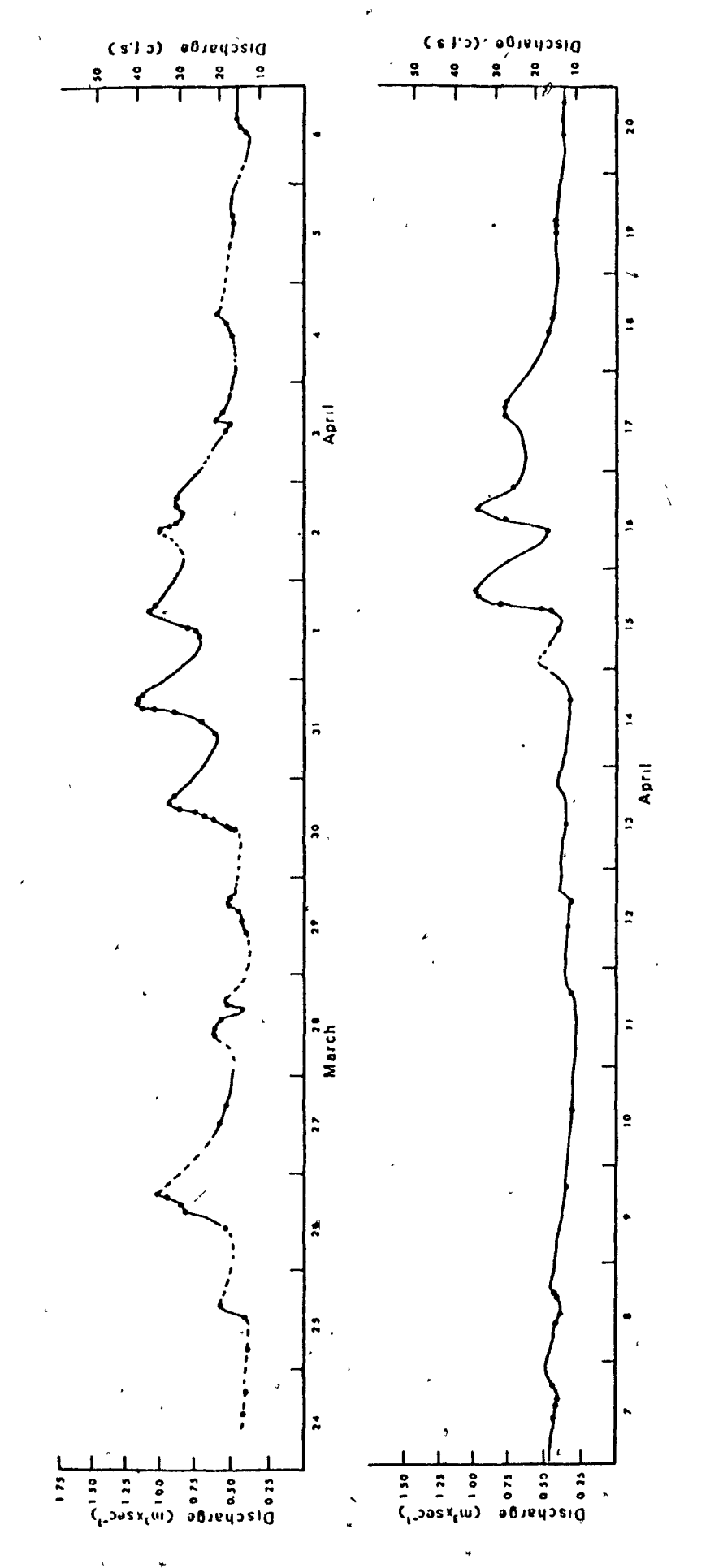


Figure 3.1b The 1973 spring flood hydrograph,

composed of non-calcaseous slates, and 1.2 and 0.7 percent of quartz and grey granite respectively. Several red siltstone, limestone, volcanic and one conglomerate particle were also spotted in the studied reach.

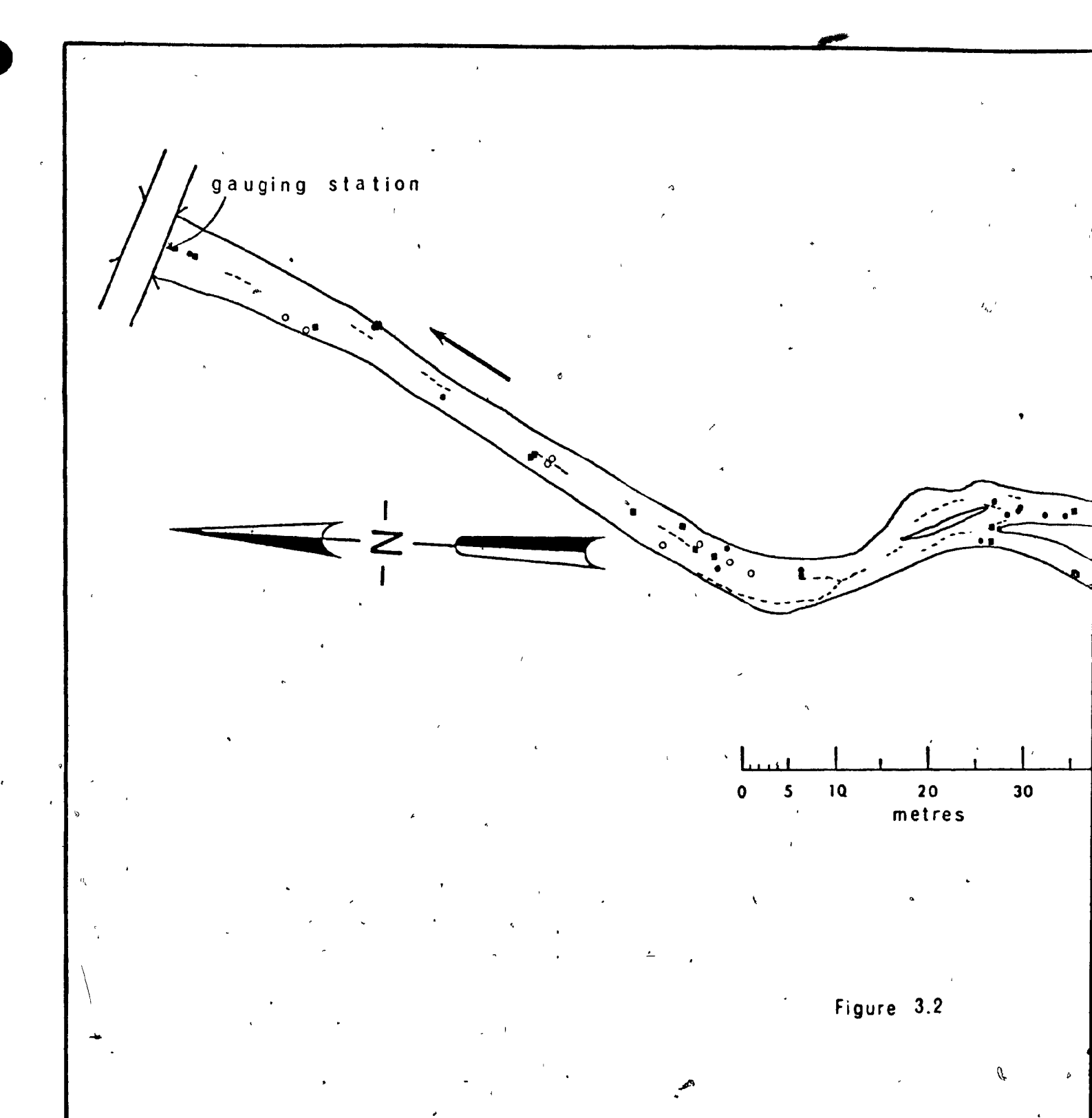
#### 3.2 Macromorphology

## a) Channel Patterns and the Longitudinal Bed Profile

reach (Figure 3.2). Channel boundaries were determined according to high-water marks (sand accumulation and swept twigs) of the May 4 - 5th flood of 1972, which discharged at its peak 5.25 m<sup>3</sup>/sec (186 ft<sup>3</sup>/sec). Figure 3.2 shows that the single channel is divided in several localities in low and medium flows by islands of raised ground. These landforms are not central bars in the accepted sense. Presence of one or more large boulders is usually associated with the small patches of raised ground, which are very distinct due to the growth of grass and occasionally a tree on them. Such boulders protect bed-material of the more usual cobble size ranges, and very fine material (down to and including sand) is also found there.

The larger patch of raised ground, the island depicted in the centre of the map, is clearly of another type. Here, the material is considerably finer than that in the adjacent channels. Sand, silt and some gravel were trapped by grass and were deposited on several island areas during the large flood of 1972. Because this raised ground is thickly covered with grass and trees, the resistance to flow is very high (Manning's n = 0.15, from Barnes, 1967) and flow velocity between these various protruberances was observed to be very low, thus causing deposition of saltating particles that landed here by chance as well as deposition of coarse suspended sed-

Figure 3.2: Map of the studied reach showing the location of recovered particles.



· l' of

SEALE'S BROOK LEGEN o re**s** 

LEGEND road thalweg channel boundary- May 4,1972 (22:09)  $Q = 5.75 \, \text{m}^3/\text{Sec}$ training walls-wood, sond & boulders cement starting point of pebbles **(**) direction of flow blue green red yellow low-water island r e d yellow

green

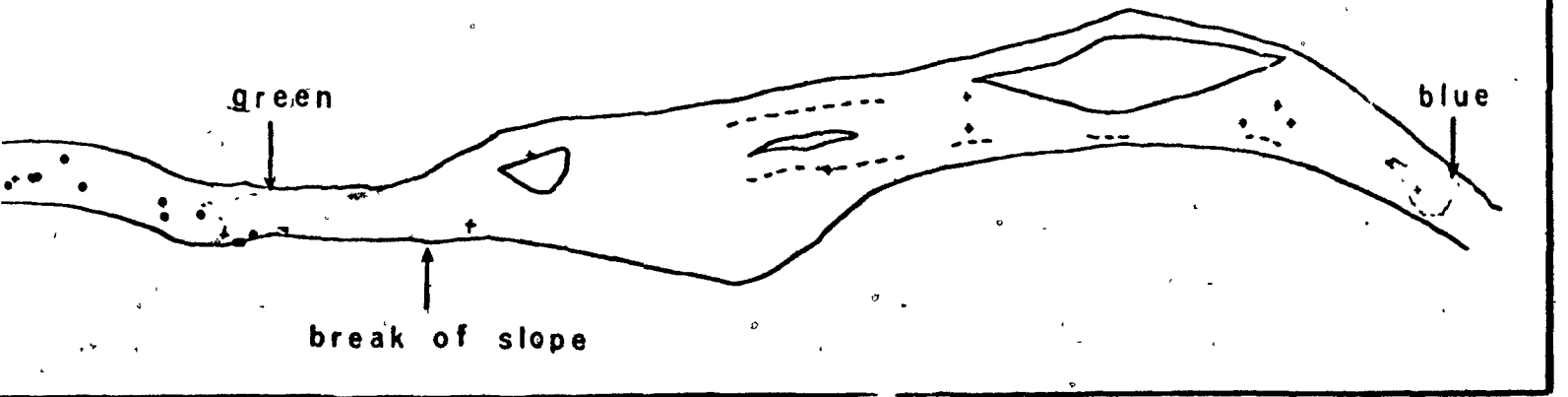
break of slope

3 %

break of slope

lers

2:00)



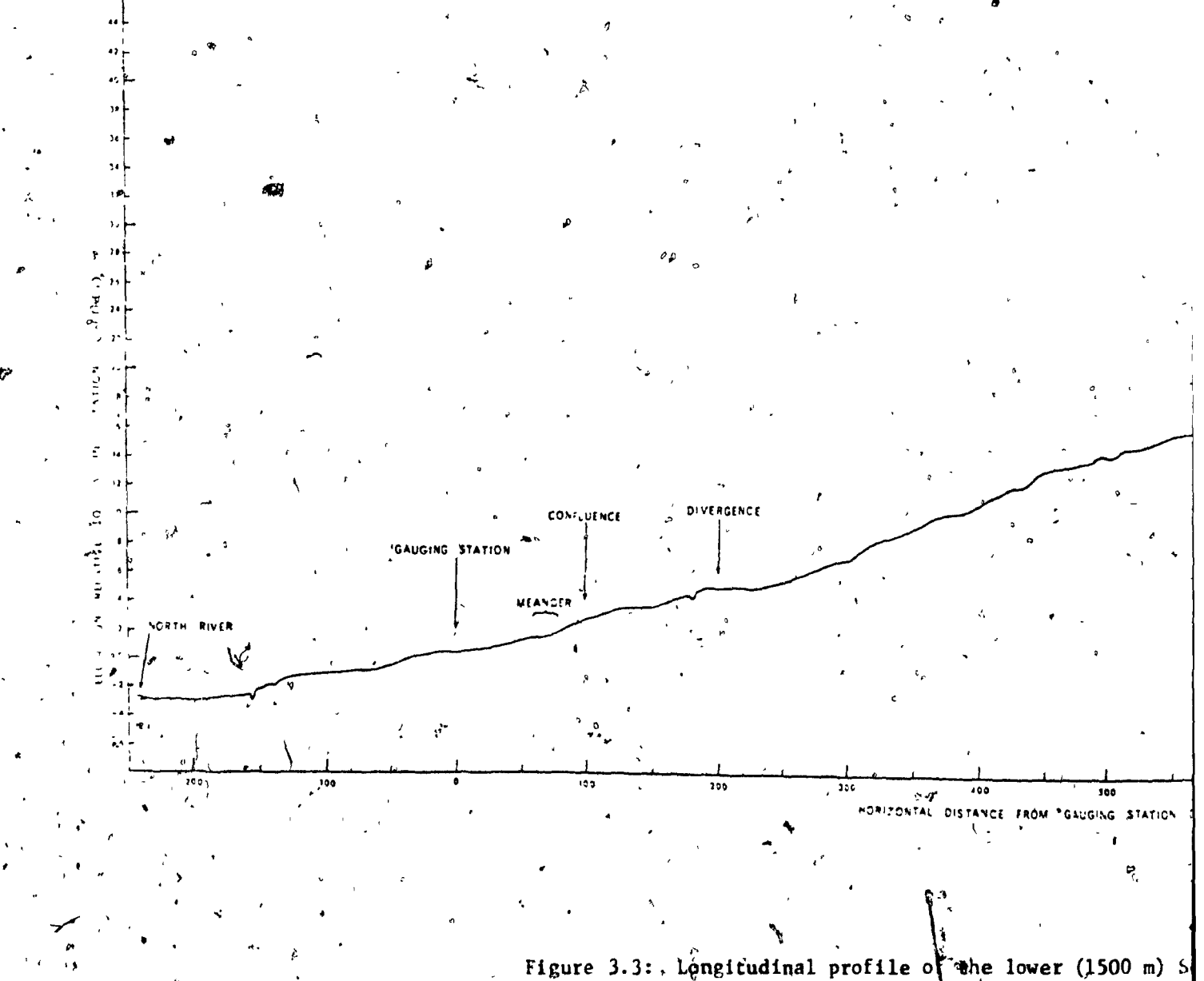
4 014

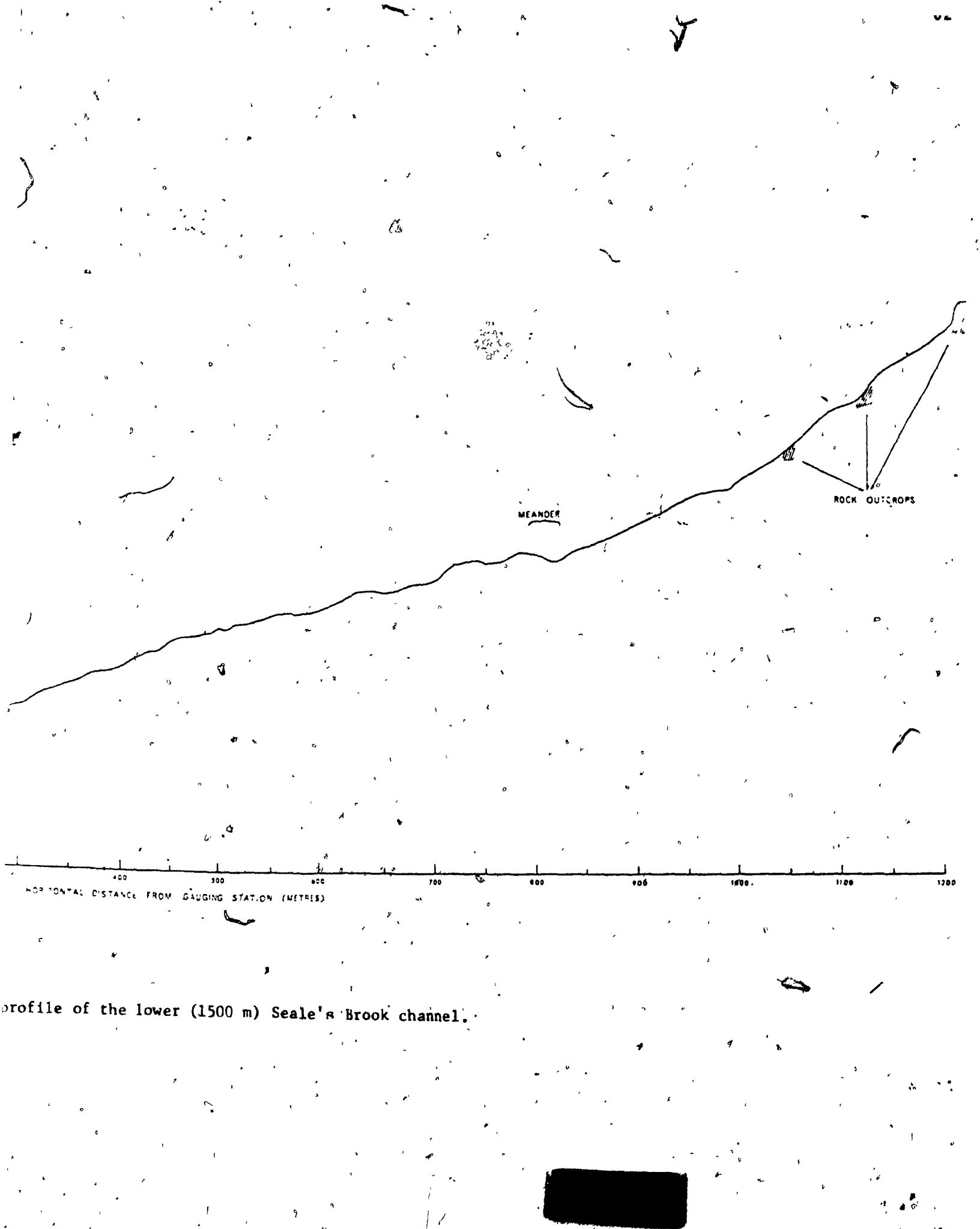
iment. The island may have been formed at the present site of divergence by a fallen tree. Fallen trees, and the debris that accumulates upstream and downstream of them (logs, branches, leaves and bed-material) are frequently encountered along the whole channel network of Seale's Brook and other small streams in the area.

The only location where the brook braids (i.e., where the formation of central bars and anabranches is a process which changes temporally and areally in a similar manner to the one described by Leopold and Wolman, 1957) is in the vicinity of its confluence with the North River. However, the location of the main stem is here less prone to areal changes than in wide alluvial plains due to the abundance of high ground thickly covered with weeds and trees. The rest of the Seale's Brook channel network is made of slightly curved reaches, and where straight ones occur, they seldom exceed a length of 20 m.

The long profile of the channel bed was measured along 1480 m (4850 ft) upstream from the confluence with the North River (Figure 3.3). For lengths of channel exceeding 10 channel widths, slopes range from 0.021 (excluding the horizontal, lowermost reach) to 0.086. Shorter reaches sometimes have a negative slope or one exceeding 45°. This range of slopes is similar to the one reported by Miller (1958) in his study of high mountain streams in New Mexico. In Seale's Brook, channel slope changes abruptly only due to bedrock contacts or in the presence of very large boulders. None of these changes is a result of tributary junctions:

Similar to many channel slopes mentioned in the literature (e.g., Hack, 1957), the measured portion of the long profile is also concave, although several rather long portions are straight or even convex. Channel slope is steeper and is generally convex in both channel branches depicted





in the centre of Figure 3.4. The average bed slope in these narrower channels is 1.2 and twice larger than the ones of the lower and upper-bordering reaches respectively. This absolute and relative increase in bed slope is in accordance with other field and flume observations (Leopold and Wolman, 1957). In two meanders (see Figure 3.3), of which one is actually a 90° change in flow direction, slope decreases considerably throughout the curving reach.

The long profile is extremely irregular rather than smooth (Figure 3.4 does not show all large-scale irregularities associated with large boulders), but no riffle pool sequence was detected. The bed morphology offers, nonetheless, a similar phenomenon to riffle-affiliated gravel bars on sandy, ephemeral streams (Leopold et al, 1966). At low flows the channel bed resembles stepping stones (Figure 3.5); concentrations of boulders occupying most of the channel width are separated by reaches 0.5 - 5 channel widths long and comprising finer bed materfal. At higher stages these are all indiscernible and there are no riffle-pool sequences (as defined by Yang, 1971).

McDonald (1972), who refers to these above-mentioned features as transverse ribs, describes them as "a series of regularly spaced pebble, cobble or boulder ridges extending across the channel and oriented transversely to current direction. They are widespread on braided alluvial plains and in high-gradient single-channel streams where they result in a stair step a rangement forcing water to flow [at intermediate flows] through a series of regularly spaced cascades." McDonald, who has formed these ribs experimentally, maintains that they are a result of the transportation of particles by supercritical flows and their deposition in

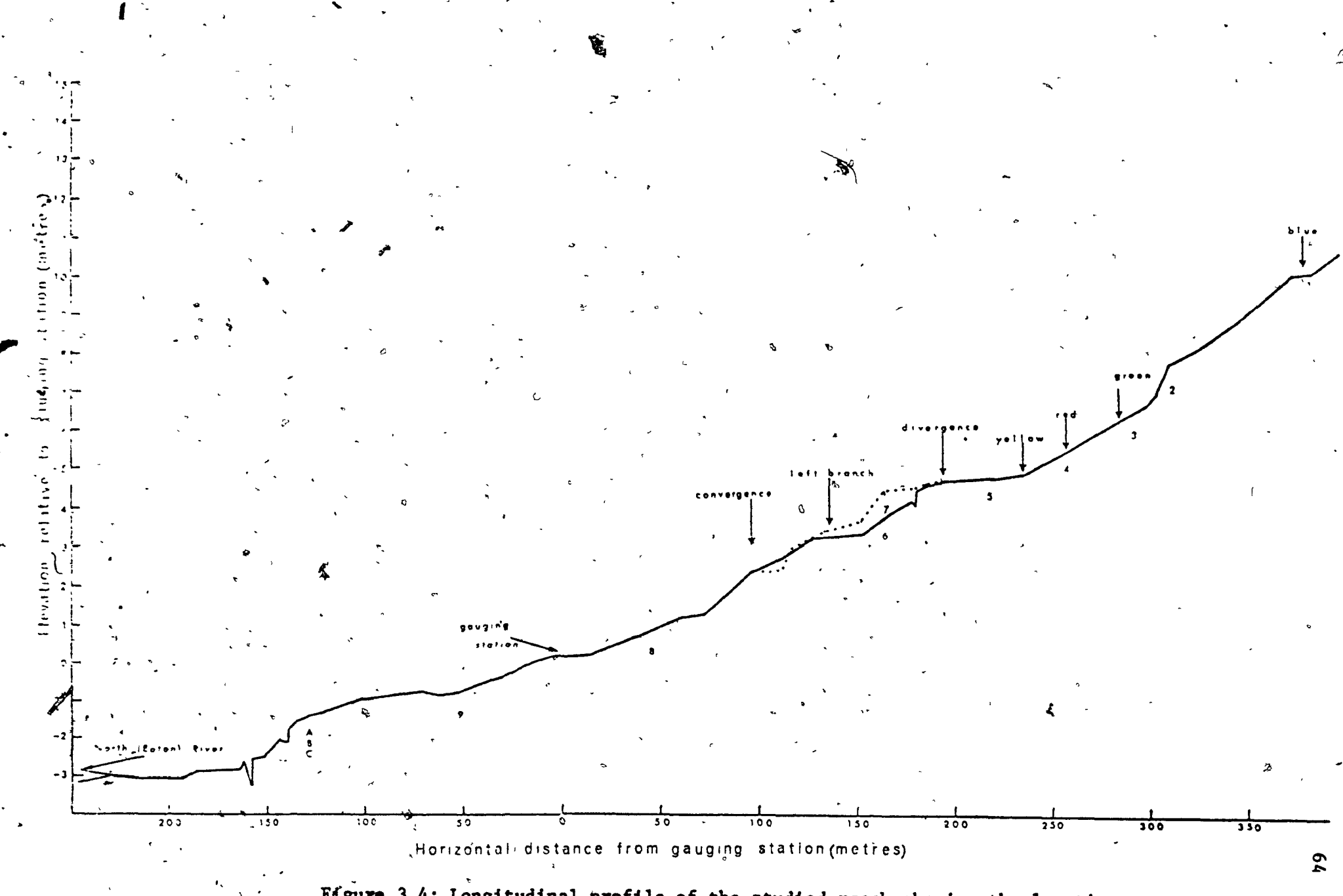


Figure 3.4: Longitudinal profile of the studied reach showing the location of the \$2 gauged cross-sections.



Figure 3.5: Transverse ribs in the right - hand channel of Seale's Brook, looking upstream. June, 1973.

a transition zone containing a hydraulic jump where the flow reverts to subcritical. Both flume and field studies (McDonald, 1972) have shown that transverse rib spacing increases with increase in particle diameter.

As indicated in Chapter I, a preliminary attempt, which failed, to measure bedload discharge directly was made during the early part of the spring of 1972. The trap site is indicated in Figure 3.2 at the upstream end of the main island in the middle of the studied reach. Gates were constructed to concentrate flow into the main (right hand) channel, in which a removable front-loading trap was located. Many difficulties were experienced and eventually the attempt was abandoned; the trap was removed and both gates were kept open. It is believed that very little interference to bedload movement along Seale's Brook was caused by this activity; attempts to use the trap system were brief and mostly confined to low-to-medium flows. Figure 3.2 does indicate a small impondment of the flow above the trap site during the 1972 peak flow, but this is misleading because the extra flow width was merely a shallow overbank area of water.

# b) Cross-Sectional Profiles and the Thalweg

Cross-sectional profiles were surveyed in the right channel branch immediately downstream of the divergence. Figure 3.6 depicts the five profiles, each 1 - 2 m apart. Although the short reach where the 5 cross-sections were measured is not representative of the whole right branch in degree of heterogeneity, similar changes characterize many other closely-aligned cross-sections throughout the channel network. These changes in cross sectional shape are frequently due to the presence of large boulders. A series of 12 cross-sections, fairly representative of the channel in which they are situated, are depicted in Figures A.1 - A.2

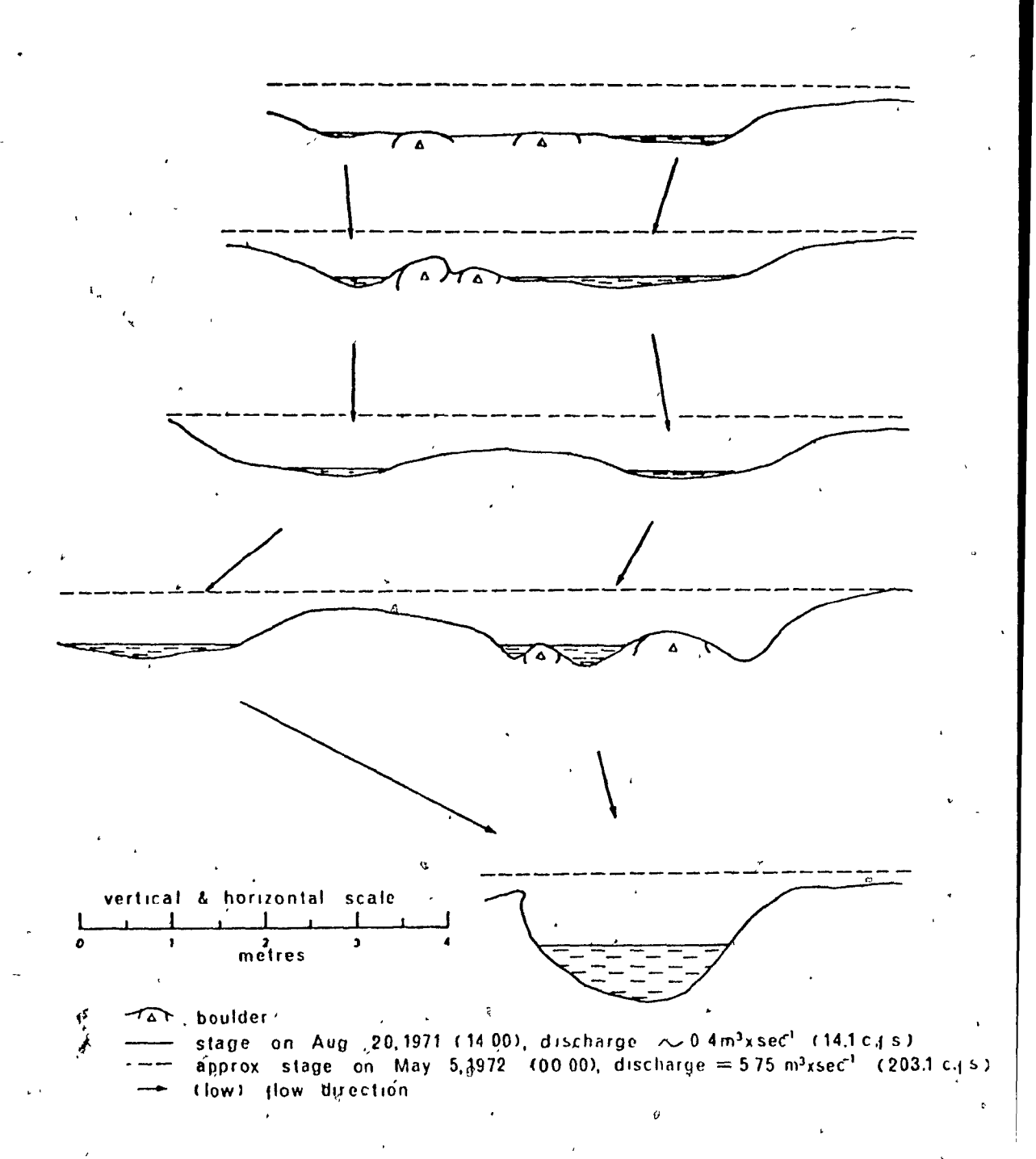


Figure 3.6 Five cross sectional profiles of the upper right-hand channel, Seale's Brook, 1971.

of the Appendix. Apart from showing the representative channel shapes in the studied reach, these profiles also give an indication of the increasing irregularity in channel shape with increase in percentage of very coarse material. In fact, because of the vast areal changes in calibre of surficial bed-material, bed slope, cross-sectional shape and thalweg shifting throughout the uppermost portion of the studied reach, the channel shapes depicted in Figure A.1 are not very representative of this particular channel reach.

The map survey also included locating the position of the thalweg in the channel (dashed line in Figure 3.2). The bed-material of Seale's Brook is comparable in size with that of streams of the Sangre de Cristo Mountains (Miller, 1958), but even at very low flows the thalweg here is not always discernible. In order to determine whether the thalweg's position shifts, its cross-sectional location was measured on the map (Figure 3.2) every 5 m. Considering only the slightly curved and the straight reaches, the thalweg is found in 26 percent (of the 40 measurements) in the outer two-fifths of the channel (i.e. in the bankward one-fifth of each side). The intermediate two-fifths and the central fifth of the channel width account for 40 and 34 percent respectively.

Results from at-a-station hydraulic geometry data show the kind of variability that should be expected between different but neighbouring cross-sections in a coarse-bedded channel. Stage measurements were taken at the bridge (gauging station in Figure 3.2) almost every day throughout the two spring flood periods. Water discharge was calculated from depth and velocity (at 0.6 depth, using a type A small Price current meter) and from a stage discharge rating curve (Figure 3.7). The best fit line is represented

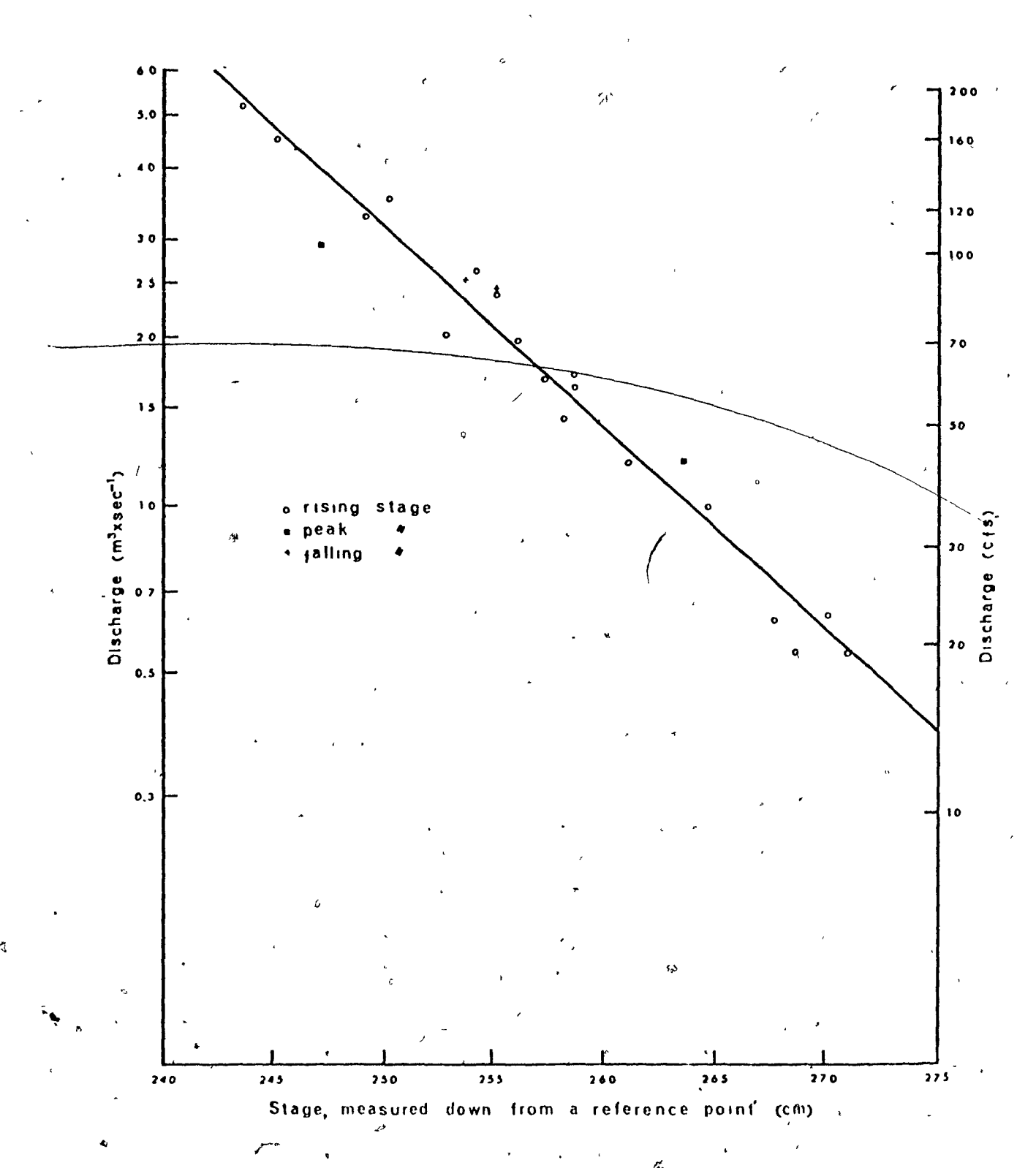


Figure 3.7 Discharge rating curve for the gauging station, Seale's Brook.

by a semilog-arithmetic relationship with a correlation coefficient of 0.978, where the value of the population correlation coefficient lies between 0.96 and 0.98 at a confidence level of 95 percent. Stage staffs were placed in 12 places along the channel. The cross-sectional form of the channel at each of these spots is shown in Figures A.1 - A.2 and their location is depicted in Figure 3.4. It had been assumed (and later found true) that discharge of water increased very slightly with distance downstream in the studied reach, because no tributaries enter it except one at its braided and lower part. Thus, a relationship between the stage at each of the cross-sections and the bridge and knowledge of the cross-sectional shape enabled construction of an at-a-station hydraulic geometry. The results of the calculations, given for three neighbouring cross-sections in Table 3.1, indeed show that both width and average values of velocity and depth differ widely. This is also true for the increase of each of these parameters with increase of discharge.

A concluding remark on this morphological description is that bed slope and cross-sectional shape change areally in a continuous and often abrupt manner. This indicates that formulae based on average conditions must be drastically reappraised in the heterogeneous environment of coarse alluvial channels.

# 3.3 Micromorphology of the Channel Bed

As mentioned in the foregoing chapters, it is believed that the micromorphology of bed-materials is of great importance in bedload studies. Although researchers in the field invariably emphasize that there may be nothing in common between the pransport of glass balls in flumes and the transport of natural materials in streams, such experiments are still

Table 3.1

Increase and Rates of Increase of Width, Average Velocity and Average Depth with Increase in Discharge, Seale's Brook, Spring, 1973.

Cross- Section No.	Q (m³/sec)	A (m <sup>2</sup> )	ū (m/sec)	<b>w</b> (m)	<u>d</u> ⟨m)	m	, b	. <b>f</b>
2 ,	0.5	0.340	1.28	3.50	0.111	0.31	0.19	
	1.5	0.863	1,30	4.30	0.200			0.53
3	0.5	0.696	0.72	4.72	0.148	0.37	0.10	
	1.5	1.383	1.08	5.26	0.263			0.56
4 .	0.5	0.760	0.66	2.84	.0.008	0.54	2 22	0.00
•	1.5	1.258	- 1.20	4.30	0.292		0.38	0.08

D\_

Q, A,  $\overline{u}$ , w and  $\overline{d}$  are the discharge, cross sectional area, average velocity, width and average depth of flow respectively. m, b and f are the exponents of Q in the hydraulic geometry equations with  $\overline{u}$ , w and  $\overline{d}$  respectively.

undertaken today. In fact, even the most recent flume studies are mainly dedicated to uniform bed material. Thus, effects of form and structure are almost completely ignored. Maddock (1968) summarized part of this problem when he stated: "There is nothing wrong with the great number of data collected in the study of flow of water in flumes with movable beds. What is wanting is a system of analysis that will take into consideration the mutual interdependence of variables and particularly, the effects of changing bed-forms." Observations of this study tend to show that for bed-materials with a wide range in particle size, the structure of these forms is vitally important — perhaps more so than the forms themselves.

An unfamiliar observer of coarse-bedded channels becomes confused by the overwhelming complexity of the structure and composition of the bed. In fact, he tends to note that the dominant motif here is one of disarray. A closer observation of the bed reveals, however, several highly developed trends, structures and microtopographic characteristics.

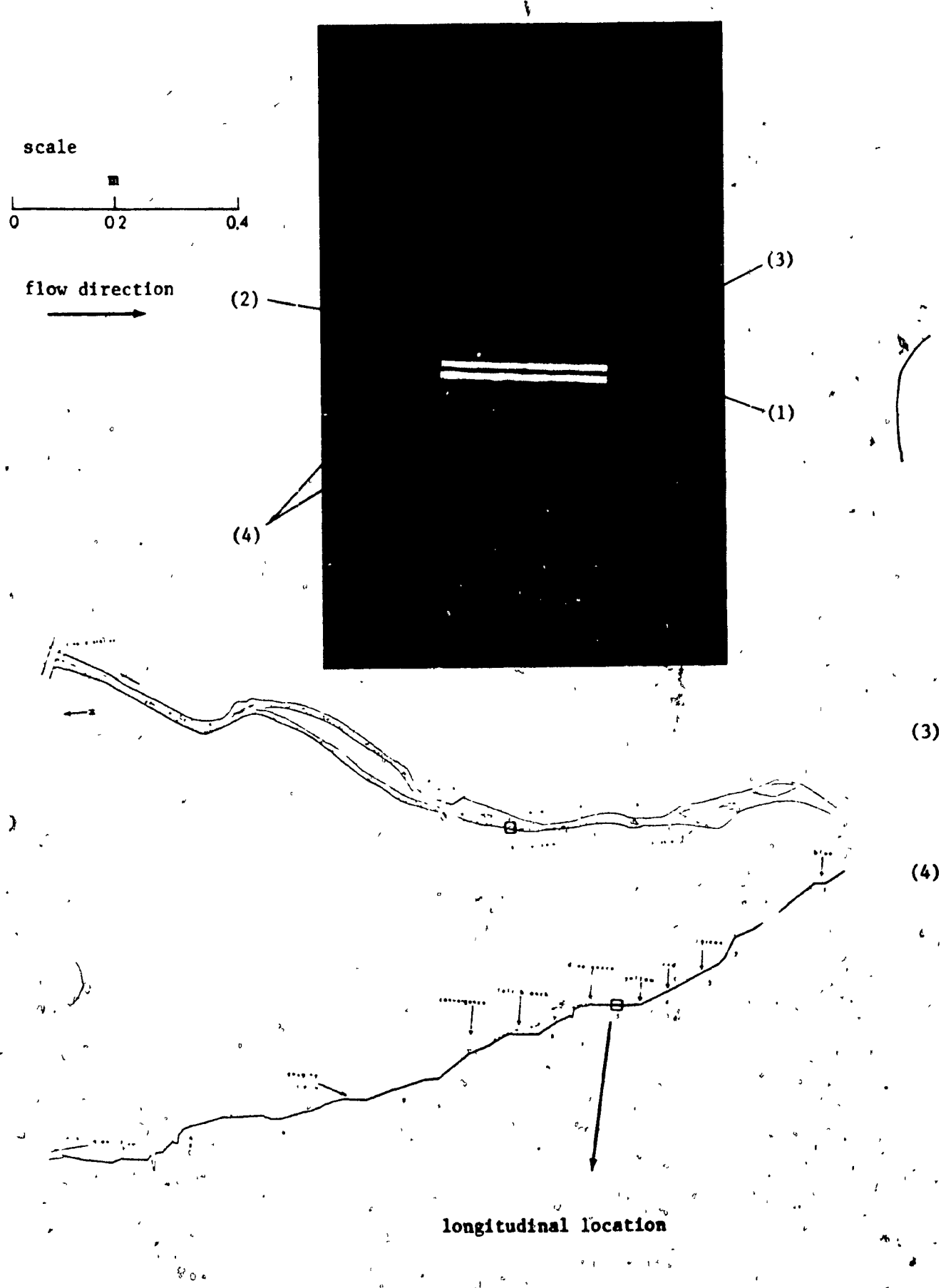
More than 100 photographs were taken of the Seale's Brook bed.

Each photographed bed area includes at least one of the labelled and recovered particles. The full length of the ruler in the photographs is 305 mm and the millimetric scale always points to the direction of flow, increasing downstream. The photographs that are incorporated in the thesis are each on a separate page, accompanied by a longitudinal profile and a map of the channel showing the exact position of the photographed bed area.

Pertinent data on the coloured bed fragments are also included.

## a) Bed Relief

Three types of bedforms, whose dominant characteristic is their relief above or below their immediate surroundings, have been distinguished



Recon

Weigh

Dista

Spher

Shape

Local

Loca

b-ax

a-ax

c-axi

, ,

60

(3) bar a

(4) relat

-

- Figu

Recovered Particle No.	-	113 <sup>(1)</sup>	114 <sup>(2)</sup>
Weight	-	97.29 gm	93.30 gm
Distance of Transport	-	86.32 m	86.02 m
Sphericity $(\sqrt{bc/a^2})$	-	0.24	0.54
Shape (c/a)	~	0.24	0.36
Local Slope	<u>.</u>	0.001	0.001
Local Slope/Average Slope	_	0.053	0.053
b-axis	<b>-</b>	25.5 mm	52.1 mm
a-axis	٠_	101.3 mm	64.3 mm
c-axis		24.4 mm	22.9 mm
Cr. Sec. Location*	-	180.20 cm	180.20 cm
		_ <b>f</b> o	4

\* see explanation to Table A.2.

(3) bar axis

(3)

(1)

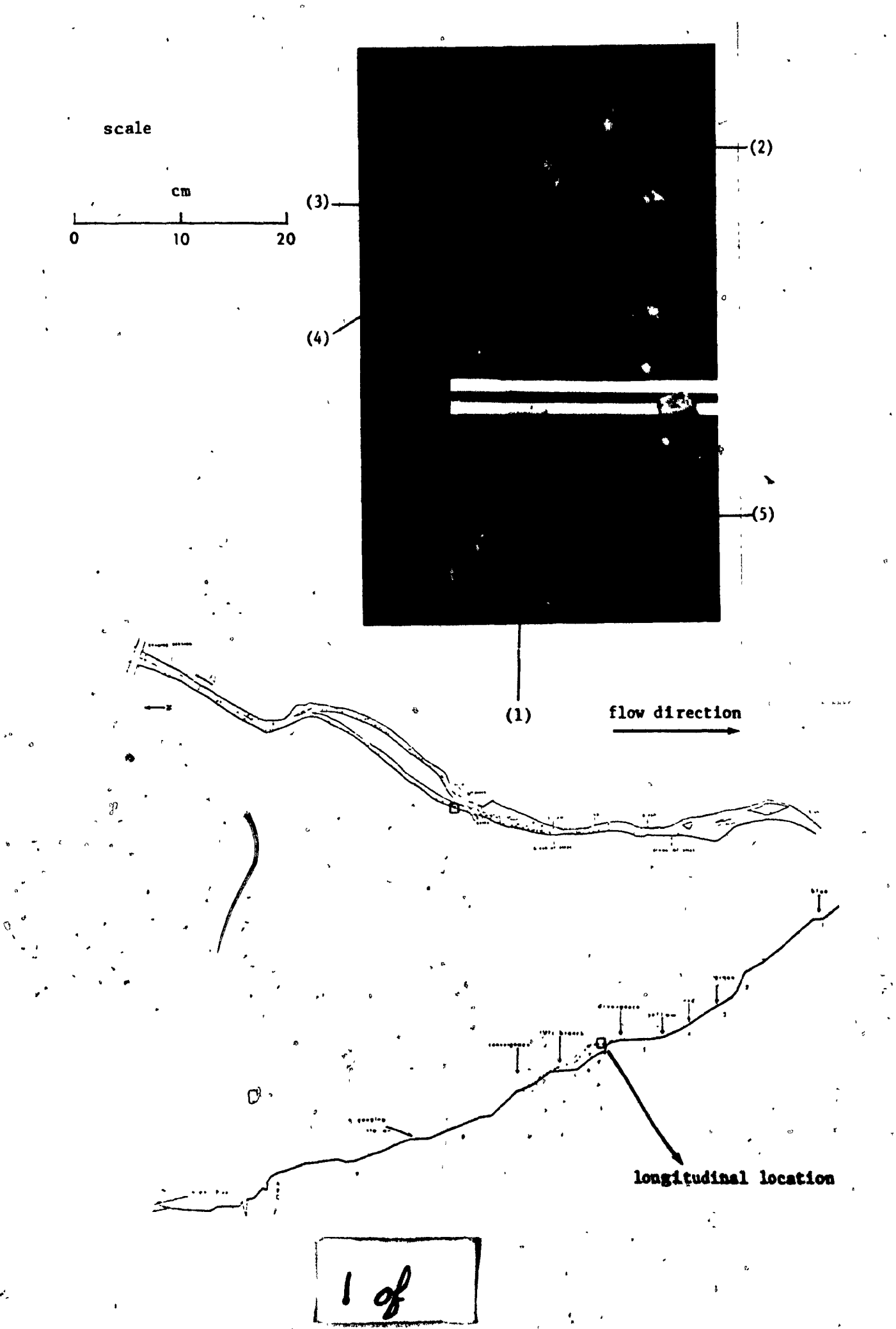
(4) relatively deep flanks of the bar

Figure 3:8: Miniature longitudinal bar. Water depth is approximately 15 cm on the bar axis. The latter is elevated 5 - 7 cm above its flanks, which are 10 - 15 cm lower than the average hight of the bankward surface layer of the bed.

in Seale's Brook. These are miniature bars, boulder shadows and bed protruberances. Clearly identifiable morpho-structural features were observed to be associated with concentrations of relatively small particles. Although not very common, rather shallow 0.2 - 1 m long by 0.2 - 0.4 m wide longitudinal bars have been observed in several locations. The bar is characterized by a cross-sectional change in calibre of the surficial material. Two microtopographical lows which accompany the bar on its flanks and its upstream end are mostly covered with fine gravel. As the bar summit (5 - 10 cm above the lows and at a somewhat lower height than the average bed elevation in the area) is approached, the surface material becomes coarser and at its maximum is 6 - 20 mm in diameter. With increase in distance outwards from the relatively deep flanks, bed-material size increases quite abruptly. An example of such a miniature longitudinal bar is depicted in Figure 3.8.

Fine bed-material is often found in lee of boulders (Figures 3.9, 3.10 and 3.11). These gravel and pebble deposits attain their accentuated concentrations because they have come to rest in parts of the bed surface which are quiet, being hidden behind a large boulder. It is quite obvious that these boulder shadows are late features associated with lower stages of a flood recession, when flow velocity is too low to cause turbulent eddies to develop and entrain the hidden particles.

Flow protruberances are either single boulders dispersed on the bed in disorder or groups of boulders. The groups form transverse ribs (Figure 3.5) or small, usually vegetated patches of raised ground.



1

Ì

(4

(4

	(2)	
AND THE RESEARCH AND THE PARTY	-(5)	

tion

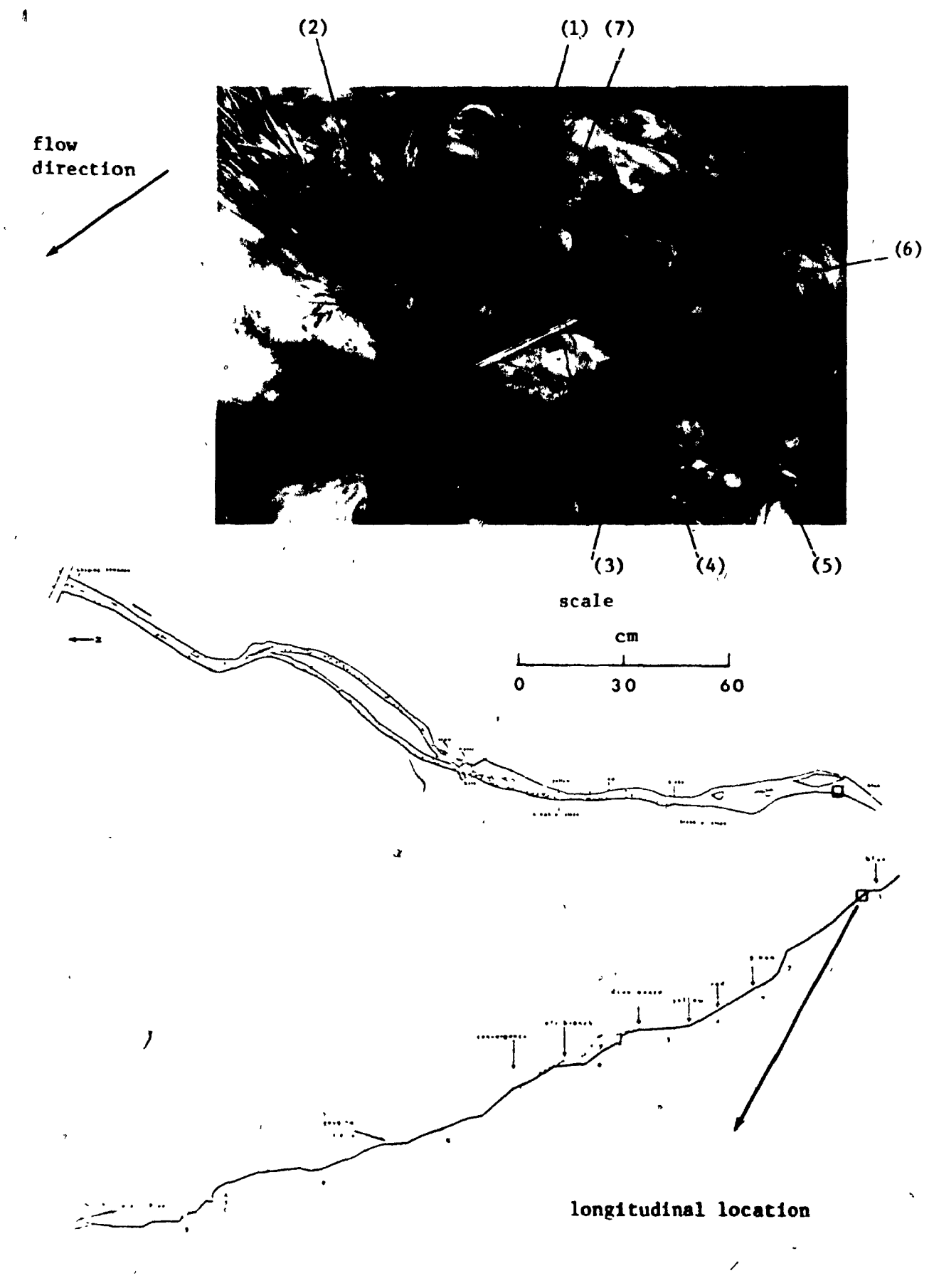
Recovered Particle No.	-	<sub>9</sub> (1)	10 <sup>(2)</sup>
Weight	-	4.29 gm	1.03 gm
Distance of Transport	<b></b>	127.08 m	207.41 m
Sphericity $(\sqrt{bc/a^2})$	~	0.62	0.73
Shape (c/a)	-	0.61	0.60
Local Slope	-	0.036	0.036
b-axis	-	13.2 ram	8.5 mm
a-axis	-	20.7 man.	9.4 mm
c-axis	•	12.6 mm	5.7 mm
Cr. Sec. Location*	- '	110.30 cm	80.30 cm

<sup>\*</sup> see explanation to Table A.2.

- (3) large boulder protruding from the surface 'layer'
- (4) gravelly and pebbly boulder shadow deposits
- (5) flat deposits characterized by uniform, open-structured bed-material

Figure 3.9: Boulder shadow and flat deposits. The boulder protrudes by approximately 25 cm from the bed area further downstream.

dinal location



Recovered Particle No.	-	241 (1)	
Weight .	-	12463.80 gm	
Distance of Transport	-	11.57 m	
Sphericity ( $\sqrt{bc/a^2}$ )	-	0.60	٠
Shape (c/a)	, 	0.51	
Local Slope	-	0.047	
b-axis	-	220.2 mm	
a-axis	-	307.3 mm	
c-axis	7	156.8 mm	¥
Cr. Sec. Location*	-	120.11 cm	,

<sup>\*</sup> see explanation to Table A.2.

- (2) grass-covered central island
- (3) tight, vertically infilled structure
- (4) imbricate structure
- (5) boulder shadow
- (6) downstream part of a large imbricate structure
- (7) boulder, with vertical a/b plane, partly underlies particle No. 241; this is an evidence that the former was transported during the spring of 1972
  - Figure 3.10: Structure and texture in the bed of the uppermost part of the studied reach. The maximum relief between adjacent spots shown in the photograph is about 1 m.

### b) Textural Associations

Because all the micromorphological features have definite textural qualities, it is somewhat misleading to treat textural associations as a separate group. In fact, texture, structure and form are all closely aligned. The distinction made herein between the three groups is merely intended to point out the dominant characteristics of these features.

The size distribution of the surficial bed-material (Figure 4.12) reveals that there is a large deficiency of fines (< 2 mm).

This deficiency is particularly marked in comparison with the textural characteristics of the surficial deposits of the area (McDonald, 1969) and of deeper-lying layers of the bed (see p. 143). The small amounts of fine surficial material tend to concentrate in various locations but particularly on channel flanks and on point bars. Figure 3.12 demonstrates that the surficial bed-material of the point bar, measuring 2x6 m in area, is even finer than the surficial bed-material further downstream. Being an elevated morphological unit on the side of the channel, water depth and velocity are low over it. Consequently, only the finer fractions tend to be transported and deposited on the bar.

Throughout the channel of Seale's Brook, channel flank deposits are consistently finer than in the vicinity of the thalweg or in the centre of the channel. This phenomenon is clearly seen where there are steep banks, which are associated with a large and abrupt granulometric change. Figure 3.13 depicts two size frequencies representing the same reach; one is for the thalweg or, where indiscernible, for the centre of the channel, and one for the whole bed

( )

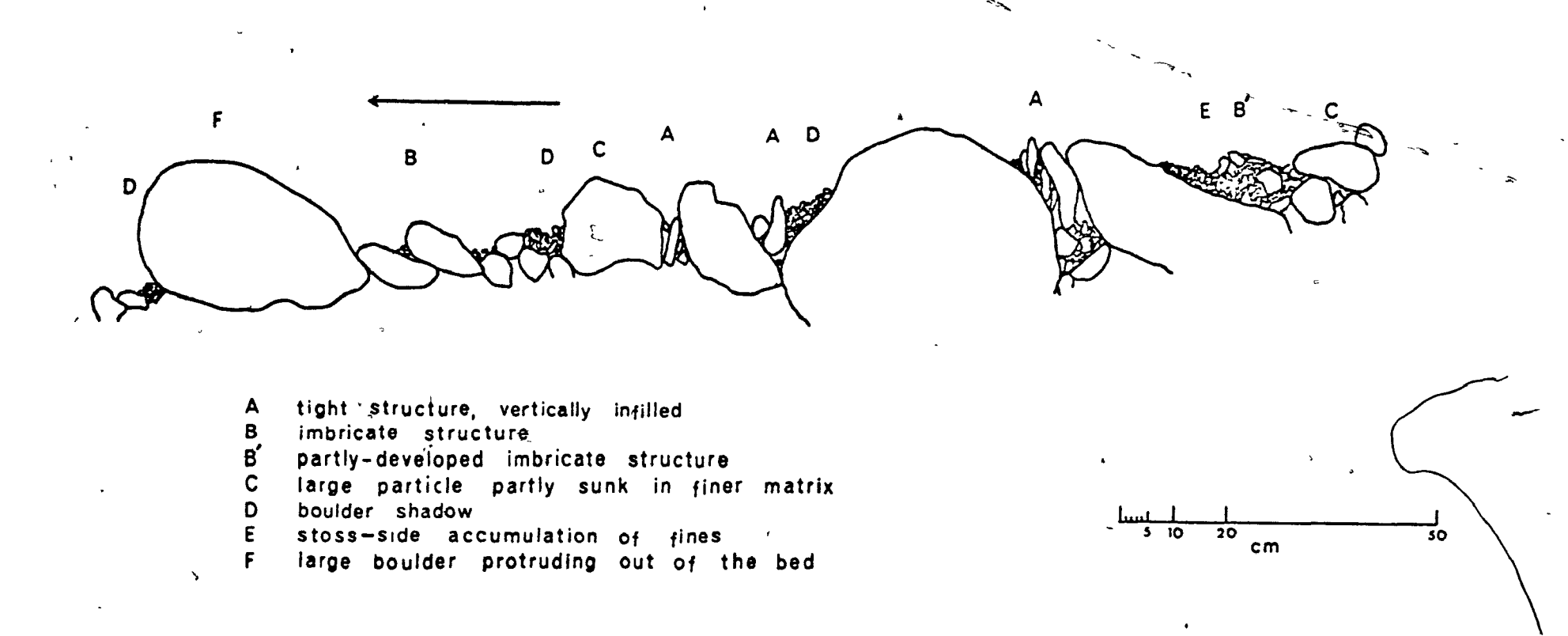


Figure 3.11 Schematic longitudinal section of the bed, Seale's Brook.

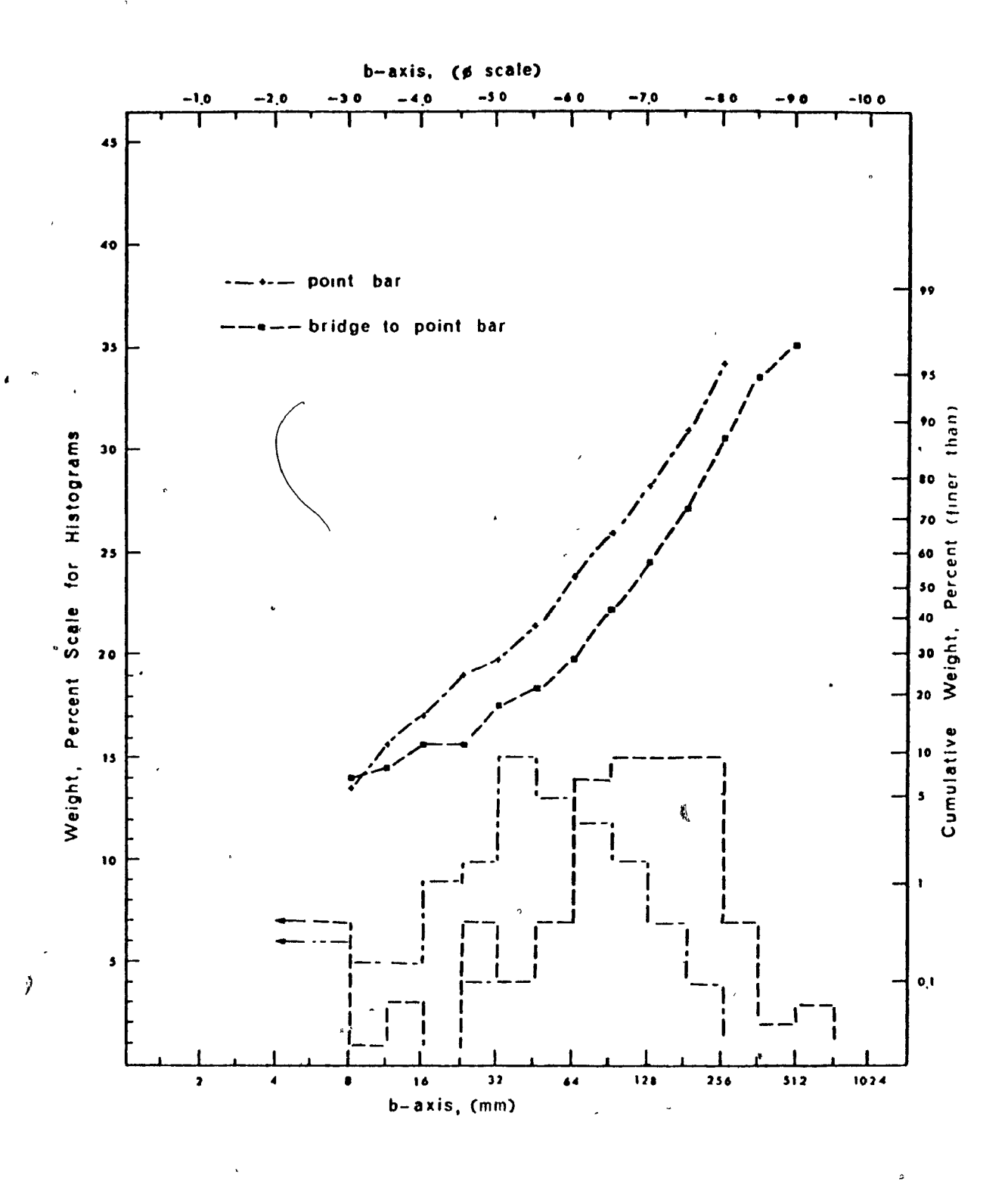


Figure 3.12 Cumulative graphs and histograms of particle sizes on the surface of the bed: point bar versus further downstream.

es.

Ψ**5.** }~~ area. It is evident that channel flank deposits are, on average, finer than those more centrally located. This clear trend for steep flanks (Figure 3.14) is also maintained when side slopes are less steep, but the change is more gradual (Figures 3.15 and 3.16).

Channel flank deposits are mostly sandy and gravelly. are often trapped by grass, branches and loose roots and tend to concentrate wherever the density of obstacles is greatest. The frequent occurrence of the obstacles-fine material 'duo' on channel flanks is readily apparent, and its formation clearly understood, if one considers these obstacles as a means by which the propelling force acting on particles is greatly diminished. Flow velocity is reduced to such an extent near the bank that any small obstacle merely reduces flow velocity still further; the total damping effect causes a decrease of velocity with nearness to the bank and the end result is that at high stages of flow, most of the water (and the coarser bedload fractions) is concentrated in the centre of the channel, where velocity and depth are greatest. During peak stages of the 5 largest spring floods of 1972, water surface in the central most turbulent portion of the channel was, indeed, noted to be raised above its sides, a phenomenon also reported by Nanson (1972) in his study of coarse-bedded mountain streams.

Flank deposits are also common in small side channels, formed concurrently with the formation of grass-covered, raised-ground patches. In fact, even a minor microtopographic change as the one shown in the right-hand side of Figure 3.17, where the channel bed is on average 5 cm lower than the adjacent vegetated bedform to its right, shows that increased resistance has a large effect on the calibre of transported

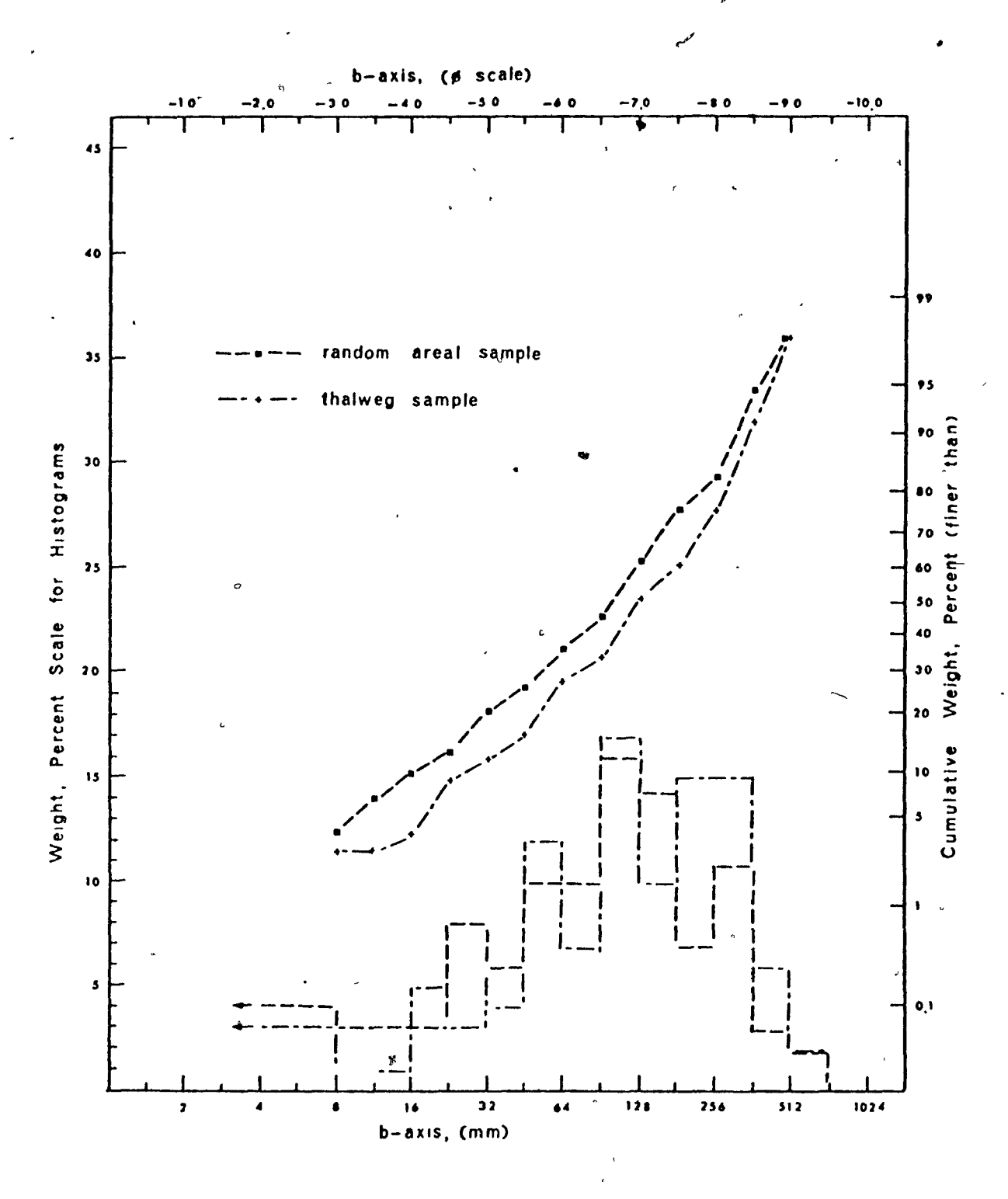
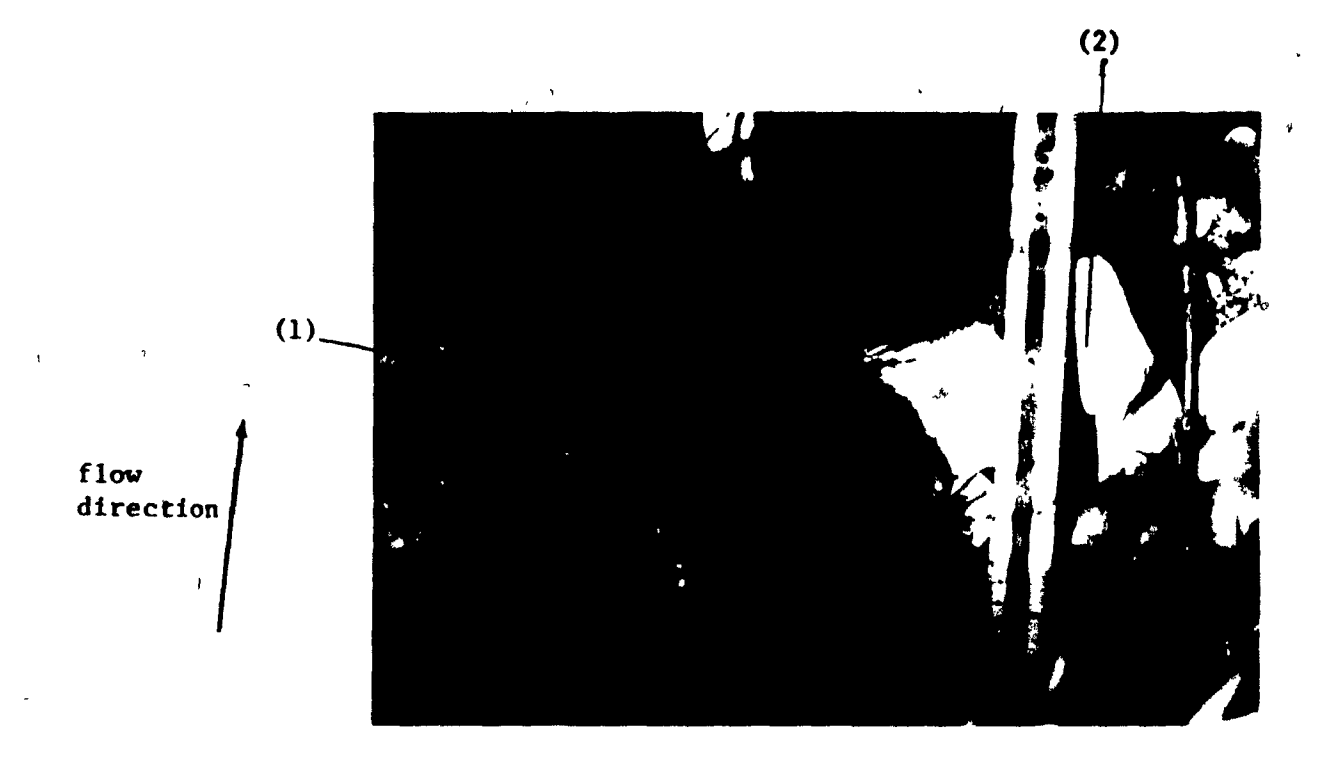
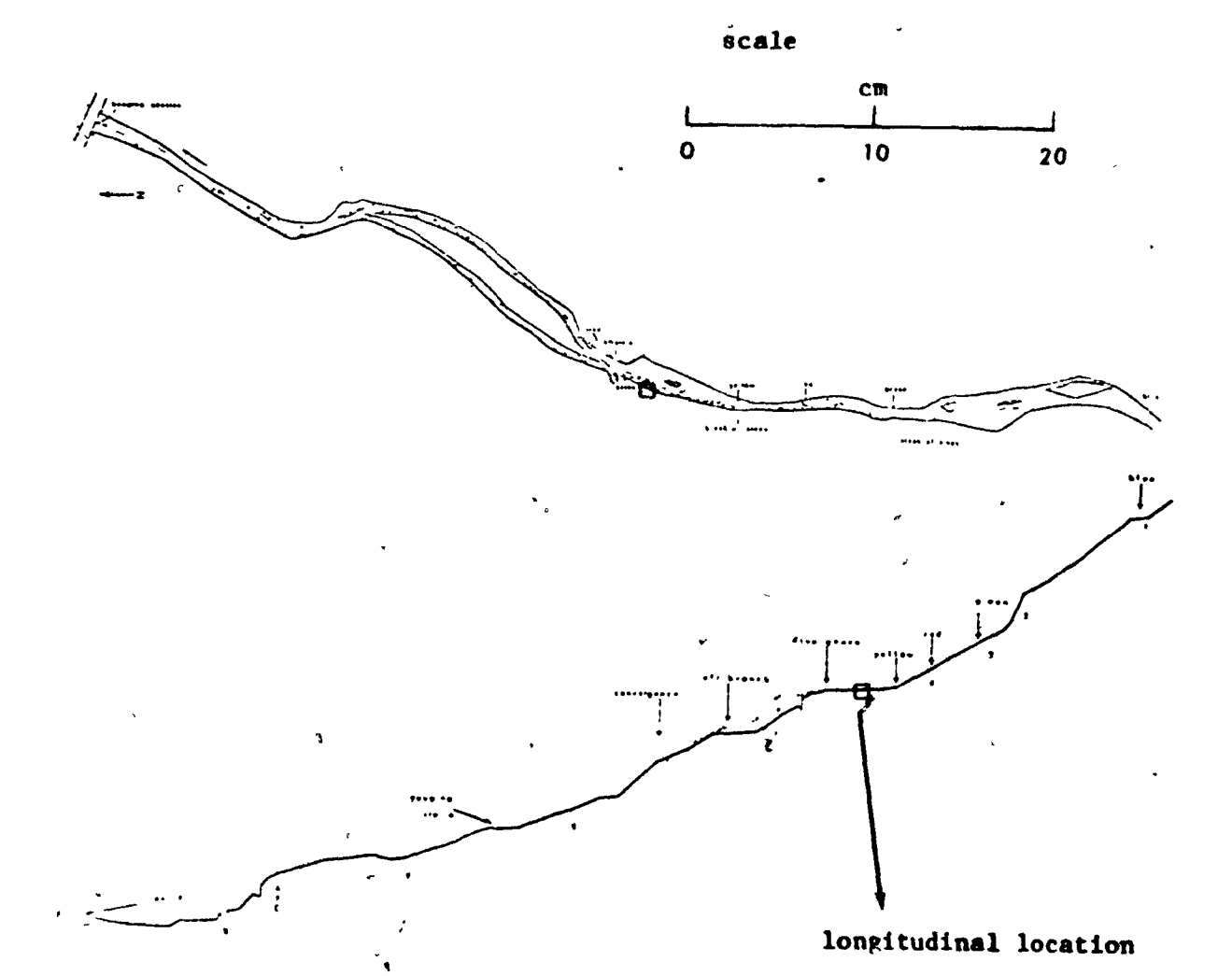


Figure 3.13 Cumulative graphs and histograms of particle sizes on the surface of the bed: random areal sample versus thalweg sample.





Mr.

Recovered Particle No.	-	181 <sup>(1)</sup>
Weight	-	5.92 gm
Distance of Transport	-	27.53 m
Sphericity $(\sqrt{bc/a^2})$	-	0.48
Shape (c/a)	-	0.37
Local Slope	-	0.006
b-axis	-	18.2 mm
a-axis	-	28.8
c-axis	-	10.6 mm
Cr. Sec. Location*	-	190.40 cm

<sup>\*</sup> see explanation to Table A.2.

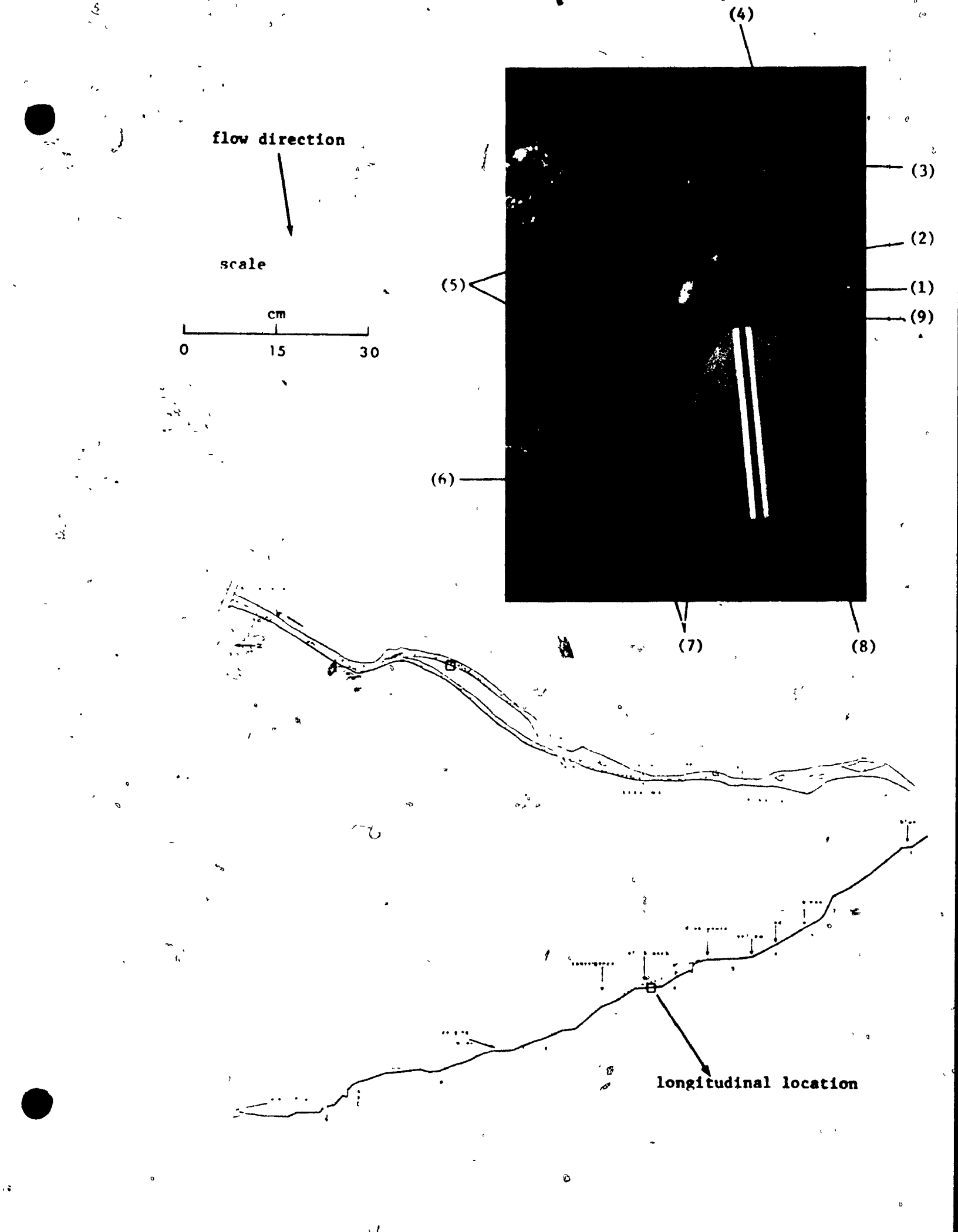
(2) this boulder is part of the man-made levee (which was constructed several decades ago) shown in this photograph

Figure 3.14: Stoss-side and steep flank deposits. Notice the partly-buried character of the pebbles in the stoss-side area.

E D

bed-material. Only few large particles are encountered on microtopographic highs because their rolling and sliding motion is usually stopped upstream of these forms. Had they moved by saltation, they would have been found more frequently on the vegetated and elevated ground rather than on the neighbouring channel bed, because once they land on such a feature the probability of their entrainment is reduced. As, an example, consider the extreme case depicted in Figure 3.17. This portion of the channel is at least 15 cm higher than the average elevation of the neighbouring stream bed, and more than 25 cm higher than the thalweg. During the flood of May 4 - 5th, 1972, pebbles and cobbles managed to roll up and on this side channel where conditions were, in terms of competence, much lower than in the centre of the channel. The bankward decrease of velocity in any stream is wellknown, and although the above-mentioned particles managed to reach such % a topographic high, hardly any of them were transported over the rougher and slightly higher vegetated surface (some did. just on the boundary). Had coarse particles moved over these surfaces with ease, no width-wise variability in calibre would have been apparent.

Patches of material of uniform calibre are not restricted to very small particles. Indeed, a considerable (20 - 30 percent, qualitatively estimated) portion of the stream bed is covered with pebbles and cobbles of uniform size (see Figure 3.18 and the downstream portion of Figure 3.9). These portions of the bed area, referred to in this study as 'flat deposits', are characterized by a very flat microtopography (represented by 'highs' and 'lows' vertically displaced by the length of the c - axis of the particles). Such bed areas are

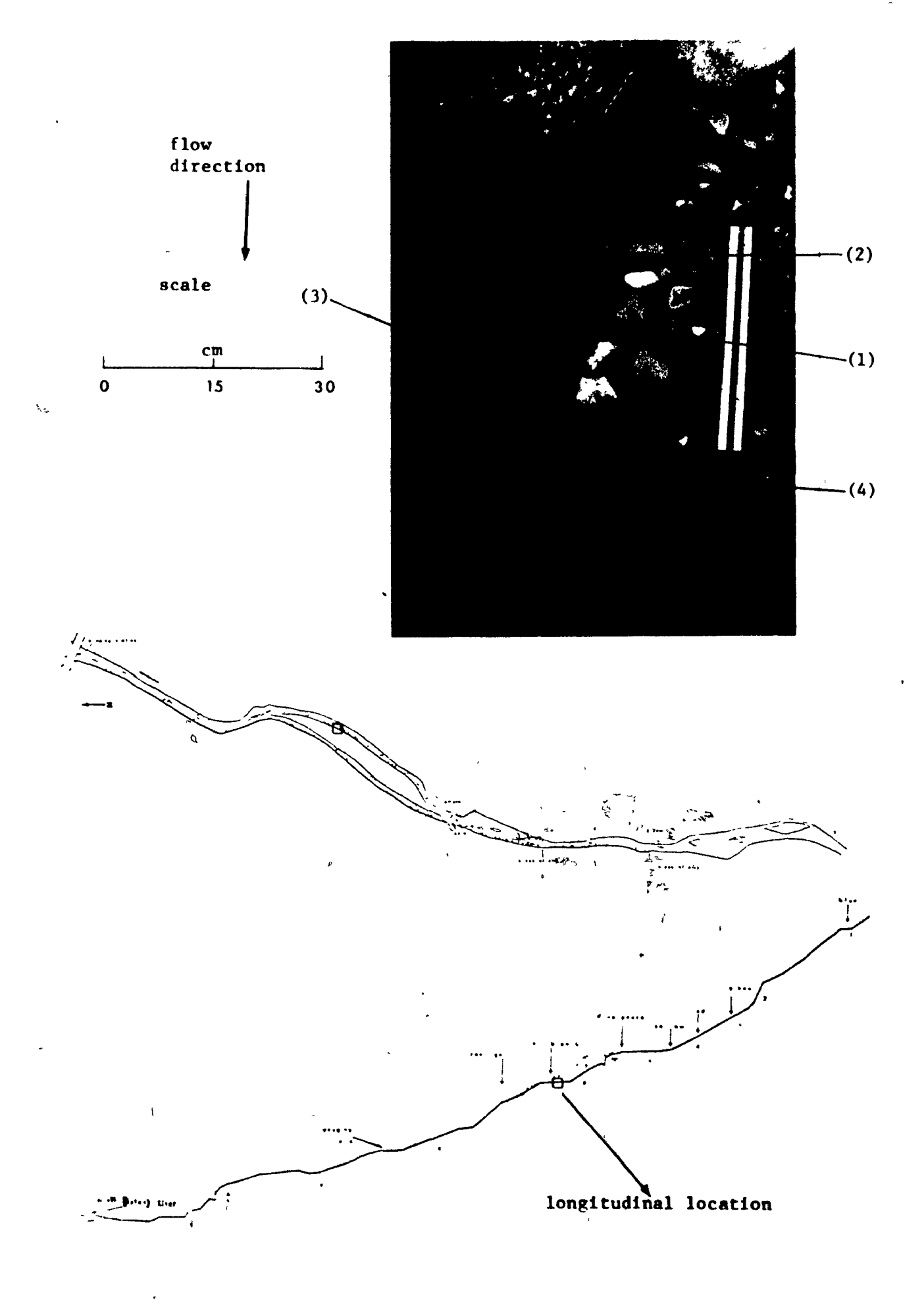


Recovered Particle No.	-	_ 26 (1) _
Weight		423.61 gm
Distance of Transport	-	104.87 m
Sphericity $(\sqrt{bc/a^2})$	••	0.59
Shape (c/a)	-	0.41
Local Slope	<u>.</u>	0.004
b-axis	-	78.7 mm
a-axis	-	92.9 mm
c-axis	-	38.0 mm
Cr. Sec. Location*	_	190.40 cm

<sup>\*</sup> see explanation to Table A.2.

- (2) stoss-side deposits
- (3) cobble with long axis aligned transversely to the flow direction is buried almost completely
- (4) 'simple' infilled (and thus, closed) structure
- (5) tight structure
- (6) vertically infilled tight structure
- (7) partly developed imbrication
- (8) lee-side deposits. These are usually somewhat coarser than the respective material on the stoss side.
- (9) notice the decrease in particle size throughout this and other (parallel) cross-sections

Figure 3.15: Gradual decrease of particle size on a low-angle flank.



Recovered Particle No.	_	29(1)
Recovered raterers no.		
Weight	-	832.02 /gm
Distance of Transport *	-	108.72 m
Sphericity $(\sqrt{bc/a^2})$	made.	0.53
Shape (c/a)	-	0.34
Local Slope	-	0.032
b-axis ·	-	124.2 mm
a-axis	-	126.0 mm
c-axis	-	42.4 mm
Cr. Sec. Location*	-	110.40 cm

<sup>\*</sup> see explanation to Table A.2

- (2) abrupt pranulometric change from coarse, thalweg deposits to boulder shadow and/or steep flank deposits
- (3) coarse textured rather open structure
- (4) tight structure

Figure 3.16: Abrupt change to boulder shadow and steep flank deposits

covered with bed-material slightly smaller or as large as the median (D<sub>50</sub>) size representative of the whole reach. The particles are usually placed one beside the other in a fairly open structure and additional surficial structures are absent. This micromorphology represents the closest approximation to idealized bed-material arrangements assumed in most bedload formulae.

### c) Structural Arrangements

Particles on the surface of the bed which are arranged in such a manner that there is hardly any contact between them are said to form an open structure. Such structures characterize flat deposists as well as various types of fine material accumulations. In addition to those concentrations of fine material mentioned previously, it is evident that these deposits are also often located on the stoss (or upstream) side of boulders, specifically where the latter dip upstream (Figures 3.11, 3.15 and 3.19). The late deposition of these materials may be inferred from their exposed locations.

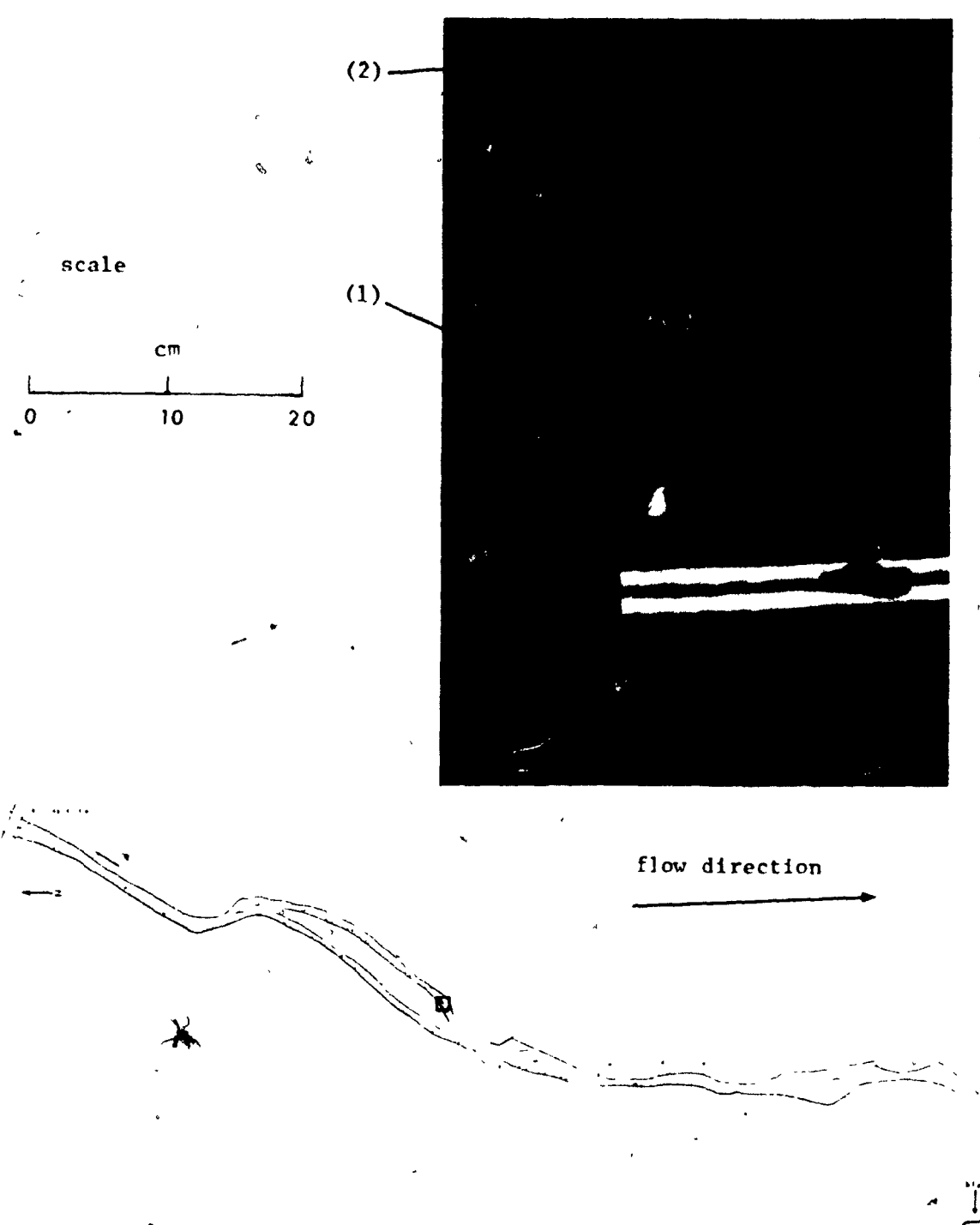
Closed structures, where most surface particles are in contact, are much more prevalent than open ones. A purely theoretical approach to coarse-bedded streams would probably incorporate the assumption that small particles fill in the voids between larger (surficial) ones while rolling or saltating and thus form infilled structures (the simplest type of closed structures). This does characterize the Seale's Brook bed but the filling of the voids is invariably incomplete (Figures 3.8 and 3.20). In other words, the surface layer is characterized by an internal relief rather smaller than the c-axis of the coarser constituents. This is usually not the case in sand-bed streams, where bedforms (e.g., ripples or dunes) are

Recovered Particle No.	<b>`-</b>	54 <sup>(1)</sup>
Weight	-	372.63 gm
Distance of Transport	-	41.18 m
Sphericity $(\sqrt{bc/a^2})$		0.39
Shane (c/a)	-	0.26
local Slope	-	0.012
b-axis	-	70.8 mm
a-axis	-	123.0 mm
c-axis	-	32.1 mm
Cr. Sec. Location*	-	160.40 cm

<sup>\*</sup> see explanation to Table A.2

- (2) steep (bankward) flank deposits
- (3) shallow flank deposits associated with increased roughness on the vegetated patch of raised ground

Figure 3.17: Low and high-angle flank deposits of a side channel.



longitudinal location

6

Recovered Particle No.	-	7 <sup>(1)</sup>	· K91.4
Weight	-	A 3.10 gm	
Distance of Transport	-	126.48 m	
Sphericity $(\sqrt{bc/a^2})$	-	0.57	
Shape (c/a)	-	0.38	
Local Slope	-	. 0.036	
b-axis	_	15.4 mm	
a-axis	-	18.2 mm	
c-axis	-	7.0 mm	
Cr. Sec. Location*	-	50.30 cm	

<sup>\*</sup> see explanation to Table A.2.

(2) right-hand part of an imbricate structure

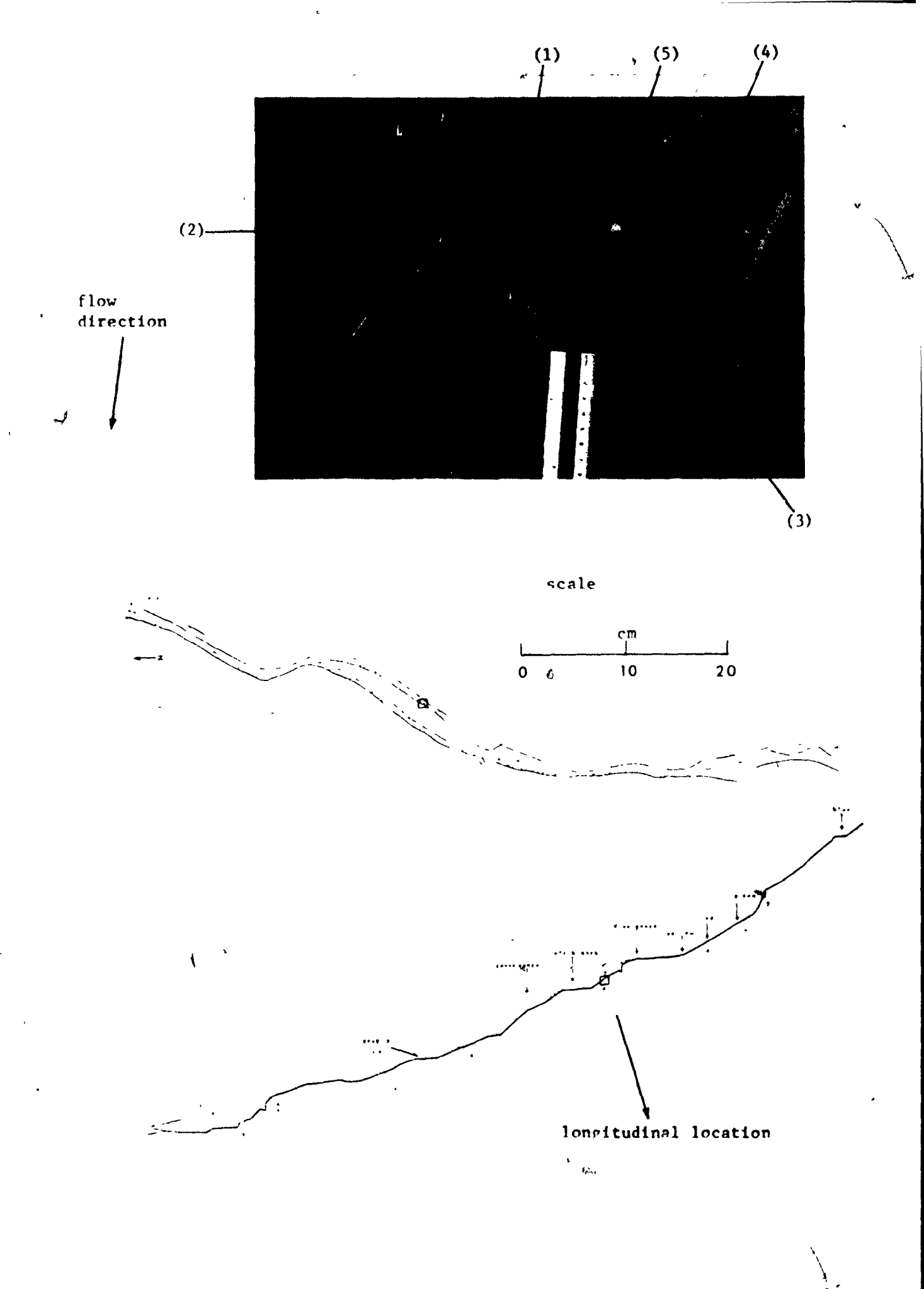
Figure 3.18: Flat deposits and open structures. Note that the structure shown in this part of the bed is not completely open; several aggregates of particles are, indeed, characterized by an infilling of interparticle spaces. Water depth is, on average 10 cm.

larger than the average particle size by one and, more often, two magnitudes. Bedforms in this latter sense are restricted in Seale's Brook to the few islands, some of the larger transverse ribs and those exceptionally large boulders found in every stream locale.

Very small particles most probably fall into hollows, rather than having been there in the first place, either by rolling and/or sliding over the large upstream particle, or by leaping in saltation. The arrangement of few small particles in between larger ones tends to be very tight, i.e., it is rather difficult to dislodge the particles, especially the small ones, without previously destroying the complete structure. When some small particles of infilled tight structures are disk-shaped, as they often are on the bed of Seale's Brook, their a/b planes tend to dip vertically (see Figures 3.10, 3.11, and 3.15). This increases the rigidity of the structure because the very finest involved particles can easily fall and settle in between flat ones (Figure 3.21).

Tight structures may be caused by a relative movement between the coarser particles (the downstream particle would, on average, move more slowly, being partly protected from the flow by its upstream counterpart). They may also be caused by a wobbling motion of the finer material (with which, in a different context, Einstein (1942) associated incipient motion) causing the smallest particles to settle further and thus tighten the structure. Tight structures are depicted in Figures 3.10, 3.11, 3.15, 3.16 and 3.20 - 3.22.

Closed, tight structures, are sometimes restricted to intermediate and large particles and then form imbrication. Imbricate (shingle block or roof-tile) structures are quite widespread on the channel beds of all coarse-bedded streams. Well-developed imbrication covers roughly 10 percent

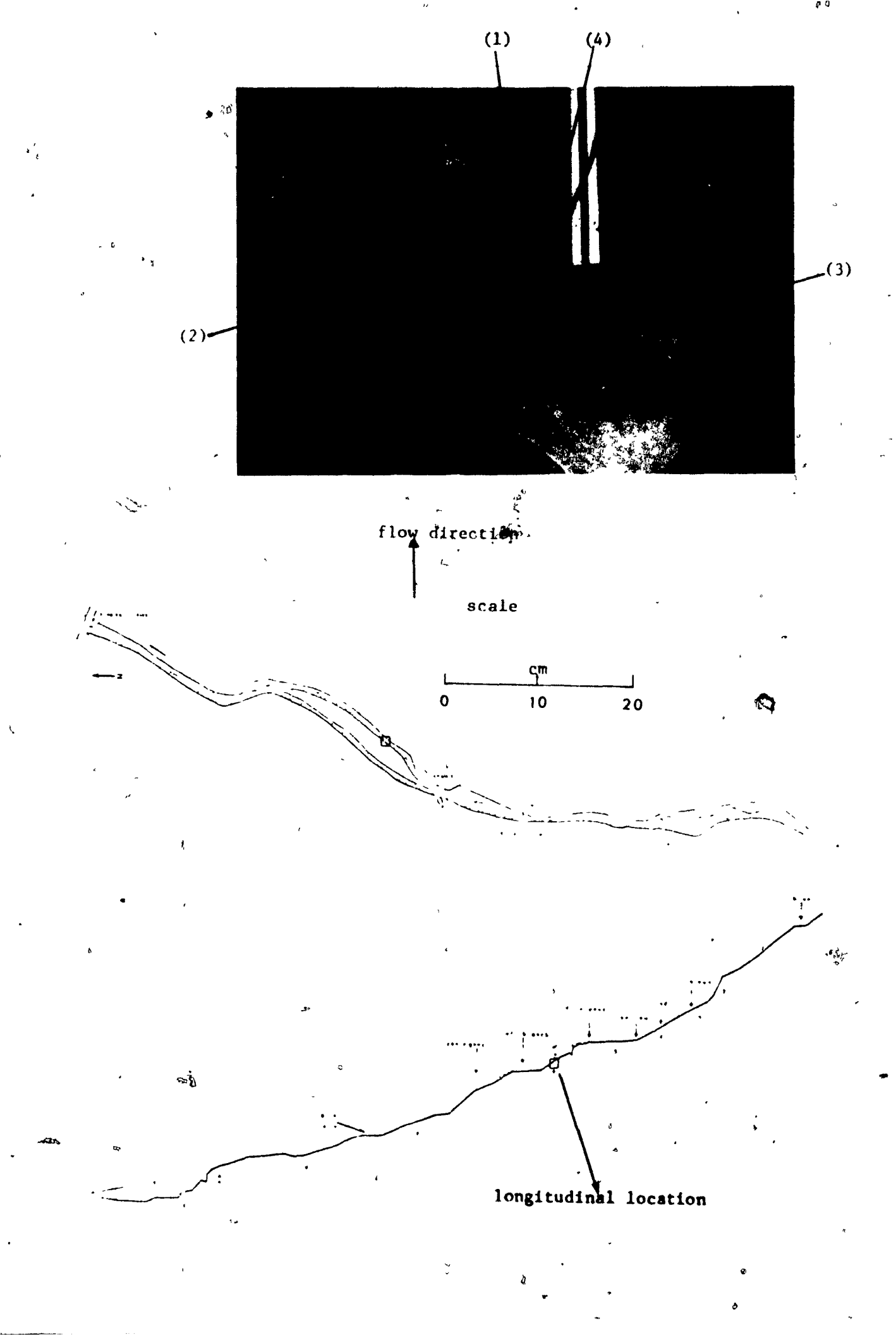


Recovered Particle No.	~	18 <sup>(1)</sup>	
Weight	~	0.96 gm	
Distance of Transport	-	64.32 m	
Sphericity $(\sqrt{bc/a^2})$	-	0.49	
ېنې Shape (c/a)	-	<b>0.30</b> °	
Local Slope	~	0.026	
h-axis	**	9.9 mm	
a-axis	***	12.3 mm	<u>ٿ</u> ر
c-axis	-	3.7 mm	
Cr. Sec. Location*	-	25.30 cm	5

<sup>\*</sup> see explanation to Table A.2.

- (2) open structure
- (3) lee-side deposits
- (4) infilled structure
- (5) tight, vertically infilled structure

Figure 3.19: Closed structures and partial infilling of interparticle voids. Notice that none of the spaces between large particles is filled to the brim...



Recovered Particle No.	` <del>-</del>	48 <sup>(1)</sup>
Weight		0.85 gm
Distance of Transport	-	253.15 m
Sphericity $(\sqrt{hc/a^2})$	-	0.24
Shape (c/a)	<del>-</del>	0.11
Local Slope	_	0.032
b-axis	-	12.6 mm
a-axis	<del>-</del>	20.8 mm Z
c-axis	<b>-</b>	2.4 mm
Cr. Sec. Location*		110.40 cm .
·		* •

<sup>\*</sup> see explanation to Table A.2.

- 2) partly developed imbrication
- 3) vertically infilled tight structure
- 4) tight structure in part of which the filling material is vertically inclined

Figure 3.20: Tight, incompletely-filled structures.

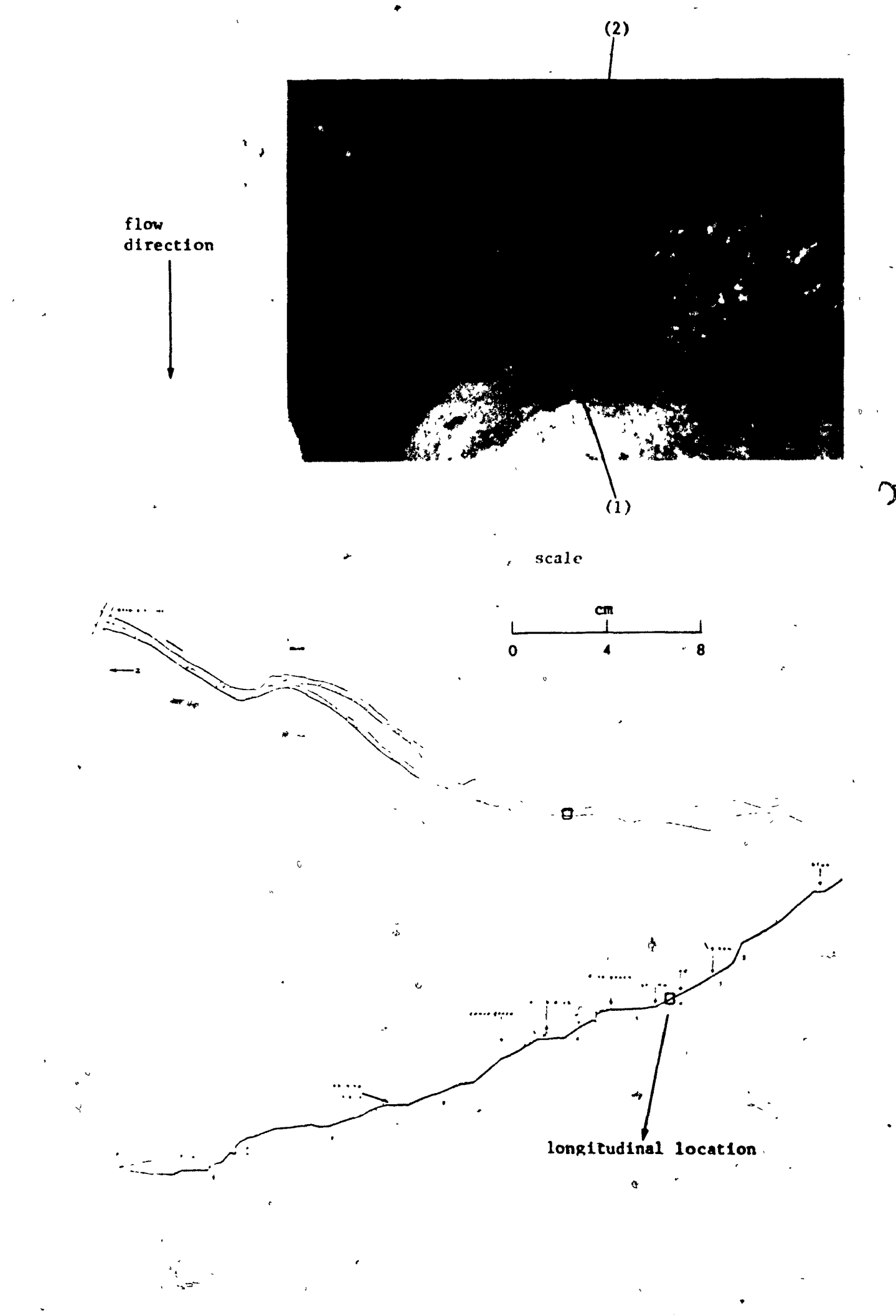
of the bed area but partly-developed imbrication is so common that it is rare not to see it everywhere, except in portions of the bed that are mostly covered with gravel. Well-developed imbrication is especially widespread in the small 0.5 - 1 m wide tributaries, probably due to the more areally-restricted turbulence and the dominant part of rolling in bedload movement.

43 ,

0

Tight structures referred to as 'imbricate' are characterized by pebbles and larger-sized particles successively leaning upon each other, commonly on a contact surface rather than on a contact point, and dipping consistently upstream. Helley (1969) and Lane and Carlson (1954) commented on the regular upstream dip of most coarse particles (i.e., on the pebble-shadow feature seen when looking upstream at the channel bed). Well-developed imbrication is shown in Figure 3.23 and others can be detected in the bed areas shown in Figures 3.10, 3.15, 3.16, 3.19 and 3.22.

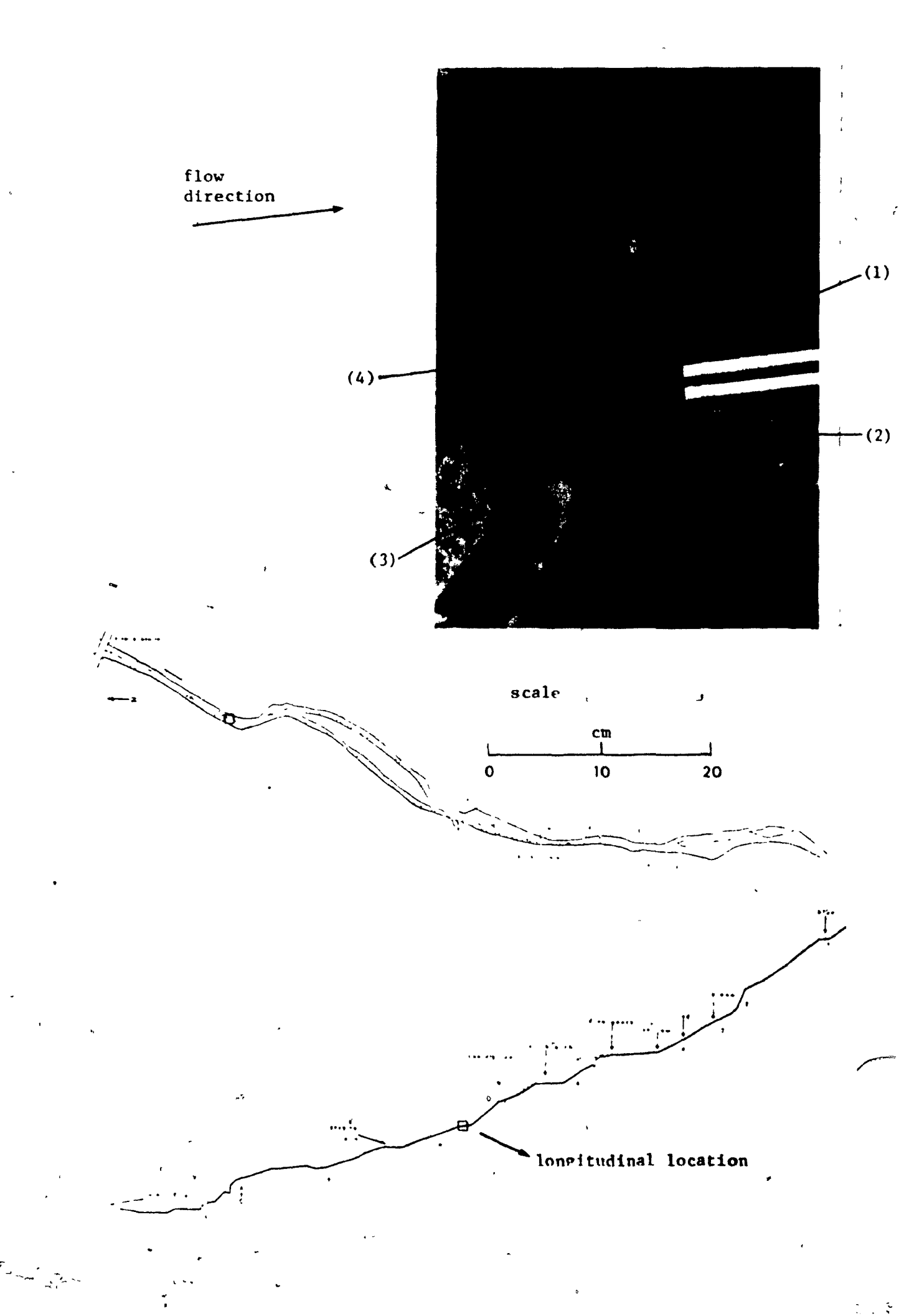
Because imbricate structures are characterized by upstream dipping particles of a very definite lower size limit (about 60 mm), their formation can only be explained by the rolling and sliding motion of bed fragments. When a coarse particle lands on a finer medium, it increases the turbulence immediately upstream of it whereby finer material underlying its upstream side is entrained and the coarse fragment sinks backwards, dipping upstream (Figure 3.19). This sinking phenomenon, on a sand bed, has been reported by Fahnestock and Haushild (1962). Any other platy particle, similar in size to the one already dipping upstream, will tend to stop its rolling/sliding motion on contact with the former, also dipping upstream. The same mechanism probably applies to particles of



\* see explanation to Table A.2.

(2) gravel particles in the tight, vertically infilled structure

Figure 3.21: The role of gravel particles in increasing the stability (or interlocking) in tight structures. Water depth in the left-hand part of the photograph is 6 - 7 cm deep.



Recovered Particle No.	-	93(1)
Weight	-	0.37 gm
Distance of Transport	-	194.68 m
Sphericity $(\sqrt{bc/a^2})$	-	0.33
Shape (c/a)	`-	0.20
Local Slope	-	0.009
b-axis	-	6.7 mm
a-axis	-	11.7 mm
c-axis	-	2.3 mm
Cr. Sec. Location*	-	260.10 cm

<sup>\*</sup> see explanation to Table 4.2.

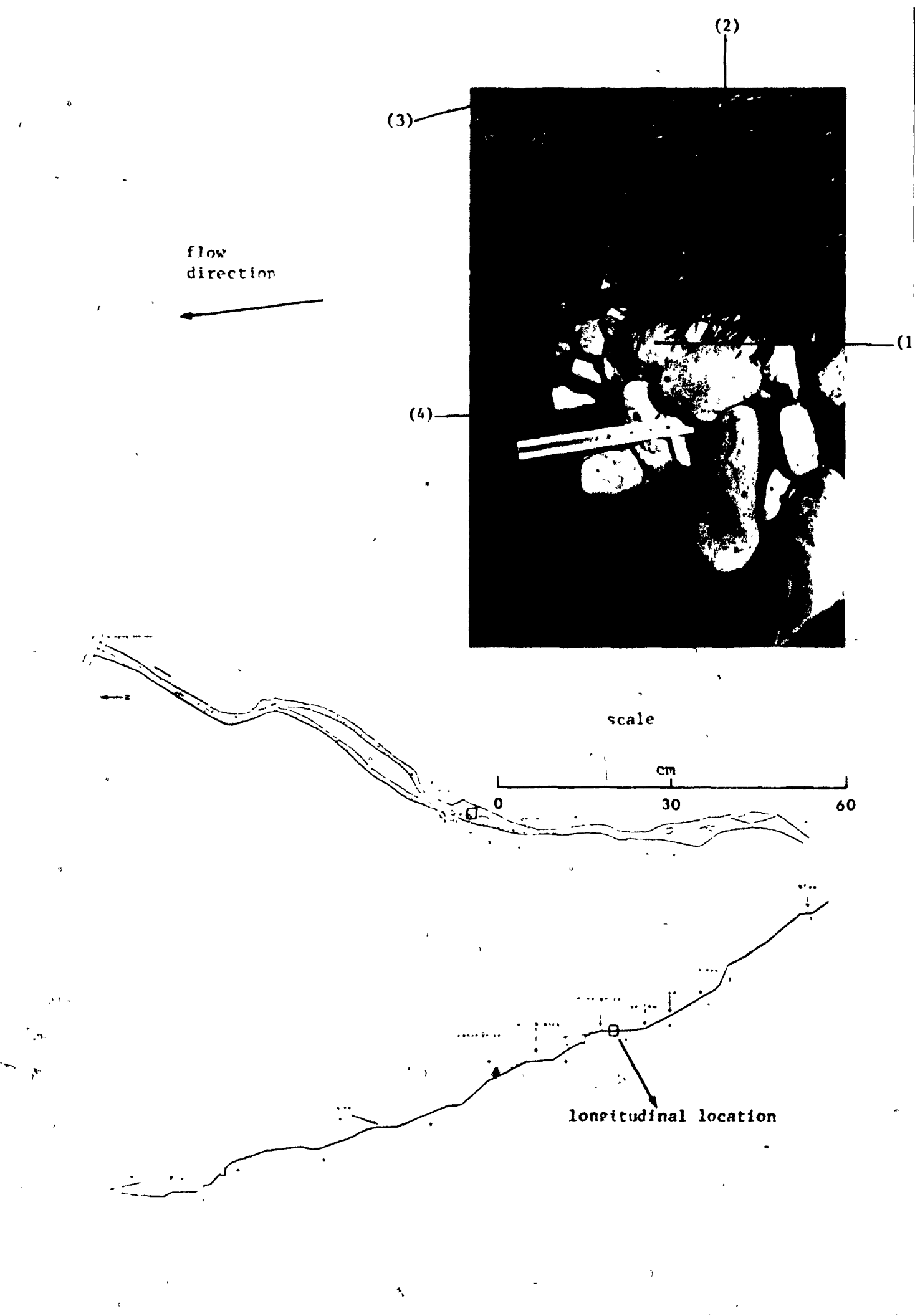
- (2) increased stability of the surface 'layer' due to infilling with fines
- (3) well-developed imbricate structure
- (4) partly-developed imbricate structure

Figure 3.22: Well-developed and partly-developed imbrication.
Water depth in the upper left-hand part of the photograph is roughly 4 cm.

other shapes, although structures of equant-shaped fragments are only partly-developed. Because gravel is often transported in saltation, or even in suspension, it will not construct such structures. In fact, few pebbles and still fewer gravel-sized materials have been observed to orient themselves with an upstream inclination.

Whether the closed arrangement of particles on the bed is an imbricate, partly-developed imbricate or any other type of tight structure, it is clear that forces greater than the submerged weight of the particles are needed to entrain bed fragments involved in these structures. This is especially pronounced in vertically-infilled tight structures, where initiation of motion of any of the particles is presumably associated with the destruction and entrainment of the whole structure. It is, however, also possible that all these structures remain stable on the bed and that particles are entrained sequentially, beginning at the upstream end of the structure. However, even in this latter case the entrainment of individual particles depends on the entrainment of the one furthest upstream, which may be very stable.

Measurements have been made of the minimal force needed to stir pebbles, cobbles and boulders in stable structures (vertically infilled and imbricate) on the bed. Two sizes of C - shaped clamps were used as a means to attach a dynamometer to a particle. The moving parts of the clamps (which held the particle) were edge-sharpened screws which, when tightened, drilled two minute holes in the particle to avoid slipping. Several methods were used in order to move the fragment. The applied force was directed vertically, horizontally or parallel to the inclination of the particle. It was immediately apparent that the dynamometer was very inaccurate for horizontal measurements. Moreover, when the applied



Recovered Particle No.	- '	171 <sup>(1)</sup>
Weight	-	1320.90 gm
Distance of Transport	-	33.43 m
Sphericity $(\sqrt{bc/a^2})$	-	0.37
Shape (c/a)	-	0.23
local Slope	-	0.006
b-axis	-	126.5 mm
a-axis	-	201.3 mm
c-axis	-	46.5 mm
Cr. Sec. Location*	-	290.10 cm

<sup>\*</sup> see explanation to Table A.2.

- (2) vegetated patch of raised ground. Notice the small, transversely aligned channel and the general fine composition of the material.
- (3) left-hand part of the bed of a side channel
- (4) well-developed imbrication of large cobbles; at least 7 large particles are seen to comprise this structure

Figure 3.23: Well-developed imbrication. Water depth in the lowermost, left-hand part of the photograph is at least 15 cm.

	Recovered Particle No.		-	171 (1)
	Weight		-	1320.90 gm
	Distance of Transport		-	33.43 m
	Sphericity $(\sqrt{bc/a^2})$		•	9.37
	Shape (c/a)		-	0.23
•	Local Slope		-	0.006
	b-axis		-	126.5 mm
×	a-axis		- ,	201.3 mm
	c-axis	0	-	46.5 mm
	Cr. Sec. Location*		-	290.10 cm

<sup>\*</sup> See explanation to Table A.2.

- (2) veretated patch of raised ground. Notice the small, transversely aligned channel and the general fine composition of the material.
- (3) left-hand part of the bed of a side channel
- (4) well-developed imbrication of large cobbles; at least 7 large particles are seen to comprise this structure

Figure 3.23: Well-developed imbrication. Water depth in the lowermost, left-hand part of the photograph is at least 15 cm.

force was directed upwards, it ultimately rotated the particle before or during its dislodgement, instead of raising it vertically. This necessarily made the measurement very inexact and quite meaningless. third method, applied to 5 particles, proved to be more useful. measurements were attempted on 100 different particles; 4 and 2 were successful (in that there was sufficient time to take the exact reading and no slipping or rotation of the particle took place) when applied vertically and parallel to the inclination of the particle respectively. Some of the unrecorded measurements were, however, successful, in that they qualitatively showed the strength of the structures. The data of Table 3.2 demonstrate the magnitude of the effect of these structures on initiation of motion. Taking  $\rho_{\rm g}=2.6$  (where  $\rho_{\rm g}$  is mass density of the particle, an average from a sample of 10 particles whose specific gravity was determined in the laboratory), the ratio of this force (probably still smaller than the actual force needed to initiate motion) to the submerged weight of a particle ranges from 1.8 to 6.1. Although this topic needs additional data to derive more accurate estimates of forces, the meager number of measurements presented herein show that this force is significantly larger than the particle's submerged weight (at 90 percent confidence interval). Moreover, the inherent interlocking friction of imbricate structures is usually augmented, rather than weakened, by water pressure on the upstream faces of the structures (Figure 3.24).

All in all, the observations mentioned in this chapter show that beds with a wide variability in calibre of bed-material have definite and systematic structures and forms. Obviously, these are interrelated with processes and specifically with bed-material transportation. Chapter IV,

Comparison between the Force Needed to Move a
Particle and its Submerged Weight

Applied Force Weight		Weight	Submerged Weight (p=2.6)
	1Ъ	1b	. 1ь
(+)	1.1	0.3	0.2
(+)	4.6	4.2	2.6
(+)	5.8	. 3.6	2.2
(+)	24.0	18.5	11.5
(I)	15.5	8.5	<b>5.4</b> ,
( )	11.0	2.9	1.8

<sup>(†)</sup> vertical pull

<sup>(||)</sup> pull parallel to particle inclination

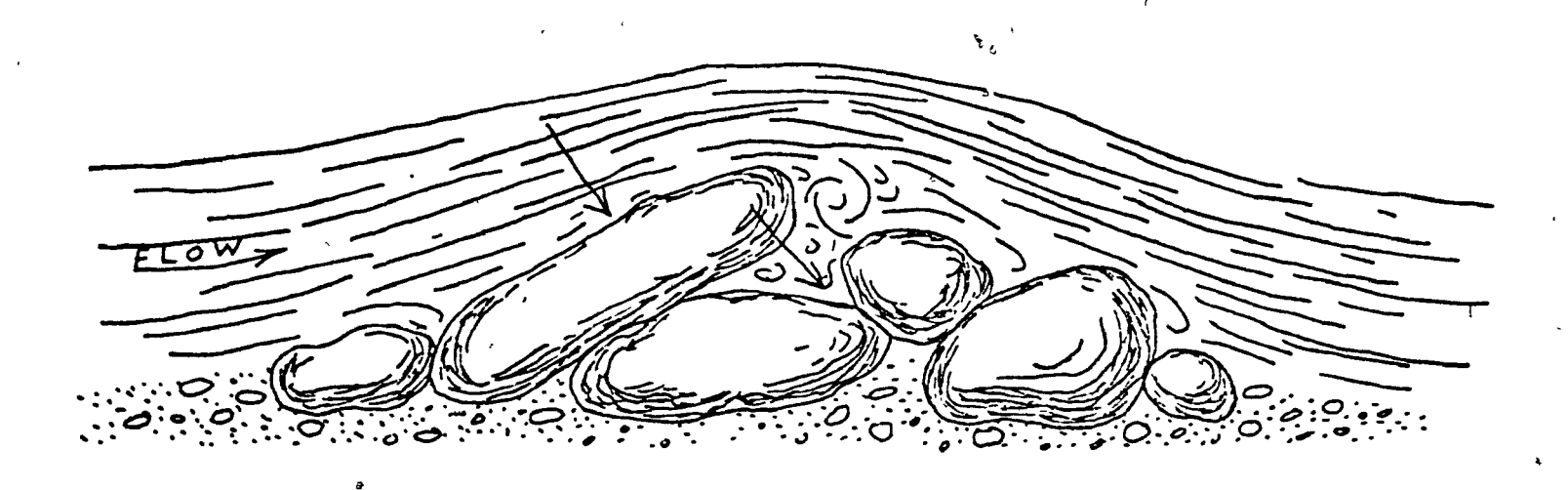


Figure 3.24 Augmentation of friction in imbricate structures (from Lane and Carlson, 1954).

dealing with coarse bed-material transportation, is written in an attempt to emphasize that an understanding of this interdependence is a prerequisite to any sound and well-founded approach to bed-material movement.

#### CHAPTER IV

#### OBSERVATIONS ON BED-MATERIAL MOVEMENT IN SEALE'S BROOK

Distance of transport of labelled bed-material can, when interpreted with care, be of much help in understanding transport processes.

The larger this distance, the greater the mobility of the particle.

Particle mobility is an indication of initial instability and duration and velocity of movement. Thus, although stability, transport duration and velocity cannot be evaluated separately from the distance of transport in a single flood, their combined effect is expressed by it.

## 4.1 <u>Collection and Preparation of Material</u>

The entire bed of Seale's Brook was covered during the winter of 1971 - 72 by a thick (0.3 - 0.6 m) veneer of ice, so that a different, but nearby, source of material was selected. Several thousand particles 4 - 256 mm in diameter were randomly picked from a portion of the bed of the North River, about 100 m downstream of its confluence with Seale's Brook. The material was washed, dried and divided into size classes from which four almost identical size distributions were assembled. Each of these was sprayed with an oil-based paint and altogether four different colours (yellow, red, green and blue) were used. Four sections were chosen in early spring wherein particles would be placed. Here, the choice depended on local bed slope and on the character of the surface layer, mainly particle size. The location of the cross-sections is shown in Figure 3.2. It was decided that the coloured material should be placed on the bed at different times in order to examine the effects of daily floods of different intensity. Date and time of particle emplacement are shown on

Figure 3.1a.

Over 20000 particles were picked from different Seale's Brook bed areas in the early spring of 1973. The treatment given to this material was identical to the one of the former year and it took altogether two weeks to prepare each of the yearly samples. Because recovery rates of 1972 labelled bed-material (see section 4.3) decreased with decrease in particle size and with increased bed roughness, the 1973 material was divided into 3 similar groups and one much larger, so that the size distribution of each group changed to a great emtent. The 1973 material was placed at or near the locations used in the former year, and inserted on March 26, 1973.

### 4.2 Disposition of Coloured Particles

Each sample of particles of a specific colour was placed on the stream bed in the following manner. The finest were disposed of first, gradually placing larger particles up to (but excluding) the coarsest fraction (180 - 256 mm). Each size group was placed about 0.1 m upstream of the preceding smaller particles. Most particles were swept a short distance downstream and altogether, the newly deposited material formed an incomplete cover and was spread downstream (especially the—smaller fragments) throughout the whole channel width for about 2 m. Because of the icy cold water, it was impossible to place the particles on the bed in structures similar to the ones most-often encountered in the studied reach. Instead, the material was either dropped at water level (in 1972) or randomly placed on the bed (in 1973), but always covering the entire channel width. Moreover, the spacings of labelled particles in each size group and for all sizes was much the same for each colour group.

The large cobbles were placed on the bed in the centre of the channel. Numbers, from 1 to 7, were previously painted on them and the initial location was such that the number increased upstream (i.e., the weight increased downstream). This was done so that their relative motion could be ascertained.

It was observed that most of the smaller introduced particles immediately disappeared between and underneath cobbles and boulders. As particle size increased, a greater percentage remained on the surface. However, it was evident that as particle size increased, particle stability (relative to the corresponding in situ ones) decreased. Thus, when several larger particles were accidentally stepped upon they moved or slid considerably, a phenomenon very uncharacteristic of the very stable bed of Seale's Brook. Another observation related to the newly-placed material was that as the percentage of coarser particles increased in a local bed area (roughly 1 m²), so the smaller labelled particles disappeared to a greater extent. When the latter were small enough, they usually disappeared between the jagged structures, and when they were large enough, they tended to roll or slide a bit and become immobilized on much finer material or, more often, on the stoss side of similar or larger particles.

Consequent to these observations, it must be realized that the transportation of the labelled bed-material was most likely uncharacteristic of the behaviour of the bed-material of the surface layer as a whole. Specifically, initiation of motion of the coloured particles conceivably commenced prior to one of their in situ counterparts. For this reason, it would be dangerous to attempt a calculation of actual bedload rates from the distances of travel of the coloured material. At

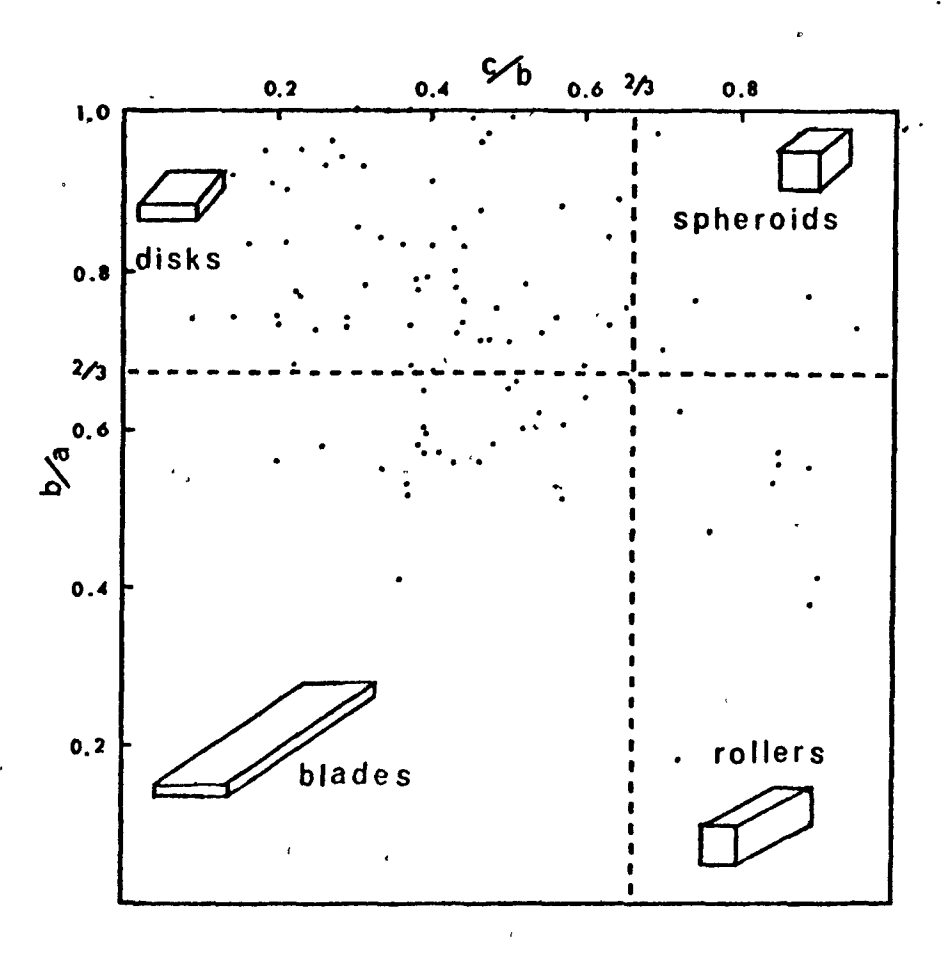


Figure 4.1 Zingg diagram depicting shapes of 100 particles of the surface layer of the reach immediately upstream of the divergence.

the same time, the variability in distances of travel in terms of particle characteristics and the post-movement locations of these particles in relation to channel morphology has yielded useful information relating to bed-material transport.

Although some difference between introduced and original materials does exist, specifically structure-wise, the transportation of the former during several flood events is, for all practical purposes, quite characteristic of the whole bed area of the specific reach.

Labelled particle characteristics are essentially identical to those of the bed (the data of Figure 4.1 show that the introduced particles have shapes very favourably compared with the ones of the original bed, shown in Figure 4.1 and the data for which are summarized in Table A.1). Once the labelled material had been transported it was deposited in stable structures identical to those characterizing the non-labelled material. Thus, the labelled particles became an integral part of the channel, and in the following transport periods they were, if recovered, a random sample that provided information on bed-material transportation.

# 4.3 Recovery Rates of Labelled Bed-Material, Spring 1972

Of the 4823 coloured particles placed on the channel bed prior to and during the spring floods of 1972, 242 (or 5 percent) were recovered. The data on number of particles introduced, number recovered and percent recovery for each colour group and size group are listed in Table 4.1. With a single irregularity introduced by the small number of recovered blue particles in the 64 - 128 mm range, percentage recovery decreases drastically with decrease in particle size and ranges from 100 percent for 3 of the 4 coarsest cobble groups to 0.5 - 1.0 percent for gravel. The recovery rates of the green, red, and yellow coloured

Number of Labelled Particles Placed on the Bed, Number Recovered and Recovery Rates for each Colour Group, Seale's Brook, 1972.

Size (b-axis)	No. introduced				No. recovered				<u> </u>	Percent recovery					
(men)	<u>Y</u>	R	- G	В	T	Y	R	G	В	T	<u>Y</u>	R	G	В	T
4-8	510	610	635	670	2425	3*	5*	3*	7*	18	0.6	0.8	0.5	1.0	0.7
8-16	406	361	376	453	1596	12	17	24	6	59	3.0	4.7	6.4	1.3	3.7
16-32	110	108	112	136	466	14	13	17	4	48	12.5	12.3	15.2	2.9	10.3
32-64	53	53	53	53	212	13	18	13	5	49	24.5	34.0	24.5	9.4	23.1
64-128	24	24	24	23	95	12	18	8	2	40	50.0	75.0	33.3	2.1	42.1
128-256	7	7	8	7	29	7	7	9 <b>*</b>	5	28≉	100.0	100.0	100.0*	71.4	96.6‡
Total	1110	1163	1208	1342	4823	61	78	74 <b>*</b>	29	24 <del>*</del>	5.5	6.7	6.1	2.2	5.0

Y - Yellow particles

R - Red particles

<sup>&#</sup>x27;G - Green particles

B - Blue particles

T - Total

<sup>\* -</sup> all but one have b-axis <6.6 mm

 $<sup>\</sup>frac{*}{*}$  - one particle had split in two

particles (originally placed in the three lowest cross-sections) in all size ranges, and in terms of total recovery, are essentially alike. However, there is a statistically significant (0.05) difference between the number of recovered yellow and blue particles, even though the actual number of yellow particles first placed on the bed was the smallest and the one of the blue the highest (see Table 4.1). This difference in recovery rates is somewhat more pronounced between the blue and the green or red particles.

The question arises as to the reason for this difference between the blue and all other particles. It was observed that neither the blue nor the green colours were very practical in terms of ease of detection. However, in this respect, both colours were very similar. Moreover, all colour coatings abraded by about the same amounts. Some particles (mostly in the coarse gravel size range) maintained their complete coating, others of all colours lost 50 - 80 percent of it, but approximately 200 particles retained as much as 80 percent of the paint.

By way of elimination, the only alternative which may explain the differences in recovery rates is burial or rather, selective burial. It has been found (see Figure 4.14) that in terms of particle size, Seale's Brook bed-material is made of two different populations - a coarser surface layer and an underlying, finer material. The finer material must have attained its buried position by some mechanism other than falling into large interparticle spaces, simply because it is actually buried beneath the surface. Fine material either remains in its deep-seated location, even when being transported, by moving as part of a sheared array of solid particles (where the smallest are always furthest from the surface),

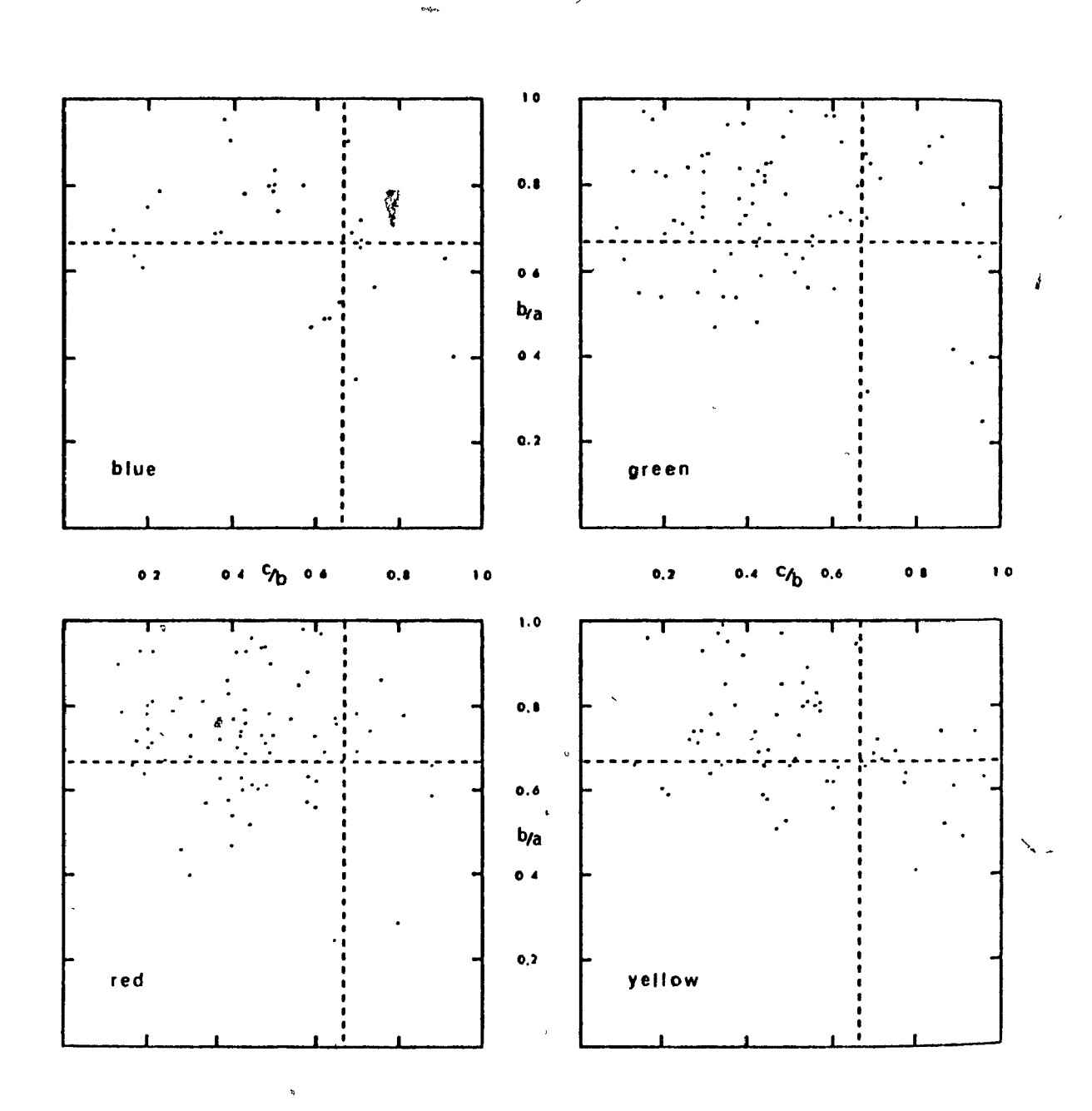


Figure 4.2 Zingg diagrams depicting the shapes of the 242 recovered particles.

and/or by being gradually covered by larger fragments of the bed-material, the latter rolling and sliding quite independently of the finer, wherein, with cessation of movement of the coarser fractions, most of the fines are buried.

Whatever the exact nature of the burial process, fine material incorporated in a coarse surface layer of a stream bed will undoubtedly be buried to some extent with activation of the layer. The finer the newly incorporated material when compared with the original one, the greater will be the burial of the former (also supported by observations on disposition of labelled materials, section 4.2). This probably explains the difference in recovery rates between the blue and all other coloured particles because of the markedly coarser character of bed-material in the 'blue' reach (see section 4.6a).

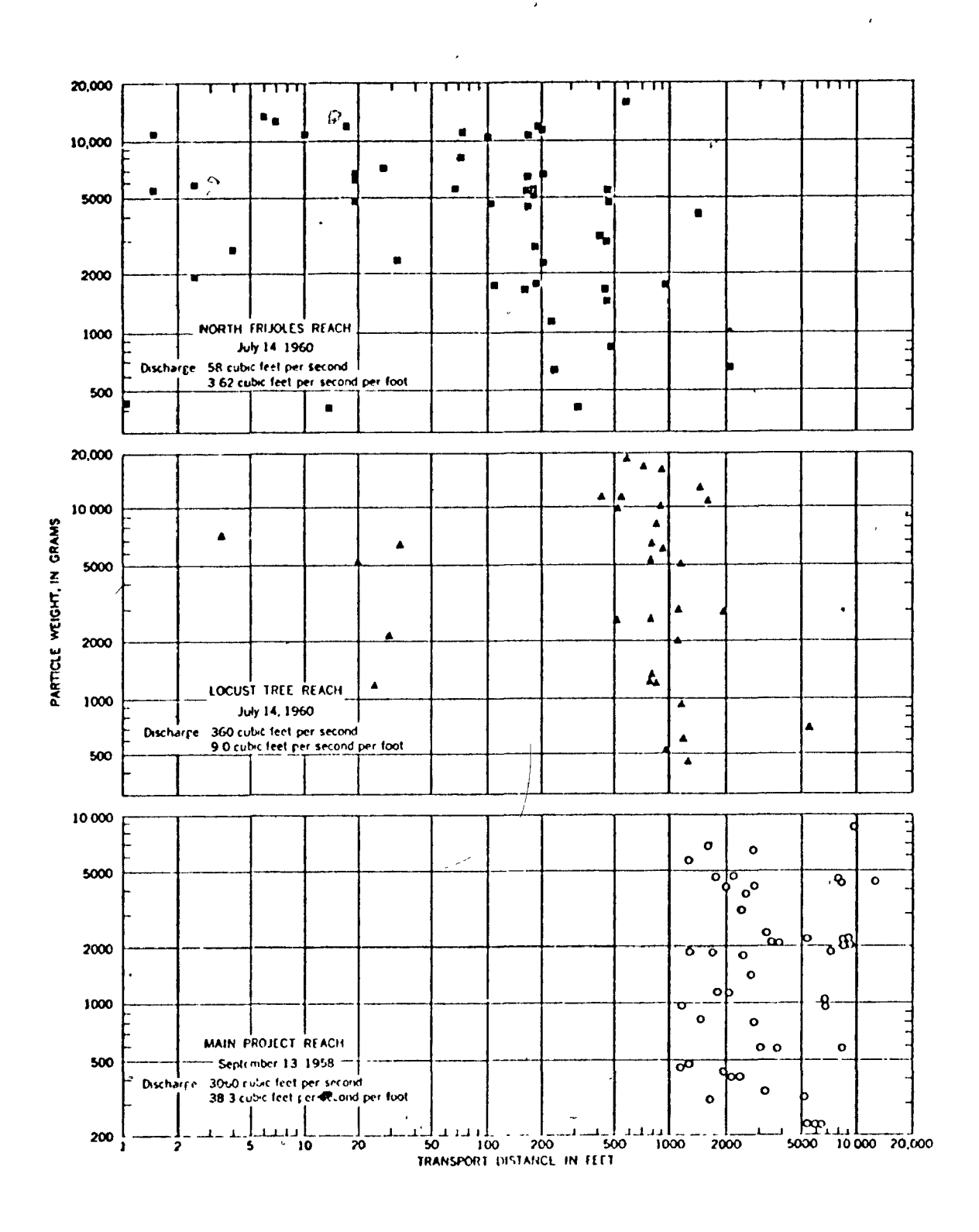
The green, red and yellow particles were placed on the bed at different times (Figure 3.1a) with two considerably large flood peaks intervening. Nevertheless, the total recovery rates of all three are much alike. The initial instability of the newly-placed material has already been considered. Because the three recovery rates are so alike, it is inferred that the main effect of the April 19 - 20 floods on the yellow and blue fragments was to transport them to more stable positions while most of the bed-material remained essentially immobilized (see the table on Figure 4.16). Had there been a general mobility during these two early floods, much smaller recovery rates of yellow particles would have been anticipated. The reason for this is that it has already been shown (Sayre and Hubbell, 1965) that with time, dispersion of labelled bed-material becomes more homogeneous with depth in the bed and also with distance from the source. The relevance of

Sayre and Hubbell's conclusion in this context is that, with time, the number of labelled particles on the surface of the bed decreases due to their simultaneous enrichment in more deep seated layers. This conclusion is applicable to sand-bed streams and for the finer fractions of altogether coarse bed -materials. However, the coarser particles, whether labelled or not, will tend to remain unchanged in their predominance on the surface. This has also been demonstrated to hold in ephemeral channel beds, where the percentage of coarse materials is much smaller than in Seale's Brook (Leopold et al, 1966). Data from this same study also show that recovery rate decreases as cobble size diminishes.

The striking decrease in recovery rate with decrease in particle size is a result of the modes of transportation of different sizes of bed-material. Admittedly, it could be maintained that low recovery rates of small particles is merely due to difficulty of detection. However, the channel bed of the whole studied reach was inspected very slowly and any particle which seemed to be painted (and there were many) was picked from the bed. A person who for half an hour studies a stream bed 5x5 m in area has had sufficient time to detect any labelled bed-material lying on the surface, including sand -sized particles positioned in relatively deep interparticle hollows. It is, indeed, believed that none, or at most very few coloured particles were left unnoticed in the surface layer (which does include the interparticle hollows where some fine material was detected - see Figures 3.20 and 3.22). In fact, the roughest, steepest and most upstream part of the studied reach was inspected with deliberate care. Still, very few small particles were recovered there. Additional

inspection of the studied reach upstream of the bridge revealed that the number of detected particles decreased very much with each inspection, and it was zero with the fourth and last. Moreover, because only 2 of the 242 recovered particles had been fractured, it is concluded that the decrease in recovery rate with diminished calibre is not due to fracturing of the fines to an extent whereby their detection is hardly possible.

It could also be assumed that large amounts of the smaller-sized particles were transported completely out of the brook. Nevertheless, the lower reach (extending from the North River and as far as the bridge) was also inspected with care. Two particles (red and yellow), about 10 mm in diameter, were indeed detected there on May 12th. However, labelled particles were first picked (and their distance of travel recorded) from the bridge going upstream, and by May 28th, the bed of the lower reach had been completely covered by a thin veneer of clayey deposits. No further detailed inspection of the lower reach was attempted. Figure 3.2 shows, however, that only 6 particles, of which none was a blue fragment, were found in the 50 m long reach upstream of the bridge. It is consequently concluded that distances of transport of different sizes of coloured bed fragments tend to have quite a well-defined upper limit although the absolute limit was not recorded. This tendency is also characteristic of the transportation of cobbles in several studied ephemeral channels (Leopold et al, 1966), as exemplified by Figure 4.3. Thus, although some very small particles may have been transported out of Seale's Brook, it is unlikely that their number was large. This inference does, however, indicate that (unlabelled) gravel-sized particles that originated in the lowermost reach were, to a large extent and especially during the rising



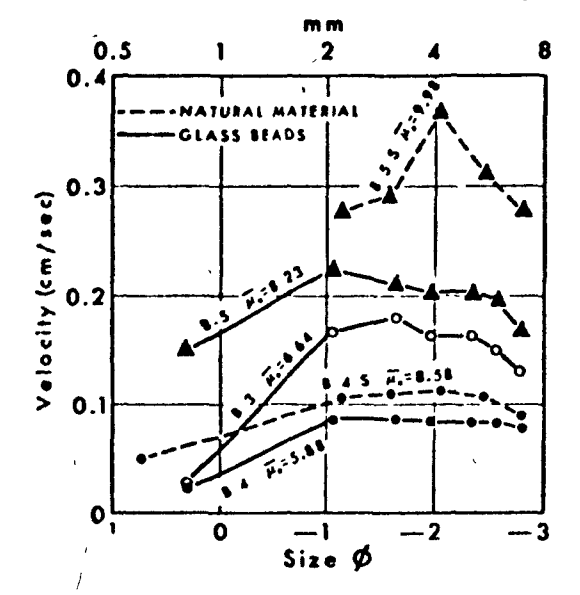
()

Figure 4.3 Transport distance of coarse particles as a function of particle weight, after Leopold et al, 1966.

stage, evacuated from the brook during the main spring flood of 1972.

Large particles were most probably transported only during the highest flood stages. This period of time depends on the magnitude and duration of the flood, on prevalent bed-material forms and structures as well as on the calibre of the particles concerned. For the flood of May 4 - 5, 1973, this duration was approximately 1 - 4 hours. It has been shown (Meland and Norrman, 1969) that highest particle velocities of bedmaterials with normal  $\phi$  size distribution (where  $\phi = -\log_2 (b - axis)$ ) are associated with particles in the intermediate size ranges (Figure 4.4a). For rectangular size distributions this is somewhat changed (Figure 4.4b). If one may assume that these relations also hold for coarser materials (these figures only relate to D < 8 mm), then low velocities in conjunction with short transport durations ascribed to very coarse particles may explain their relatively short distances of transport. The finest commonly-found (gravel-sized) particles of the bed-material also have low velocities according to Figure 4.4a, and the duration of their transportation is largely dependent on the mobility of the intermediate and coarse particles which, on cessation of movement, bury the fine material. Thus, it seems that the (practically-identifiable) limit to distance of transport depends on the average distance of transport of the intermediate sizes (down to about 20 mm in diameter or approximately 10 gm - see Figure 4.5) and on the distance of transport of the few and finest particles that managed to avoid too many stationary conditions induced by 'hiding' in interparticle hollows or by burial underneath larger bed fragments.

In conclusion, the data from Leopold et al (1966) and Meland and Norman (1969) are interpreted as supporting the view that the lower' recovery rates associated with smaller size fractions are not due to a



4.4a

4.4b

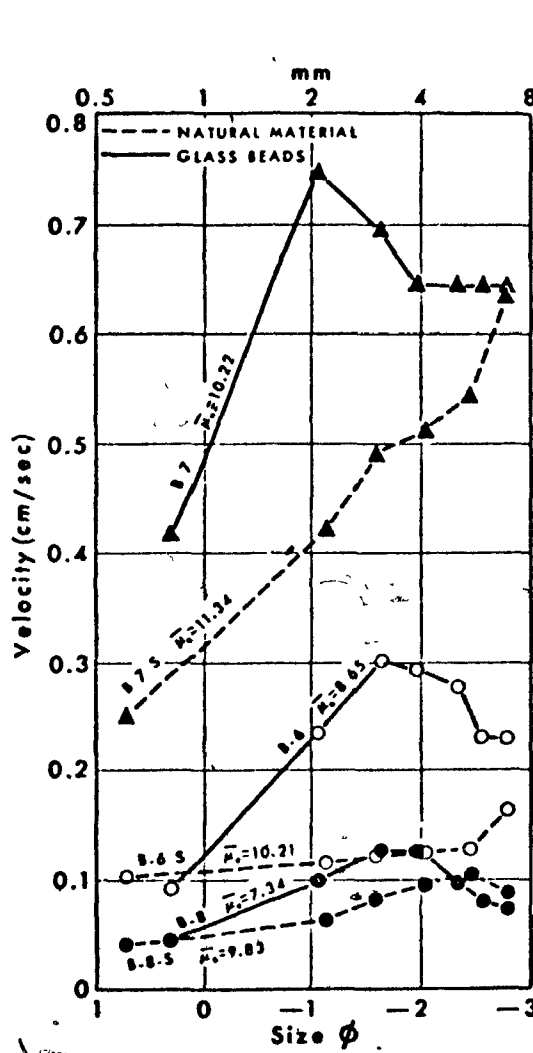


Figure 4.4: Particle size - particle velocity relations; normal (4.4a) and rectangular (4.4b) \$\phi\$ distributions, after Meland and Norman, 1969.

(

-----

complete removal of this material from the drainage basin but, rather, that burial of fine material is an important part of the transport processes of bed fragments of widely varying calibre.

Burial may be brought about in one of two ways. Bagnold's (1966) concept of a moving 'carpet' of bedload, a sheared array of non-uniform solid particles immersed in a fluid, may be one explanation. Here, deeper and slower moving layers of the 'carpet' are associated with smaller particles. The latter tend to remain buried during transportation. This results from the activated dispersive stress (proportional to the second power of particle diameter) which causes larger particles to remain on the surface. In another but similar transport mechanism, Bagnold's concept holds over restricted areas of the bed characterized by accumulations of fine bed-material. Large particles move over most of the bed area by rolling or sliding, quite independently of the smaller particles there which may roll, saltate or even become suspended between periods of entrapment and burial by larger bed fragments.

If all the bed-material, from sand to boulders, were alive and formed a 'carpet', the larger fragments would remain on the surface, which is also the fastest moving bed layer, and for all particle sizes, particle velocity would increase with size (this is also in accordance with Figure 4.4b). Now, because most of the finer bed-material is buried underneath the surficial bed layer, it is mobilized only after incipient motion of the intermediate and coarse particles has begun. Being slower, and having similar durations of transport, distances of travel associated with small particles would be shorter than those associated with coarse

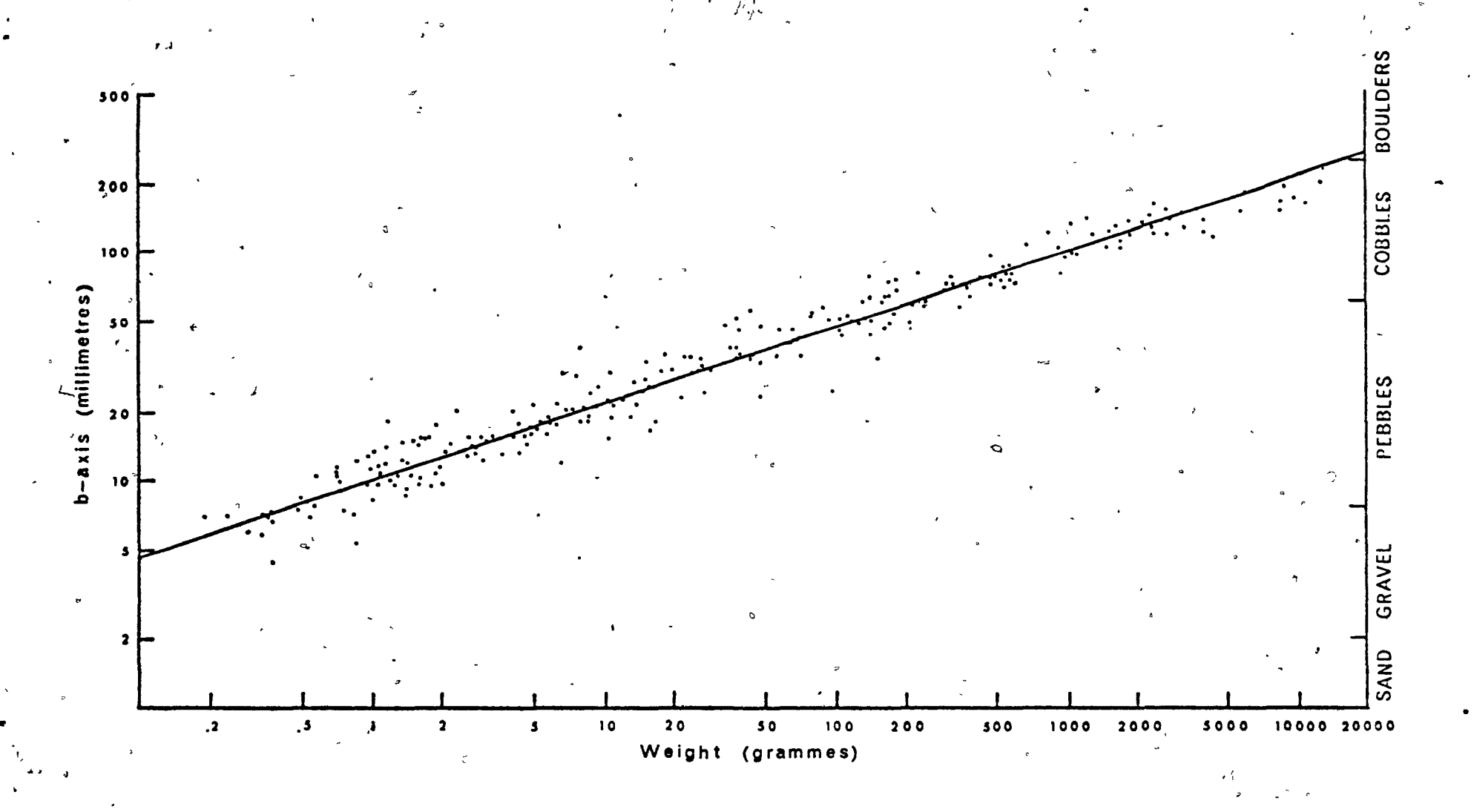


Figure 4.5 Particle diameter - particle weight relationship for the 242 recovered particles.

وموثاه

ones (i.e., distance of travel increases with particle size). This latter conclusion, based on Bagnold's own theory, is contradictory to data from this and other studies.

Burial may, however be brought about by a combination of Bagnold's concept and a 'carpet'-independent motion of large particles. Here, finer bed-material remains deep-seated in the bed due to the disperssive stress as well as by burial underneath rolling and sliding larger bed fragments. Small particles will not remain on top of larger ones for two reasons: Firstly, they will be very unstable. Secondly, and possibly more important, when small particles land on a larger mass (from saltation) the momentum is transferred almost entirely to the small particle. Moreover, small particles in motion will avoid large objects in their path simply because this is also the general direction of the streamlines. Their deposition will not occur on the stoss side of a protruberance because velocity there is greatest, and it will not occur in lee of it because the development of wakes will entrain them anyway. Thus, larger particles will tend to remain on the surface or, at most, will become partly buried on their stoss side.

## 4.4 Distance of Transport of Labelled Bed-Material

particles in the top layer was recorded. After a particle had been detected, its distance from the thalweg or, if the thalweg was unrecognizeable, its distance from the centre of the channel was measured with a graduated rod 1.7 m long. The accuracy of these measurements is about ± 5 cm. Because distances along the channel had been measured and marked prior to the collection of the particles, the same rod was sufficiently

long to determine the longitudinal location quite accurately. The absolute accuracy of measurement depended here on the distance from the source. The greater this distance, the lower the accuracy. The relative accuracy remained constant at about ± 1 percent. Most of the recovered particles were photographed before being collected and brought to the laboratory. No measurements were made on labelled bed-material introduced in the channel in 1973 because all of it, except the smaller, gravel sizes, remained immobile during the whole spring and early summer periods. In fact, it is very probable that most or all of the distance of transport of the gravel resulted while the material was carried to more stable localities or merely transported because it was left suspended 1 - 2 cm above the bed.

Measurements of several parameters of the recovered particles were undertaken. These included particle weight, a, b and c - axes, specific gravity and roundness. The data on particle roundness are incomplete and are not presented here; assessment of roundness is somewhat subjective, especially because most of the particles have similar roundness coefficients of 0.65 - 0.85. The specific gravity of 10 sampled particles varied from 2.48 to 2.71.

Particle weight was measured with three different scales with capacities of 160, 1200 and 28000 gm and accuracies of ± 0.001, ± 0.01 and ± 1.0 gm respectively. Thus, accuracy of weight exceeded 0.1 percent. The particles were weighed after having lost most of their water content by allowing them to dry for one month at room temperature. A test was also conducted to evaluate the amount of remaining water content by drying several particles of all size ranges in an oven for one day.

Results of Stepwise Regression - Correlation Programme:

Correlation Matrix

	RYX	RYA	RYB	RYB'	RYC	RYZ	RDA	RDB	RDB 1	RDC	RDZ -
yellow	-0.39	+0.78	+0.43	+0.15	*	*	+0.83	+0.27	*	*	+0.14
æed	-0.39	· +0.60	*	*	*	*	-0.19	*	*	+0.11	+0.11
green	-0.58	+0.63	+0.22	+0.12	*	*	+0.32	*	-0.14	+0.16	+0.12
blue	-0.76	+0.24	-0.32	-0.39	*	*	*	*	*	*	*
all colours	-0.47	+0.27	* ,	+0.27	*	*	*	*	*	+0.10	+0.11

- Y log(distance of transport)
- X log(weight)
- A average slope of the reach through which the particle was transported
- B local bed slope

- Z sphericity  $(bc/a^2)$
- C shape (c/a)
- \* smaller than |0.1|
- D Y predicted(Y)<sub>x</sub>

Their dry weight decreased on average 0.5 percent.

Axis length was measured with engineering calipers accurate to 0.01 mm. The axes of the coarsest particles were measured with a ruler of 0.5 mm scales. In addition, two particle shape factors were calculated. These data are presented in Table A.2 of the Appendix.

Data on distance of travel of each recovered particle, its cross-sectional location and weight, local slope of the bed where it was detected and the ratio local slope/average slope are also incorporated in this table.

A regression correlation programme was run to determine the dependence of distance of transport on particle weight, shape (c/a), sphericity ( $\sqrt{bc/a^2}$ ), average and local (5 - 20 m channel length) slope and the ratio local slope/average slope were determined. The correlation of each of these with the distance residuals, from the regression of log(distance) versus log(weight), was also determined and the results are given in Table 4.2.

The most obvious conclusion, also supported by Keller's (1970) data, is that there is no relationship between particle shape and distance of transport or its residuals. It would seem from the data matrix of Table 4.2 that distance of transport is highly dependent on average slope, but these correlations are merely different means of describing the longitudinal profile. The importance of slope could not be evaluated from these relations but a longitudinal profile (Figure 4.6) indicating the location of recovered particles by size class does show that there are patches where particles tend to be deposited. This could indicate that there are 'stable' environments in the macromorphology similar to the stable structures in the micromorphology. However, it is very likely that the

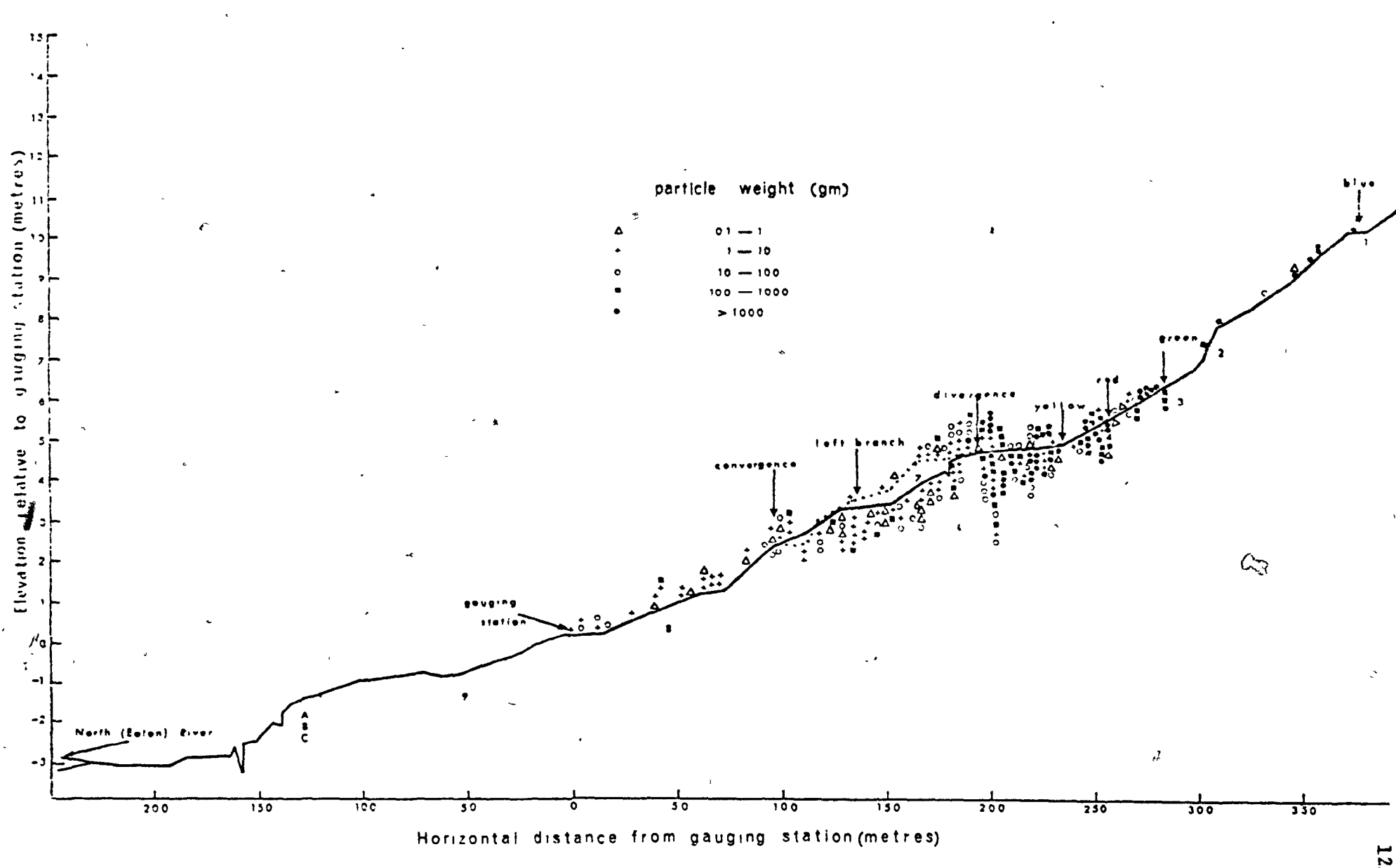


Figure 4.6: Longitudinal profile of the studied reach showing location and weight of recovered particles.

patchy appearance owes its existance to the relationship between size and distance transported. No obvious size <u>versus</u> slope relationship exists. This is also in accordance with the description of the bed in Chapter III, whereby it is shown that local changes in structure and particle size are even larger than the small-scale bed slope changes. Thus, it is believed that bed slope in coarse-bedded channels does not influence initiation of motion nor bedload discharge to a large extent. This same conclusion was also reached by Helley (1969), who actually ignored bed slope.

The only consistent relationship is the one between distance of transport and weight (or size, see Figure 4.5) of particles. Regressing distance on weight yields the highest reduction in variance of distance transported, and the correlation coefficients are consistently negative.

The linear relationship between log(distance transported) and log(weight) is very convenient in terms of clarity of scatter diagrams, which include a three and a fivefold increase in the magnitude of the variables (Figures 4.7 - 4.10). An arithmetic-semilog linear relationship between distance of transport and log(weight) yielded slightly higher correlation coefficients but several other attempted transformations yielded much lower ones.

The distance-weight scatter can be approximated by a linear regression line, but the validity of the latter in terms of confidence levels is very restricted. The plotted data are not normally distributed nor do they have a constant variance about the line. Thus, although it is clear from these scatter diagrams that there is a tendency for distance of transport to increase with decrease in particle weight (or size), quantitative

Table 4.3

Linear Regression Analysis on Distance of Transport of Labelled Bed
Material: Correlation Matrix, after Keller, 1970

	•				
Experiment Number	Dependent Variable	Independent Variable	Coefficient of Correlation	Confidence Level	N —
1	distance moved	volume	-0.423	0.98	41
1	distance moved	weight in water	-0,410	0.97	41
1	distance moved	A-C axis ratio	-0.158	0.75	41
1	distance moved	specific gravity	-0.030	0.97	41
1	distance moved	diameter x s.g.	-0.522	0.99	41
1	distance moved	shape	-0.258	0.99	41
1	distance moved	effec. bot. vel. sq.	0.692	0.80	41
1	distance moved	effec. bot. vel.	0.701 ′	0.99	41
2	distance moved	volume	-0.305	0.99	65
2	distance moved	weight in water	-0.327	0.99	65
2	distance moved	A-C axis ratio	-0.057	0.50	65
2	distance moved	specific gravity	-0.286	0.99	65
2	distance moved	diameter X s.g	-0.528	0.99	65
2	distance moved	shape	-0.291	0.99	65
2	distance moved	effec. bot. vel. sq.	0.438	0.61	65
2	distance moved	effec. bot. vel.	0.470	0.99	65

estimates of this tendency and its reliability, based on linear regression-correlation results, are very unreliable. Even if the data were distributed normally with a fixed variance along the line, at a confidence level of 95 percent the correlation coefficients of these log-log relationships (for the yellow, red, green, blue and all colours) would vary to a great extent (-0.58 to -0.17; -0.57 to -0.18; -0.73 to -0.42; -0.88 to -0.52 and -0.57 to -0.36 respectively).

Results reported by Leopold, Emmett and Myrick (1966) show either no relationship at all between distance of transport and particle weight, or a very slight, negative one (for the North Frijoles Reach, see Figure 4.3). Keller (1970) does not provide a distance of travel versus weight scatter diagram, but his results, summarized in Table 4.3, indicate that distance of transport correlates with particle weight and with all other weight-affiliated particle parameters negatively in a consistent manner. Although such relations yield correlation coefficients very similar to those found in this study, the correlations should be interpreted with care. Whether the relationships are genuinely linear has yet to be established.

Inspection of the pattern of scatter in Figures 4.7 - 4.10 leads to some doubt whether a simple first-degree function is appropriate for the relationship between distance of travel and particle weight. If distance of travel is strongly controlled by velocity of travel, rather than merely duration of travel, the data of Meland and Norman (1969) (Figure 4.4) would lead us to expect quite complicated functions even in the absence of background scatter. For this reason, relations of distance of travel and weight were examined in other ways.

An analysis of variance was undertaken in order to test whether

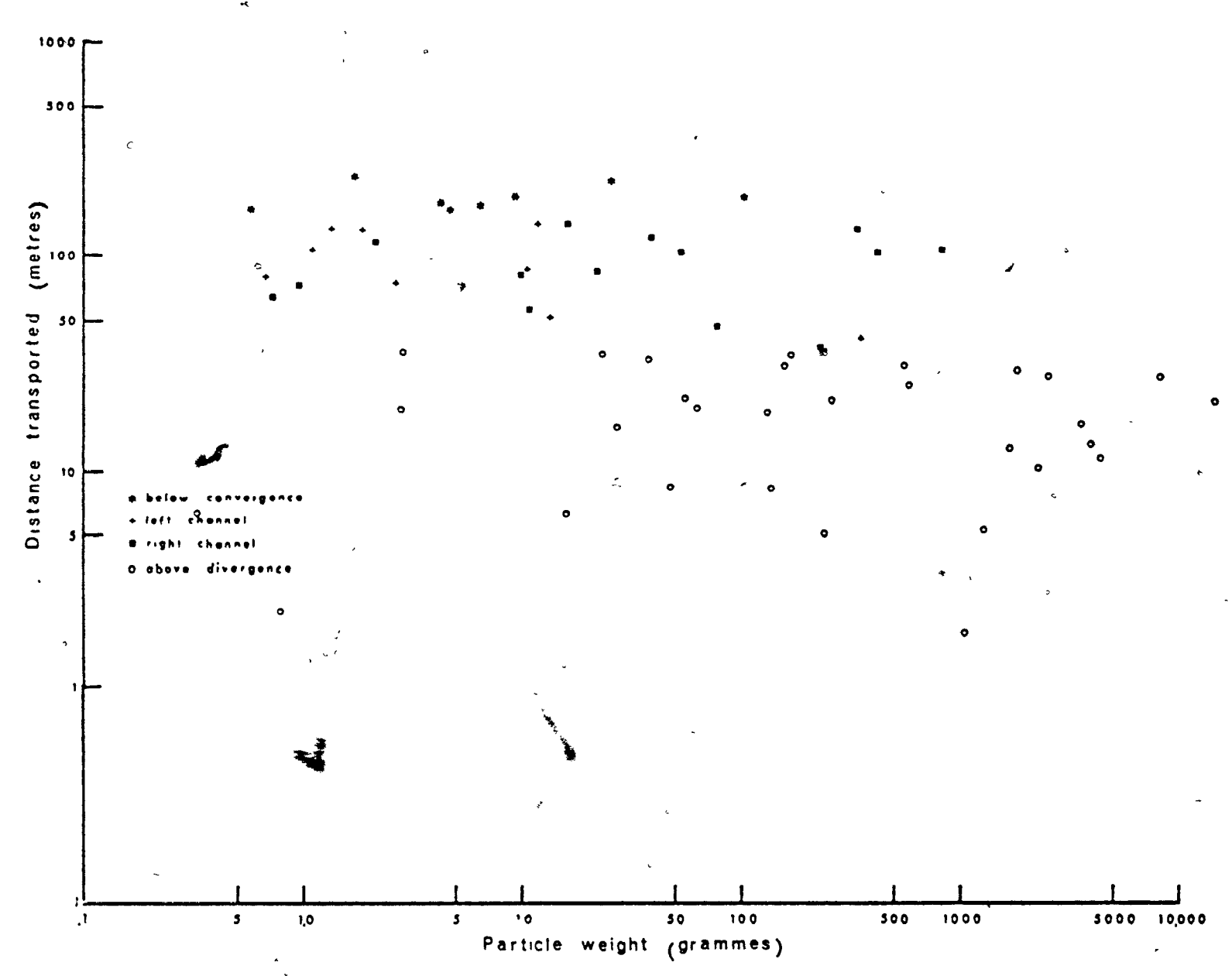


Figure 4.7 Transport distance of particles as a function of particle weight, yellow particles.

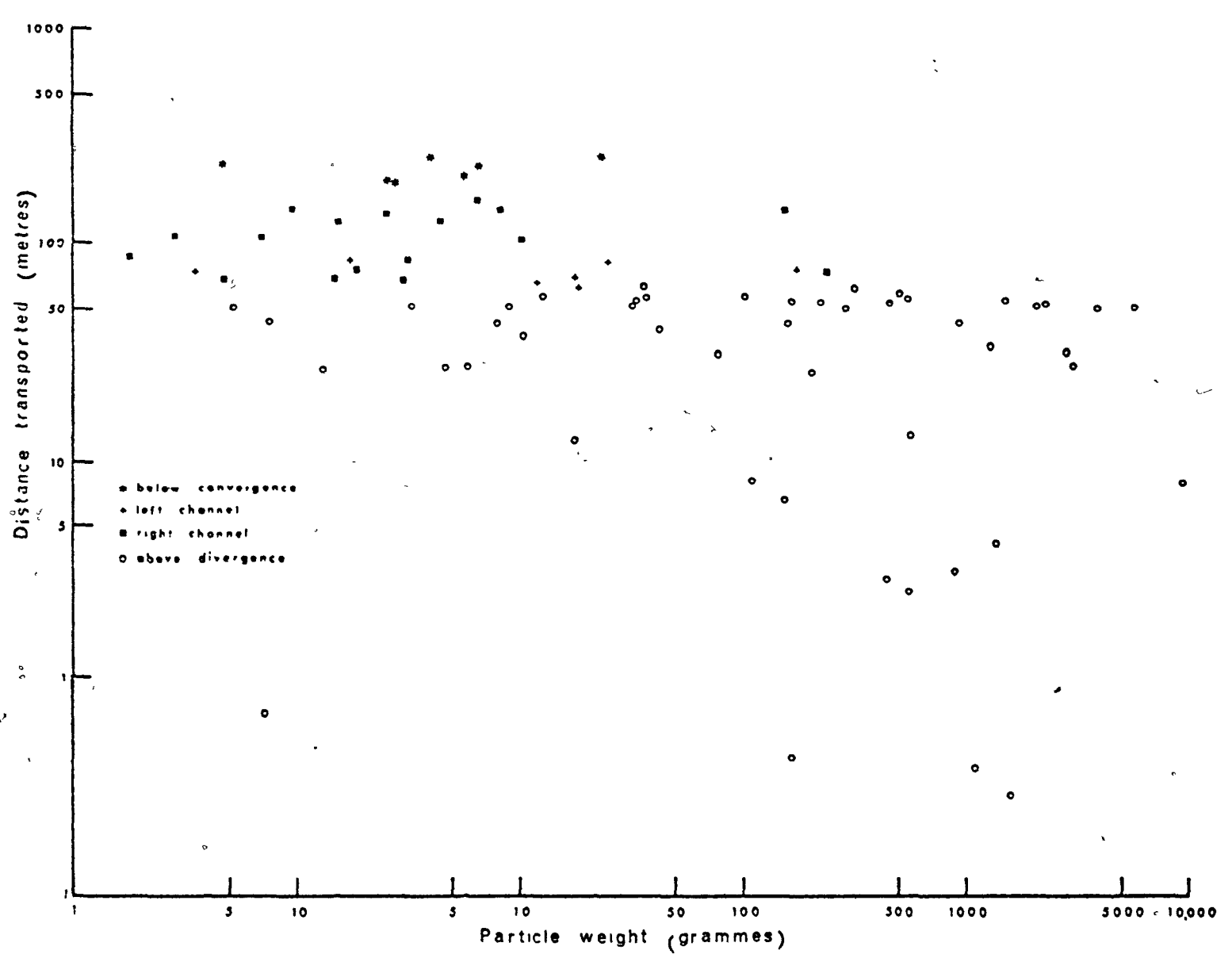


Figure 4.8 Transport distance of particles as a function of particle weight, red particles.

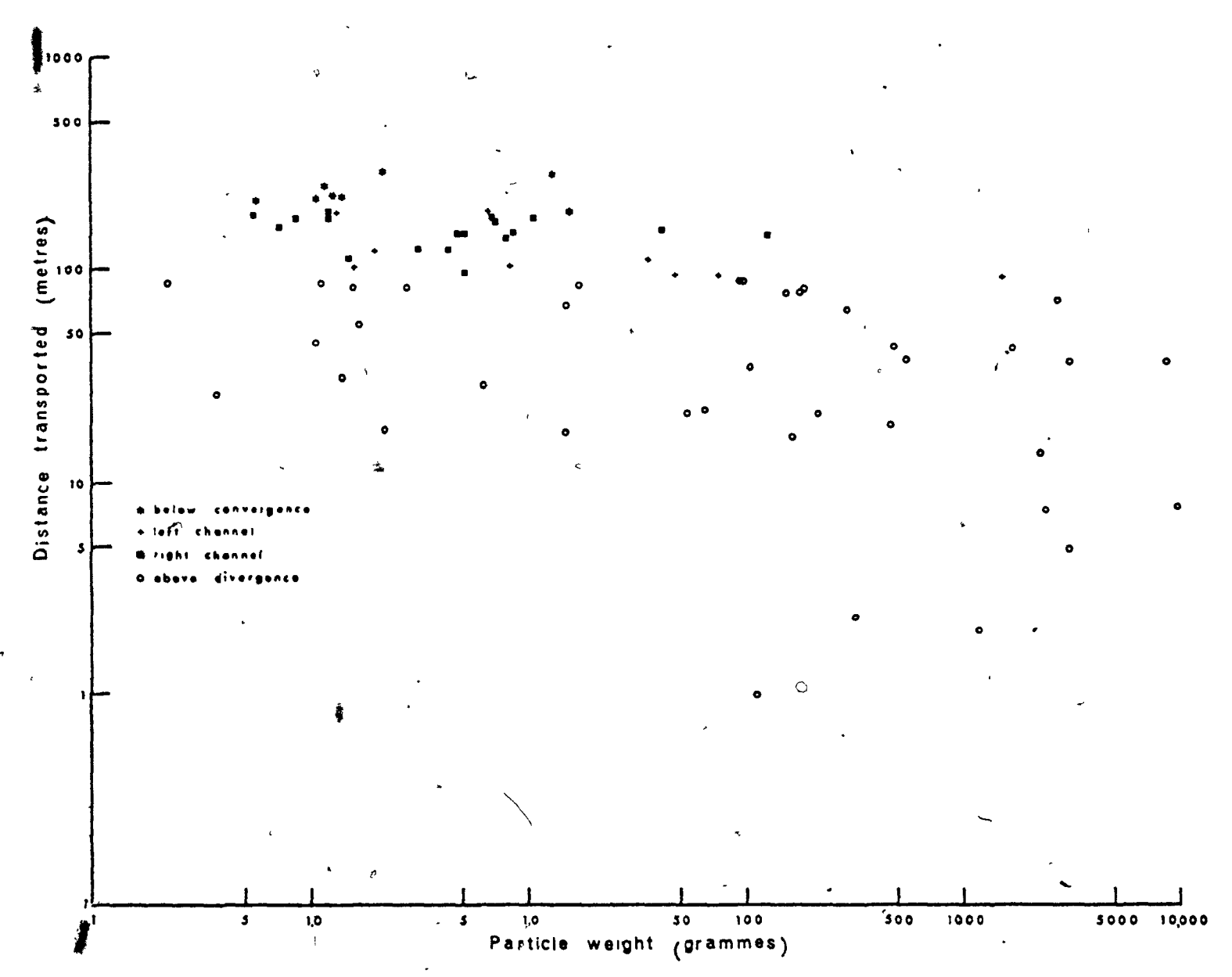


Figure 4.9 Transport distance of particles as a function of particle weight, green particles.

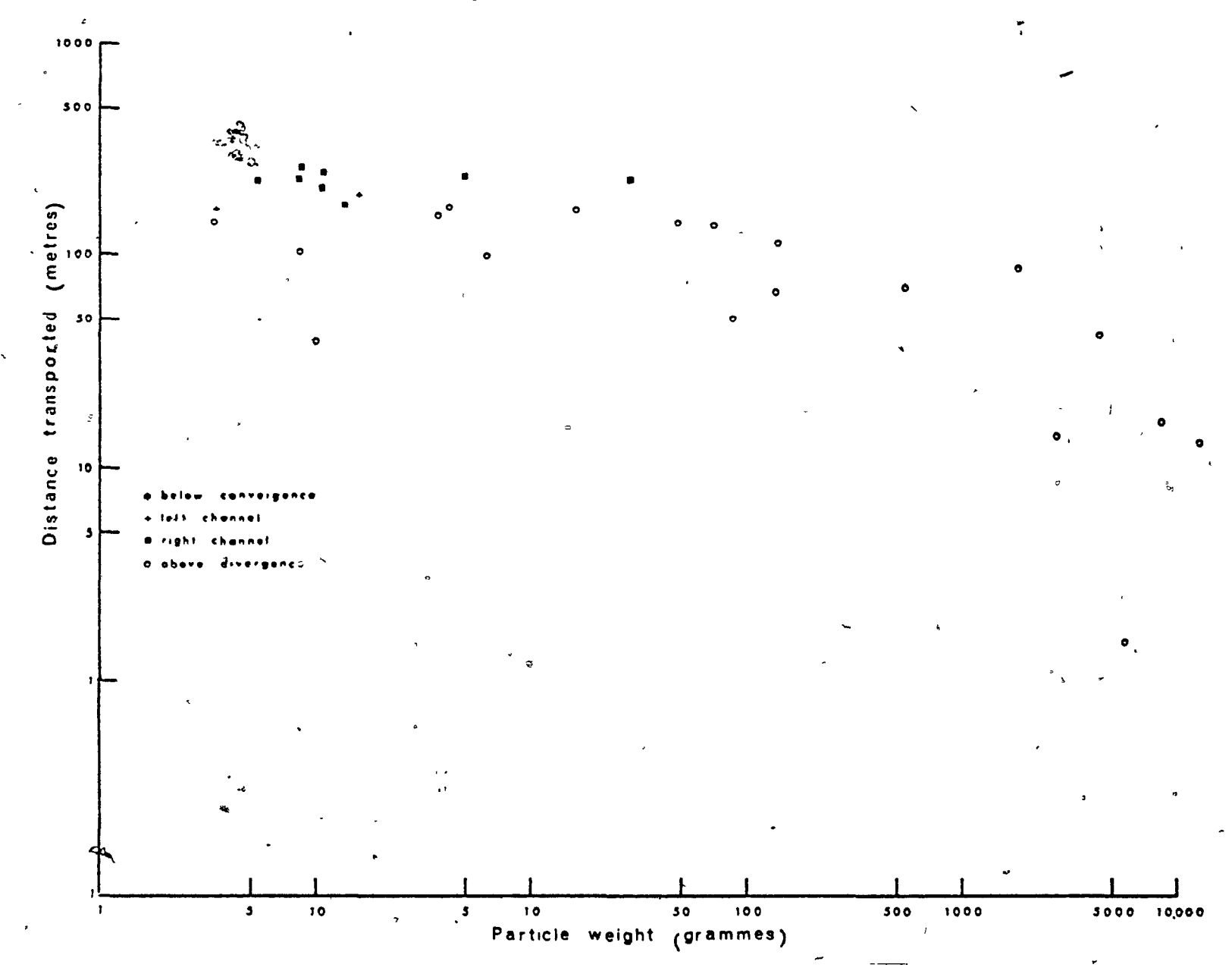


Figure 4.10 Transport distance of particles as a function of particle weight, blue particles.

the distance residuals for each size group (0.1 - 1, 1 - 10, 10 - 100, 100 - 1000 and > 1000 gm) are significantly different. For this analysis a regular F - test was done, which showed that there is a significant (0.05) difference between the average residuals of some of these groups (an F - test will not indicate where the difference lies). In order to avoid comparing each two groups (five groups in each colour, or ten comparisons) and in order to maintain the same confidence level, a test on means after experimentation (Hicks, 1964) was used, for which least significant ranges are obtained from a table. It was found that comparison between the average residuals of pairs of particle size groups yield very similar results for the four separate colours as well as for all 242 recovered particles. The average residuals of the smallest (0.1 - 1.0 gm) and the largest (> 1000 gm) groups are consistently negative (i.e., they tend to appear in the scatter diagram below the regression line) and the opposite is true for the intermediate size groups. This is consistent with Meland and Norrman's (1969) data depicted in Figure 4.4a.

The only consistent and significant difference between size groups concerns the smallest and the second smallest groups; gravel-sized particles (inferring b - axis from weight using Figure 4.5) are transported significantly less than predicted from the regression line and small pebbles significantly more. Thus, the average distance-residual for each size group can be minimized still further when the weight versus distance of transport data are approximated by a cubic relationship schematically shown in Figure 4.11. The conclusion here is that the distance of transport of bed-material increases, but at a decelerating rate, with decrease of particle size from the boulder to the pebble range. With further

. .

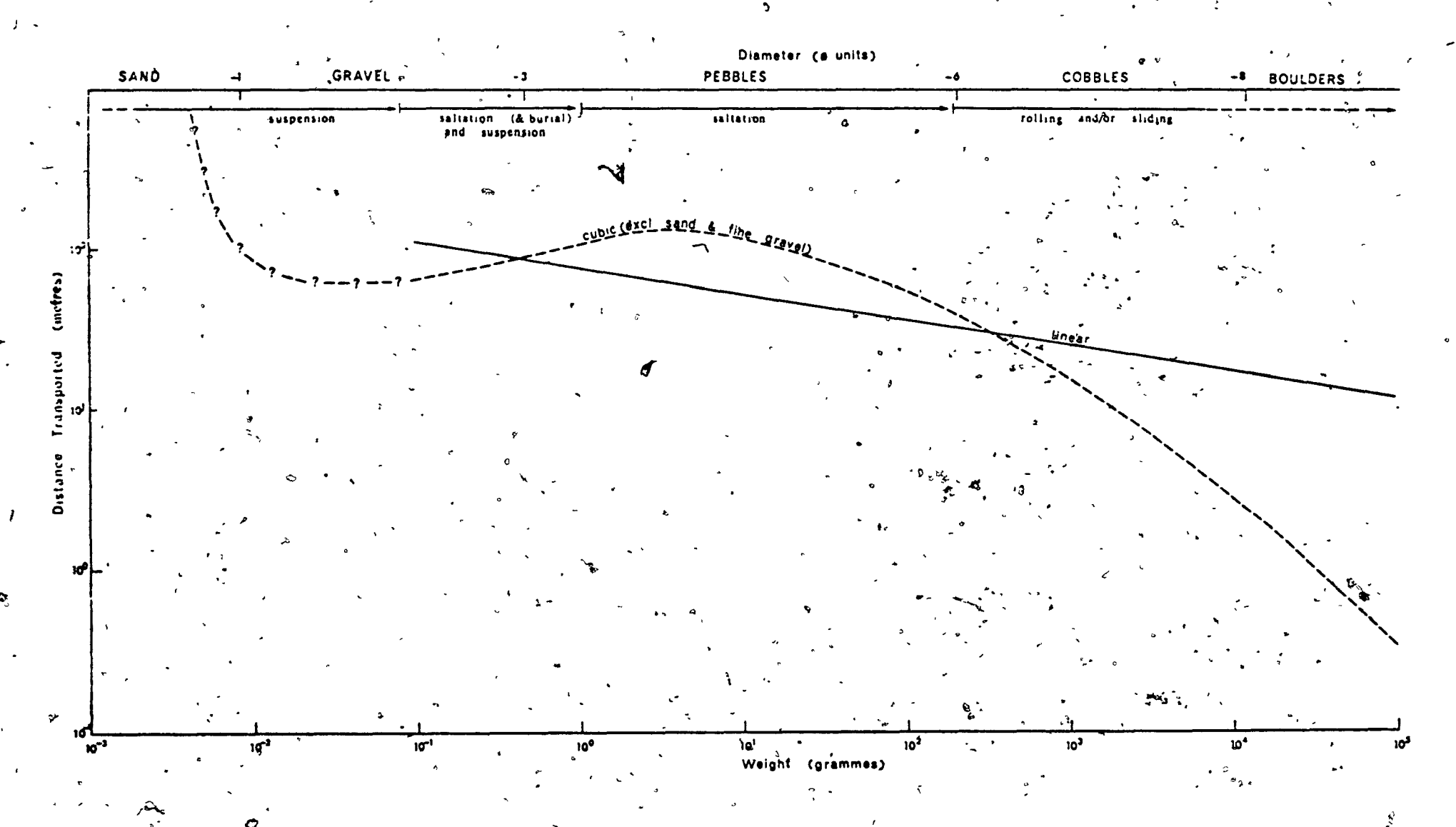


Figure 4.11 Schematic particle weight - distance of transport relationship showing different bed-material transport mechanisms for Seale's Brook, May 4 - 5, 1972.

diminution of calibre, the distance decreases, remains constant or increases very slightly. It is also logical to assume that below a minimum size (the largest sizes transported in suspension in considerable amounts), a further decrease of particle size is associated with an accelerating increase in distance of transport.

# 4.5 Structure and Form as Indicative of Particle Velocities and Transport Mechanisms

The slower particle velocities and shorter periods of travel (i.e., the relatively small distances of travel) of large cobbles on the one hand and gravel on the other can find their explanation in the composition, morphology and structure of the bed. Above everything else, the most prominant characteristics of the coarse-bedded channel of Seale's Brook is the predominance of coarse particles in the surface layer of the bed and its consequent jagged nature, as well as the localization of finer material in specific areas.

Meland and Norrman (1969) presented a theoretical but sound explanation for the differences in particle velocity. They maintained that with increase in particle size, bed stability becomes less effective in retarding, or causing cessation, of bedload transportation by sliding and rolling. The larger a particle, the larger its contact surface with the bottom consequent to which it is less likely to sink in a matrix of finer bed-material. Moreover, with increase in size the less likely will the motion of the particle be affected by bed irregularities. Thus, average particle velocities will tend to increase with increase in particle size up to a certain limit. As particle size increases above this limit,

the increase in weight overcompensates for the increased contact surface area in terms of relative stability. Thus, increase in size for very large particles is associated with a decrease in particle velocity. Bedload transportation of large particles is, consequently, inferred to be characterized by short-lengthened but fast advances with long intervening rest periods. Conditions were dynamically competent (see section 4.6) in Seale's Brook during the peak spring flood of 1972 at least for small boulders. An example of the transportation of such large particles can be seen in Figure 3.10. Here, the upright boulder, beside the grass-covered raised ground, partly covers a transported, blue-labelled, quartz-veined large cobble.

Although small particles are associated with low velocities, this is only applicable to movement by rolling and/or sliding. Particles transported largely in salitation will travel faster than will somewhat larger, rolling ones. Moreover, velocity will be greatly increased for particles in suspension. Nevertheless, as soon as particles of this latter category come in contact with the bed surface, they will tend to be buried underneath larger particles. The overall result should then be that the smallest particles commonly found on the bed would be transported extremely variable distances - depending whether they were or were not buried at the onset of a flood recession by larger particles which, at that time, become immobilized.

It has already been mentioned that the smallest particles commonly associated with imbricate structures, especially with well-developed ones, most likely form the lower size limit for bedload transportation by rolling and sliding. For Seale's Brook, this corresponds very approximately to particles with D > 60 mm, or having weights in excess of 200 gm (see Figure

4.5). This lower limit for bedload transportation by rolling and sliding should be regarded with care and it probably applies only to the peak flood of May 4-5, 1972.

The gravelly fractions have been shown to be transported significantly shorter distances than a simple logarithmic relationship would have predicted. This is a result of the extremely variable distances they were transported. In fact, the difference between the gravelly and pebbly fractions is very likely due to different mechanisms of transport. Gravelsized fragments were probably transported in suspension during the highest stages of the May 4 - 5th flood. From Sundborg's (1967) well-known diagrams showing bedload/suspension transport zones and zones of immobility, it can be seen that with a small decrease in particle size in the < pebble range, the particles are transported as bedload at much smaller velocities. It is, in fact, quite evident that much of the gravelly bed-material was transported in suspension and deposited on high channel flanks and on point bars at the onset (1 or 2 hours) of the recession of this flood, because at somewhat lower stages water depth and velocity were much too low on channel flanks and on point bars for the water to carry gravel in suspension. At the time during which considerable amounts of the moving gravel were deposited on channel flanks and banks, most of the remaining gravel in motion was being buried underneath or hidden in lee of the cobbles and boulders which concurrently became immobile. Had gravelly material been transported in suspension longer than ca  $\frac{1}{2}$  - 1 hour, the labelled gravel would have been very conspicuous on the bed of the lower reach (from the bridge to the North River), or at least as conspicuous

as on rougher, further upstream locations, where the percentage of fine material on the surface is, indeed, very small (see Figure 4.12). In fact, only two coloured particles were detected in the lower reach on the 12th of May and none of the blue gravel-sized particles were transported farther than the point bar immediately downstream of the convergence (Figure 3.2). A relatively small amount of gravel was probably transported in saltation and later by rolling and sliding during lower stages of flow subsequent to which it was deposited on the stoss side of protruberances or in miniature longitudinal bars.

Because pebbly particles tend to be located in interparticle spaces, they were probably transported in saltation during peak flow conditions, landing in the large hollows. For the same reason it is also reasonable to assume that they were not moved solely by rolling or sliding (that is, the larger particles were there originally and the pebbles could not have rolled on top of these protruberances). It is also clear that had pebbles been transported largely in suspension, they would have filled the interparticle spaces almost to the brim. They did, however, most probably roll and slide 1 - 2 hours after the onset of the recession, at the time of which they were deposited in channel flats and, more rarely, formed partly-developed imbricate structures.

### 4.6 <u>Dynamic Competence and Bedload Movement</u>

ζ,

The foregoing sections dealt with the tendencies of bed-material size groups to be transported varying distances according to associated durations, velocities and mechanisms of transport. The unanswered question concerning these tendencies is why they are so weak or, rather, complex. The results of measurements of downstream changes in particle size distribution will precede the attempt to answer this question.

#### a) Downstream Particle Size Diminution

Sampling of particles on the top layer of the bed was undertaken by using the grid-by-number method (Wolman, 1954 and Leopold, 1970). The b - axis of the rocks was measured with field-made wooden calipers large enough to encompass small boulders. All particles smaller than 8 mm were included in the < 8 mm size class, as suggested by Kellerhals and Bray (1971b). In two recent papers (Kellerhals and Bray, 1971a and 1971b) it is shown and explained that the grid-by-number sampling method yields equivalent results to customary bulk sieve analysis. It is also shown that in order to convert a set of area-by-number measurements (essentially an evaluation of the frequency distribution by number of all surface layer particles in a unit bed area) to weight-by-volume data, it is necessary to multiply each frequency of occurrence by D<sup>2</sup> (where D is particle size; see column 12 of Table A.3).

Particle size distributions of the top bed layer of four reaches are illustrated in cumulative form in Figure 4.12. The four reaches are denoted Up - from where the blue particles were introduced extending down to where the yellow ones were; Div - from the former to the divergence; Rc - the right channel branch and Br - from the coalescence to the bridge. Each grid-by-number sample contained 100 individual particles. The median diameter is seen (Figure 4.12) to decrease downstream: 152, 122, 113 and 106 mm respectively for each of the consecutively lower reaches. This decrease of particle size, going downstream, is true for practically the complete size range commonly found on the streambed. The trend was also checked qualitatively

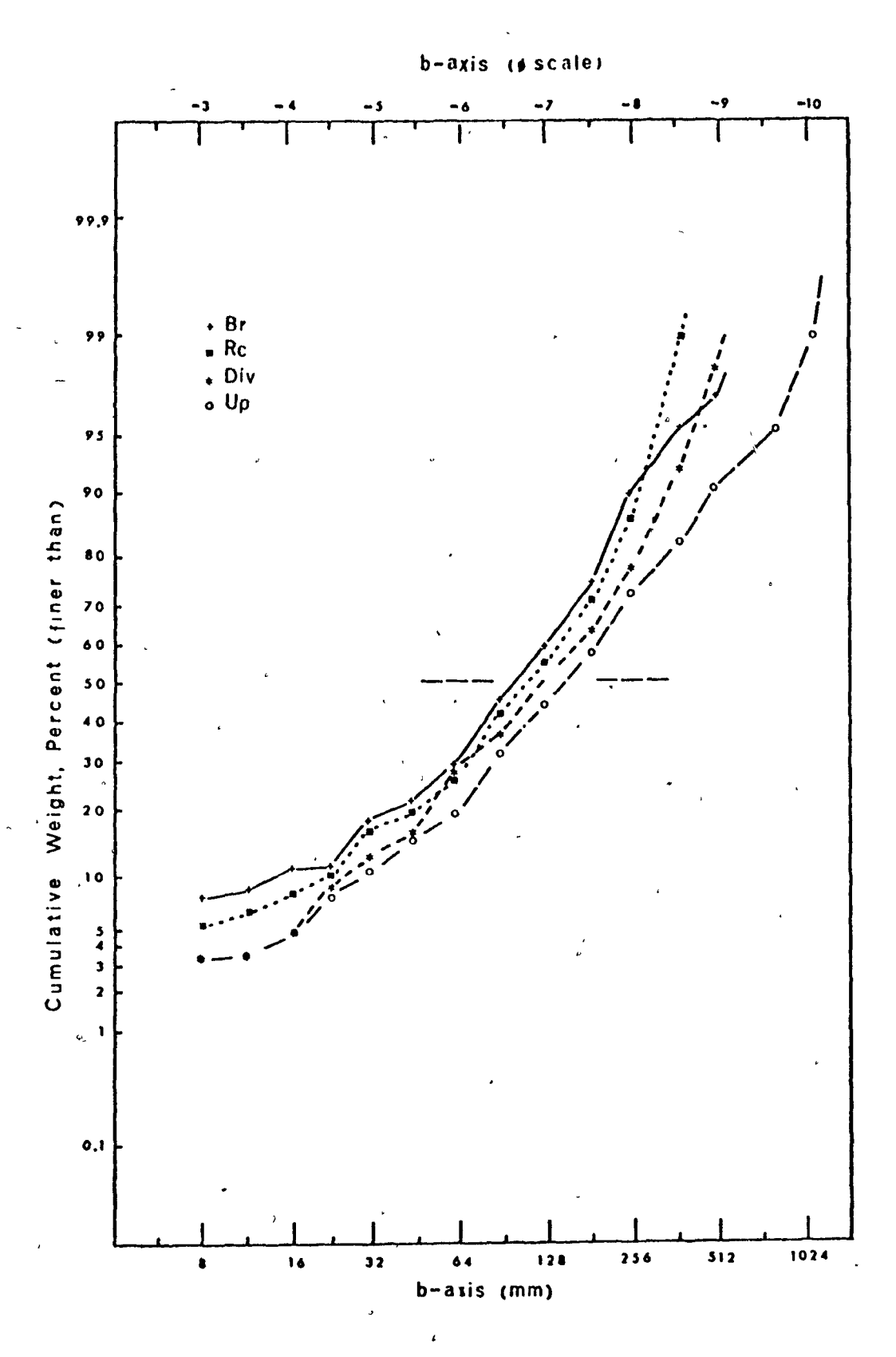


Figure 4.12: Cumulative graphs of particle sizes: downstream diminution in calibre of surficial bed-material.

throughout most of the channel and it was noted that similar small cycles are superimposed on this general trend. A small cycle usually terminates at strong bends or upstream of bedrock exposures.

What is the cause for the gradual and the cyclic decrease of particle size with distance downstream? Abrasion is one possibility, but experiments by Kuenen (1956) and by Bradley, Fahnestock and Rowenkamp (1972) show that much longer distances of travel are needed. The recovered labelled bed-material lost part of the paint coating, but abrasion was extremely small. Another possibility is fracturing. Most of the pyrite cubes, so common in the slates, are completely oxidized to limonite. This enhances fracturing of the slaty fragments, but the process is only effective for very thin particles. Of the 242 recovered particles only two were fractured. This fracturing was restricted on one occasion to a fissility plane and in another to the whole weathered mass of the particle. Some granular disintegration of the very few siltstones was observed, but on the whole, less than 1 percent of the surface material was noticed to have been freshly fractured. Weathering of particles may be associated with downstream decrease in particle size if their residence time in the channel increases downstream (due to an increase in floodplain width). The bed-material of Seale's Brook is not deeply weathered (nor the bedrock nor the coarse fractions in the drift) partly because the residence time of individual particles along the whole network is short due to the narrowness of the channel.

Particle size diminution with distance downstream can, Kowever,

be explained by hydraulic sorting (i.e., varying distance of travel). If there is no weathering-limiting situation for any of the particle size ranges, it should be expected that although much of the finer bed-material is mobilized only when the coarser fractions are entrained, the former is carried greater distances (because it moves faster) and thus concentrates in lower reaches. This, then, is regarded as a leading clue to the longitudinal size sorting of bed-material in coarse-bedded channels.

#### b) Classical Competence

Implicit in much of the previous discussion is the belief that threshold velocities for uniform material of a given size will not, in fact, prove to be competent for that size of material in heterogeneous channels where resistance is augmented by the interlocking of tight structures. Unfortunately it is difficult to prove this directly, because most competence diagrams are based on "bottom velocity" or on shear velocity, whereas data are available only on surface velocity in the Seale's Brook study. Conversion of these figures (x 0.84) to mean channel velocity does, however permit comparison with Hjulström's (1936) diagram (Figure 4.15). Detailed velocity data are available for two occasions: April 19, 1972 and peak flow conditions in 1973; mean channel velocities at these times were 2.5 m/sec and 1 - 1.25 m/sec respectively. According to Hjulström's data, these velocities correspond to competence values of 50 mm and 10 mm respectively.

The data from Figure 4.16 show that the largest labelled particle  $(D=176\ mm)$  was not moved at all, that those of intermediate sizes were indeed transported (but merely 2 - 3 m to more stable positions) and that the smallest numbered cobbles were hardly transported at all. It is

thus inferred that a stability of the newly placed material was soon attained and that conditions were not yet competent for particles of these sizes (133 - 176 mm). Moreover, it is evident that during the spring of 1973, conditions were not competent to move pebbles or coarse (> 4 mm) gravel (see section 4.4). This indicates that initiation of motion of coarse bed-materials is associated with somewhat higher competence levels than those predicted from the flume data. It reinforces the observations that coarse bed-materials are more stable due to structural arrangements which are absent in flume runs.

The few data presented here are certainly inconclusive.

Moreover, the difficulty of standardizing the criteria used by different workers to designate "initiation of motion" will always thwart this type of comparison. Verification of the role of interlocking structures in relation to "classical competence theory", based on uniform material, will necessitate much further work.

#### c) Dynamic Competence

Downstream particle size diminution varies with different reaches and with size groups (Figure 4.12). In other words, the diminution and its rate are inconsistent. In the same context, Figures 4.7 - 4.10 show that distances of travel, viewed as the means by which particle size diminishes downstream, vary to a great extent for particles of the same size category. For instance, pebbles were transported 20 and 200 m, but usually not 2 m. In this section an attempt is made to explain these differences and the associated tendencies.

It has already been mentioned that coarseness of the surficial channel bed is usually closely linked to nearby sources of coarse

material (whether bedrock outcrops or fluvioglacial deposits). lar observations were reported by Scott and Gravlee (1968), Bradley et al (1972) and others. The two above-mentioned studies showed that lack of competence is a decisive factor controlling lag formation and size sorting downstream. The dominant role of competence, in its accepted sense, seems to be refuted in Seale's Brook for two reasons. Firstly, large boulders are quite abundant downstream of these localized areas. This raises the question as to why these boulders were transported and not those in the upstream localized concentrations. The same question is applicable to all the coarse size ranges. It may be expected that the distribution of large particles in drift is partly random and not entirely localized in nests. ever, why then should the percentage of boulders and, for that matter, all coarse particles, decrease downstream and with superimposed cycles? The movement of individual large particles from their original concentrated location may be partly answered by the explanation of Leopold et al (1966) of gravel bar formation on sand-bed streams. Briefly, they observed that the closer the spacing between particles of the same size, the smaller their velocity. For instance, when labelled bed-material is placed in several spacings on a river bed, those that are more widely spaced will be associated with a greater probability of movement (Figure 4.13). Thus, once some large boulders are transported away from the local area where others are still concentrated, the distance of transport of the former will subsequently and continually increase relative to the more or less stationary population of concentrated boulders. This same reasoning would also

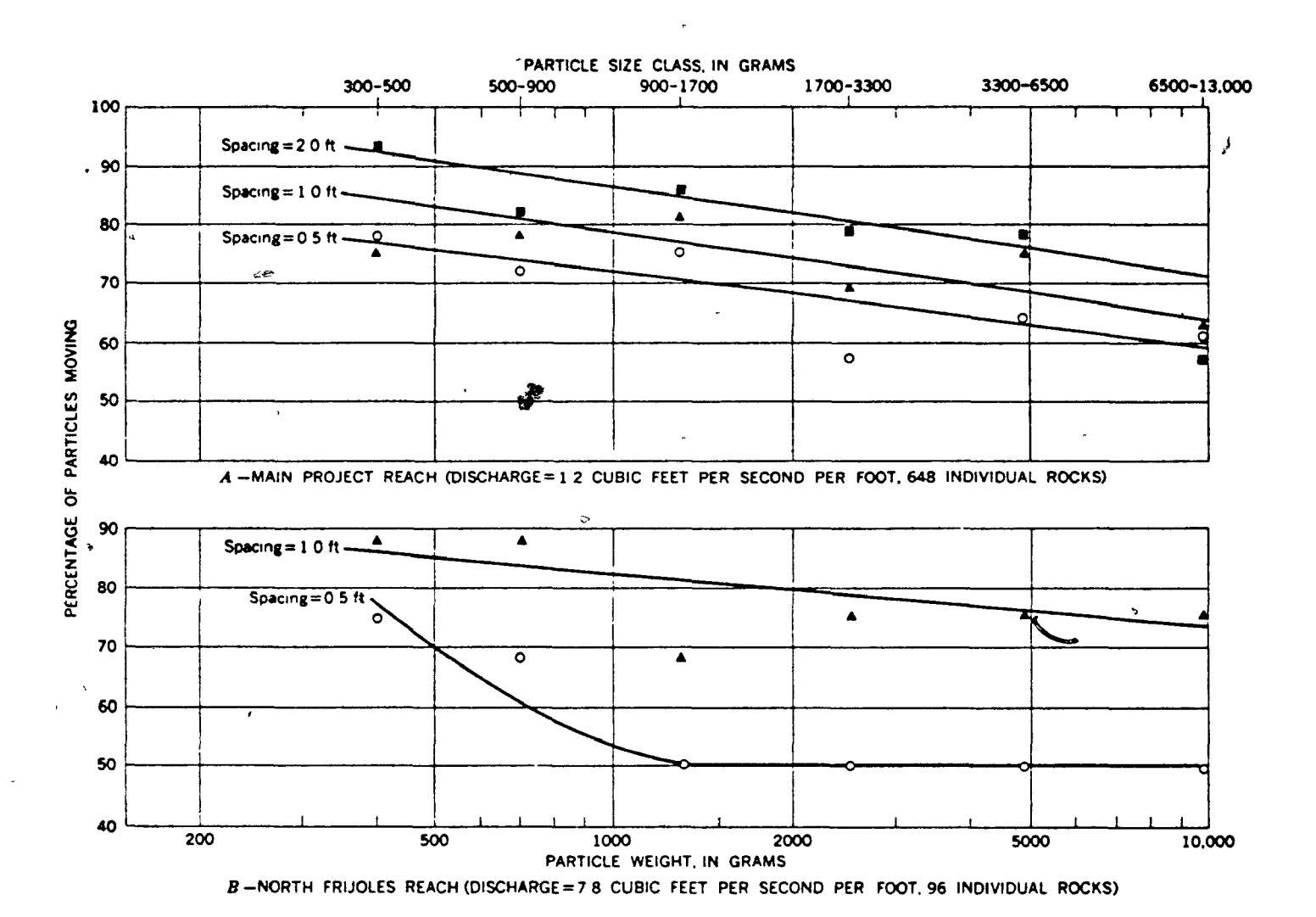


Figure 4.13: The effect of spacing on percentage of rocks moving for a given discharge and particle size, after Leopold et al, 1966.

apply to gradually smaller particles, but the basic question as to why some boulders were first transported away from their concentrated location, instead of having the whole localized group move as one, slow-moving mass, remains unanswered.

The second reason for refuting the dominant role of competence in this context is that the recurrence interval of floods capable of moving quite large boulders (see p. 132) is as low as 2 - 4 years (Chapter V). If such competent floods are so frequent then the reasons for the size sorting downstream, the smaller distances travelled by coarser particles and especially the ejection of coarse particles from localized concentrations must be explained in a different way.

The concept of dynamic competence, which is introduced here, is especially applicable to coarse-bedded channels; it needs definition, proof and explanation. A review of the literature on competence and initiation of motion of large particles reveals that competence, as such, is the ability of a stream to entrain a certain maximum size of particles for which, in turn, flow conditions are said to be competent.

It is a well-known fact that all alluvial channels and specifically natural, coarse-bedded ones, are characterized by nonuniform sizes of bed-material on the surface and in the bed as a whole. If, then, flow conditions are competent at a certain stage to move a specific maximum particle size, with flood recessions this competence and the associated particle size decrease. An inspection of the bed-material at low flow should then reveal a nonuniform bed-material with a very definite layering of particle sizes, fining towards the surface.

However, such layering is very restricted in natural channels and it is only common on the most bankward (or quiet) portions of channel beds.

Moreover, it is known that the composition of the surface layer is usually coarser than that of more deep-seated bed layers. In fact, this was also found to hold for Seale's Brook.

The area-by-number sampling technique was applied to a small bed area measuring 0.5 x 0.5 m by spraying it with paint. Each particle was picked and its b - axis was measured. The small amount of surface gravel was brought to the laboratory where it was washed, dried, sieved and the number in each size class was recorded. Because some of the larger surface particles had left deep holes partly filled with water, the underlying layer could not be sprayed. Instead, a volumetric sample, roughly 0.1 m deep, was dug out of the same location. Care was taken not to lose any fine material. The data from these two samples are found in Table A.3 of the Appendix. Figure 4.14 depicts the cumulative frequency distributions and the histograms of the calibre of the surface and the underlying particles (see also Table A.3). Clearly, the surface material is much coarser and the lack of fines in the surface layer is especially notable.

If, instead of considering the usual competence term, one considers the cross-sectional and downstream variations as well as fluctuations of flow parameters (e.g., velocity), which are caused by microtopographical, structural and channel-configuration changes, and if one considers in the same category of importance the natural variability in bed-material composition and structure, then the formation of totally nonuniform layers, in terms of particle size composition, is

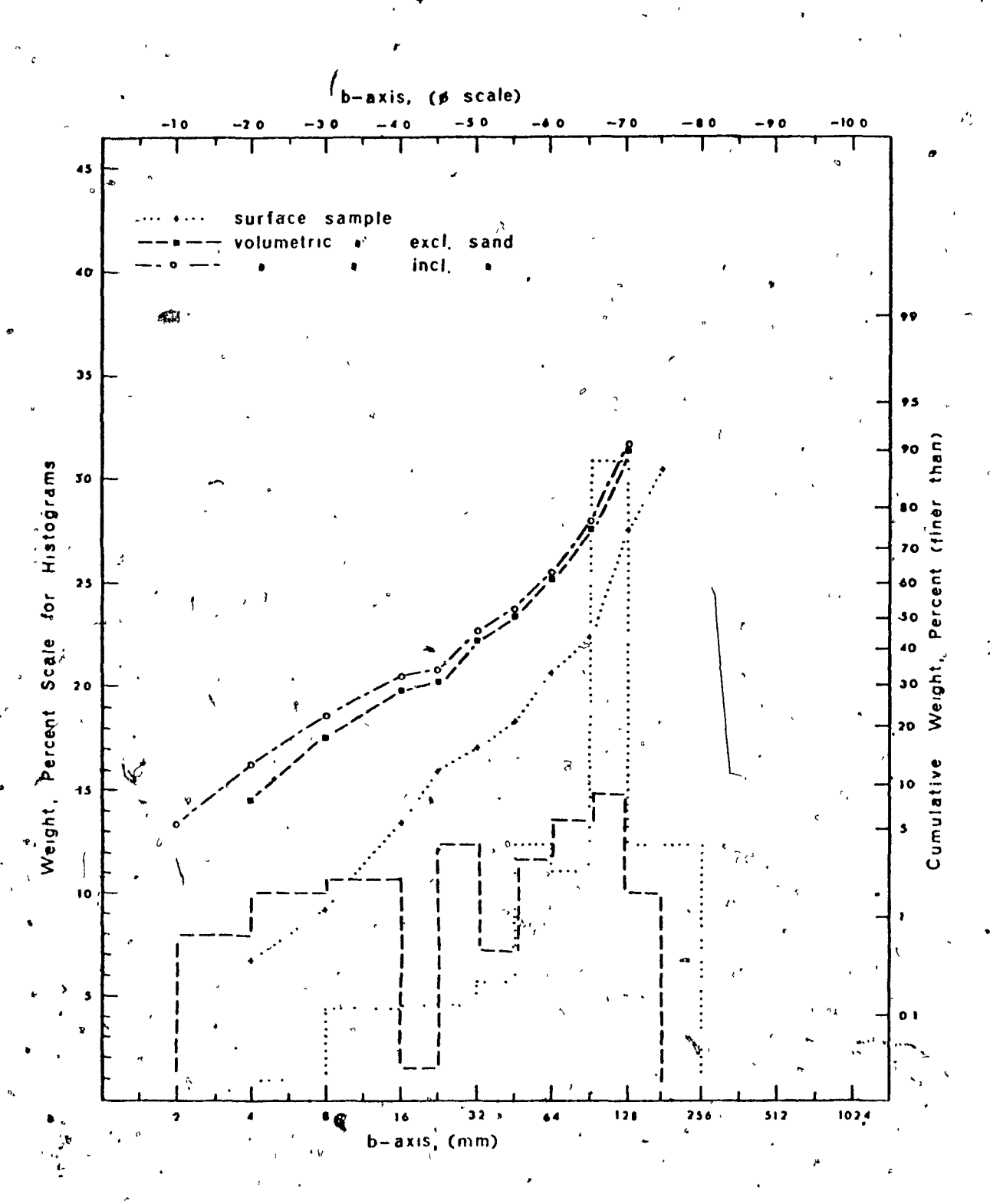


Figure 4.14: Cumulative graphs and histograms of particle sizes:
surface layer versus underlying material.

readily apparent. This also explains why conditions may be competent to move some boulders from their 'nest', but not all of them.

The discriminatory nature of the transport mechanism which moves only few large particles at a time from a bed area that is very coarse is both a matter of chance and bed stability. In this context, Einstein's (1950) statistical approach (probability of being transported) is useful. The specific large particle that is entrained and transported away from other large particles was initially less stable than those particles that did not move and it was subsequently moved from one unstable position to another until it reached a stable one. Its mobility and initial instability are not only a function of its inherent characteristics (e.g., size or shape) and of the hydraulic conditions (e.g., stream power or velocity) but also, and probably to a great extent, of the stability of the structure of which it is but one component. Had it been rolled against a very stable bed structure (e.g., another but much bigger boulder), its movement would have ceased. Moreover, if its initial position had not been, partly by chance, unstable, it would, have not moved in the first place. Thus, the hydraulics-chance-areally variable bed stability approach can, in fact, explain the formation of distinct gravel bars on sand-bed streams and the areally variable bedmaterial composition in coarse-bedded streams.

In conclusion, the concept of dynamic competence involves areal and temporal changes in competence. Moreover, a stream may be competent to transport boulders but the dynamic competence related to the structures of the channel bed and to the hydraulics of the situation may be such

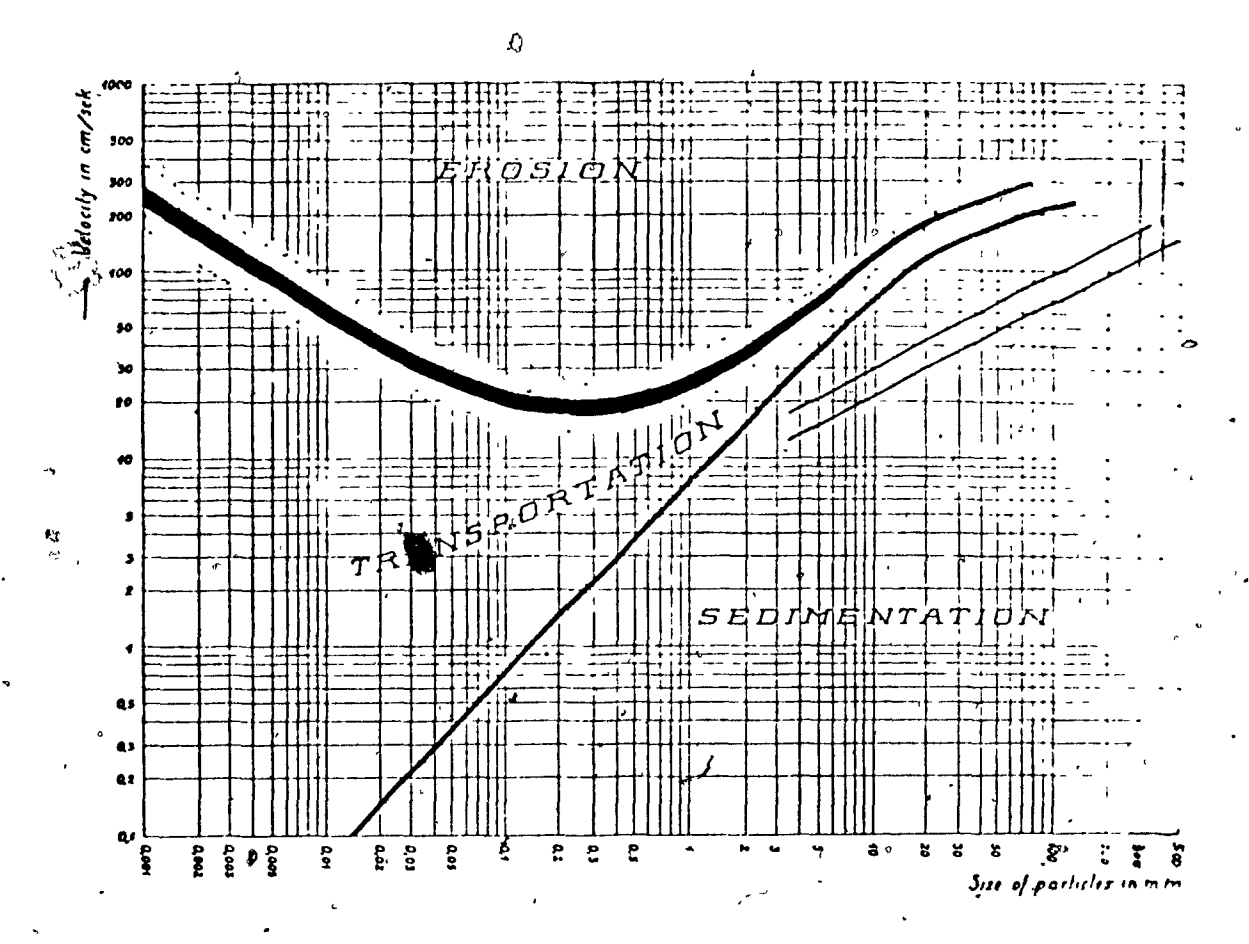


Figure 4.15: Hjulstrom's (1936) curves for erosion and deposition of a uniform material.

No	Weight (gm)	Distance (m)	De tance (m)
1	104934	000	21 42
2	82/7 9	0.36	27 82
3	4592 4	1 24	11 97
4	3613 9	2 62	1722
5,	2291 2	3 28	1067
ó	2516 9 €	0 24	28 52
7	1851 8	0 22	3047
4			

114 2116 · AVERAGE

odistance, of transport between April 15 and April 23, 1972.

during the whole spring of 1972.

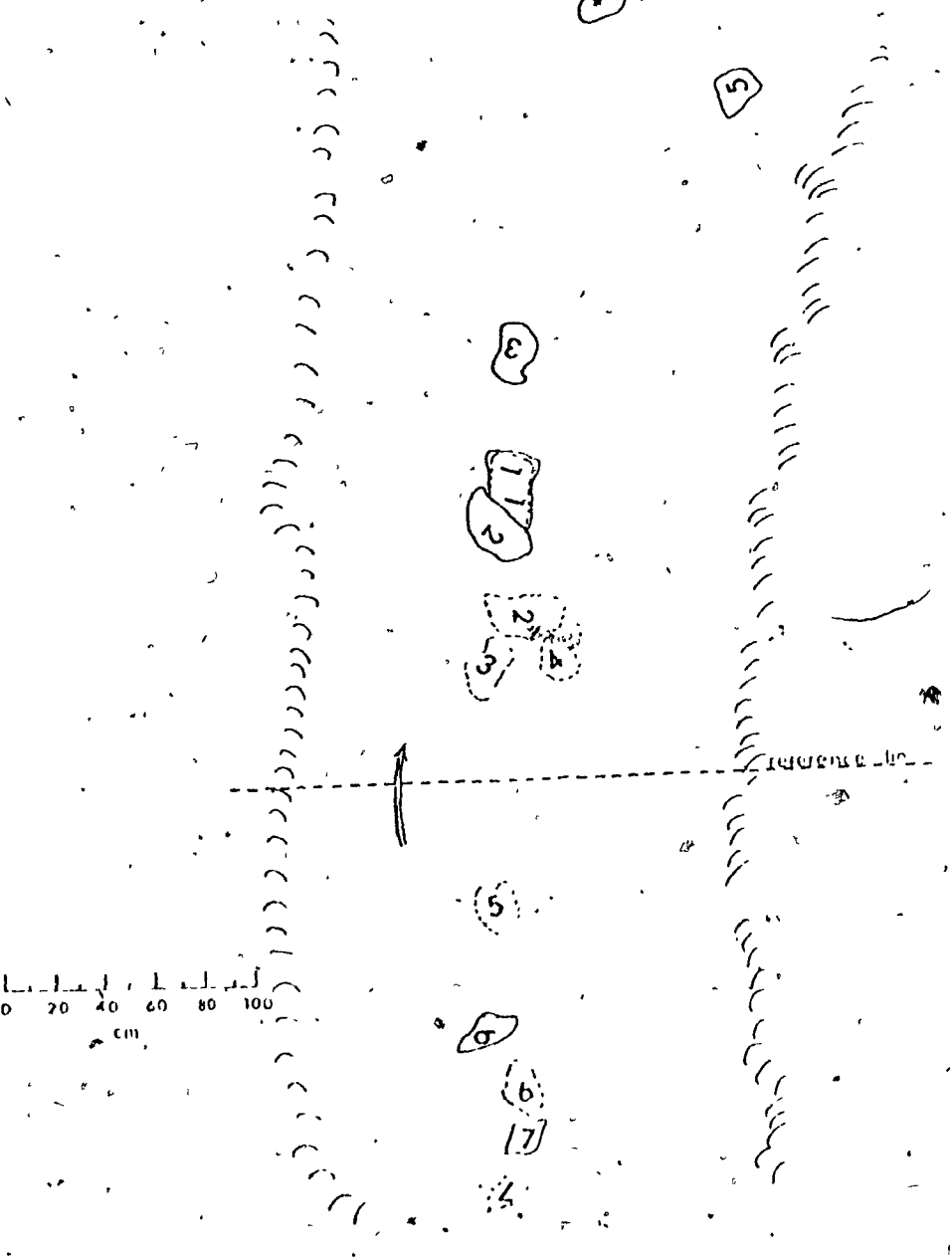


Figure 4.16: Map showing locations of 7 yellow cobbles on April 15 (dashed lines) and on April 23, 1972.

that boulder structures are stable enough to prevent release, and only a few, unstable boulders can be moved. Thus, dynamic competence may be regarded as the ability of a stream to destroy the most stable structures. Competence, in the common sense, differs from dynamic competence in that it is associated with the initiation of motion of individual particles rather than with threshold conditions of structures.

## CHAPTER V

## CONCLUSIONS

This study attempts to show that field observations of the morphology of coarse-bedded channels and the structure, composition and relief of their beds are in great need today. Theoretical and experimental studies reveal trends and relations that may or may not hold in nature. Whatever the theory, at some point it must be validated in the field for which, in fact, the relations and trends are sought.

The problems of sampling bedload, most of which are simply a result of the character of bedload transport mechanisms, have not yet been solved. In fact, the usefulness of present bedload sampling techniques is and will continue to be questioned unless sampler efficiencies are determined in natural channels. None of the prevailing theories can be checked as long as a solution is not found to bedload sampling. Thus, it is somewhat useless to expand still more the vast literature on bedload theories, based on general physical (and usually hydraulic) concepts as well as on flume experiments, without first studying in detail the actual characteristics of the natural system. The natural open system associated with bedload transportation is comprised of flowing water, its conveyor - the channel, and the latter's constituents - the individual bed and bank fragments. 'Although many studies dealing with the behaviour of water in natural alluvial channels have been undertaken, much still remains to be understood. The great gap between fact and theory still lies

today in the actual description of channels and bed-materials. This is especially true of coarse-bedded streams.

The lower reach of Seale's Brook was studied in order to evaluate and understand channel and bed-material characteristics. It was found that cross-sectional shape, channel slope and configuration, although following certain trends, change in a continuous and usually abrupt manner. Thus, average values of slope, width and, to some extent configuration do not convey the actual character of the channel.

The surficial bed layer was found to be considerably coarser than underlying layers. This was also observed whenever a particle was picked from the bed; more often than not, it overlay much finer material. The surface layer also shows a tendency for particle size to diminish towards channel flanks as well as with distance downstream.

The surficial layer of this coarse-bedded channel is composed of fragments of variable sizes and shapes. These, in conjunction with more complex bedforms such as transverse ribs, give rise to a very jagged bed relief. Consequently, only a small portion of the bed surface approximates a flat, ideal surface so often assumed to exist in the development of bedload equations.

Particles are arranged on the bed in several well-developed structures such as imbricate ones. Almost all of them are closed and it is obvious, as has been shown, that greater forces are needed to attain threshold conditions than those expected from theoretical studies.

Thus, an infrequent flood event preceded by one with a lower probability of occurrence (during which very large particles may be mobilized and

be incompetent to initiate motion of any but few particles. Structure, in this sense, is obviously important in understanding incipient motion.

The flood of May 4 - 5, 1972 transported labelled particles, part of which were subsequently recovered. It was dynamically competent to destroy all but the most stable structures on the bed, and entrained boulders as large as Dgo - Dgo, depending which river reach (particle size distribution of the surface layer) is considered. Pre-1972 discharge data for Seale's Brook are nonexistant. However, if it can be assumed that the severity of the peak spring flood of 1972 at Seale's Brook, in relation to previous floods there, was much the same as for the Eaton River at East Angus, then the return period of the 1972 spring flood, as identified by the largest daily mean flow that occurred during the snowmelt period, is of the order of 4 years (25 percent probability of occurrence) (Carson, 1972). This, then, raises doubt as to the stability of coarse-bedded channels, so often viewed in the geomorphological literature as armoured and practically immobile.

It is believed that further micromorphological studies of natural river beds, and specifically coarse ones, are necessary to enhance our understanding of bedioad transport mechanisms.

## REFERENCES

- A.S.C.E. Task Committee.
  - 1966: Sediment transportation mechanics: initiation of motion. A.S.C.E. Proc., 92(HY2), 291-314.
- Bagnold, R.A.
  - 1954a: The Physics of Blown Sand and Desert Dunes. Methuen, London, 265 pp.
  - 1954b: Experiments on a gravity-free dispersion of large solid spheres in a Newtonian fluid under shear. Roy. Soc. (London) Proc., sec. A, 225, 49-63.
  - 1956: The flow of cohesionless grains in fluids. Roy. Soc. (London)
    Philos. Trans., ser. A, 249(964), 235-297.
  - 1966: An approach to the sediment transport problem from general physics. U.S. Geol. Survey Prof. Paper 422-I, 37 pp.
- Barnes, H. Jr.
  - 1967: Roughness characteristics of natural channels. <u>U.S. Geol. Survey</u>
    <u>Water-Supply Paper</u> 1849, 213 pp.
- Bird, J.B.
  - 1970: Some aspects of the geomorphology of the Eastern Townships of Quebec.

    Rev. Geogr. Montr., 24(4), 417-429.
- Blench, T.
  - 1955: Regime formulas for bed-load transport. <u>Internat. Assoc. for Hydraulic Res.</u>, Proc. of the 6th Gnrl. Mtg., The Hague, Netherlands, 4, Dl-l to Dl-7.
- Bradley, W.C., Fahnestock, R.K., and Rowenkamp, E.T.
  - 1972: Coarse sediment transport by flood flows on Knick River, Alaska. Geol. Soc. of Am. Bull., 83, 1261-1284.
- Brooks, N.H.
  - 1958: Mechanics of streams with movable beds of fine sand. A.S.C.E. Trans, 123, 526-594.
- Brown, H.E., Hansen, E.A., and Champagne, N.E. Jr.,
  - . 1970: A system for measuring total sediment yield from small watersheds.

    Water Resources Research, 6(3), 818-826.
- Brune, G.M.
  - 1953: Trap efficiency of reservoirs. Am. Geophys. Union Trans., 34, 407-418.

Cann, D.B., and Lajoie, P.

1942: Soil survey of Stanstead, Richmond, Sherbrooke and Compton Counties in the Province of Quebec. Canada Dept. of Agric., Publ. 742, Tech. Bull. 45, 59 pp.

Carson, M.A.

1972: Sediment production in the Eaton River Basin, southeastern Québec, during spring runoff, 1970 - 1972. Final report to the Ministère des Richesses Naturelles du Ouébec. 87 pp.

Cartier, L., and Leclerc, A.

1964: Rivière Eaton: caracteristiques topographiques du bassin versant.

Service d'Hydrométrie, Ministère des Richesses Naturelles du

Québec, Bull., HP-5, 32 pp.

Charlton, F.G.

1972: Discussion of "Sediment transport measurements in gravel river" by Hollingshead, A.B., A.S.C.E. Proc., 98(HY8), 461-462.

Chepil, W.S.

1961: The use of spheres to measure lift and drag on wind-eroded soil grains. Soil Sci. Soc. Am. Proc., 25, 343-346.

Chien, N.

1956: The present status of research on sediment transport. A.S.C.E. Trans., 121, 833-884.

Clément, P.J.

1972: Observations sur l'exportation de produits en solution par certains cours de l'eau appalachiens de la region de Sherbrooke, Québec, Canada. Congrès U.G.I., Montréal, 1972.

Colby, B.R.

1961: Effect of depth of flow on discharge of bed-material. <u>U.S. Geol.</u>

<u>Survey Water-Supply Paper</u> 1948-D, 10 pp.

1964a: Discharge of sands and mean-velocity relationships in sand-bed streams. U.S. Geol. Survey Prof. Paper 462- A, 47 pp.

1964b: Scour and fill in sand-bed streams. U.S. Geol. Survey Prof. Paper 462-D, 32 pp.

1964c: Practical computations of bed-material discharge. A.S.C.E. Proc., 90(HY2), 217-246.

Colby, B.R., and Hembree, C.H.

1955: Computations of total sediment discharge, Niobara River near Cody, Nebraska. U.S. Geol. Survey Water-Supply Paper 1357, 187 pp.

Colby, B.R., and Hubbell, D.W.

1961: Simplified methods for computing total sediment discharge with the modified Einstein Procedure. U.S. Geol. Survey Water-Supply Paper 1593, 17 pp.

Cooke, H.C.

1950: Geology of a southwestern part of the Eastern Townships of Quebec.

Geol. Survey of Canada, Memoir 256, 2496, 142 pp.

Davis, W.M.

1902: (Reprinted 1954, Dover, New York). <u>Geographical Essays</u>. Ginn. Boston, 777 pp.

Einstein, H.A.

1942: Formulas for the transportation of bed-load. A.S.C.E. Trans., 107, paper 2140, 561-597.

1950: The bed-load function for sediment transportation in open channel flows. U.S. Dept. Agr. Tech. Bull. 1026, 78 pp.

Einstein, H.A., and Chien N.

1956: Similarity of distorted river models with movable beds. A.S.C.E. Trans., 121, 440-462.

Einstein, H.A., and El-Samni, E.A.

1949: Hydrodynamic forces on a rough wall. Rev. of Modern Physics, 21(3), 520-524.

Fahnestock, R.K.

1961: Competence of a glacial stream. U.S. Geol. Survey Prof. Paper 424-B, 211-213.

1963: Morphology and hydrology of a glacial stream - White River, Mount Rainier, Washington. U.S. Geol. Survey Prof. Paper 422-A, 67 pp.

Fahnestock, R.K., and Haushild, W.L.

1962: Flume studies of the transport of pebbles and cobbles on a sand bed. Geol. Soc. Am. Bull., 73, 1431-1436.

Fair, G.M., and Geyer, J.G.

1954: Water Supply and Waste-Water Disposal. Wiley, New York, 973 pp.

Federal Inter-Agency River Basin Committee

1940: Equipment used for sampling bed load and bed material, in "A study of methods used in measurement and analysis of sediment loads in streams." Rept. 2, 57 pp.

Gagnon, R.W., Pollack, D.M., and Sparrow, D.M.

1970: Critical meteorological conditions for maximum flows, the St. Francis and Chaudiere River Basins, Quebec. Climatological Studies, 6,

Dept. of Twansport, Meteorological Branch, Toronto, 85 pp.

Garg, S.P., Agrawal, A.K., and Singh, P.R.

A 1971: Bed load transportation in alluvial channels. A.S.C.E. Proc., 97(HY5), 653-664.

Gilbert, G.K.

1914: The transportation of debris by running water. <u>U.S. Geol. Survey</u>
<u>Prof. Paper</u> 86, 363 pp.

Grey, B.

1972: Sources of suspended sediment in the Eaton River (Quebec) during spring runoff: Thesis presented to McGill University in partial fulfilment of the requirements for the degree of Master of Science.

Hack, J.T.

1957: Studies of longitudinal stream profiles in Virginia and Maryland. U.S. Geol. Survey Prof. Paper 294-B, 45-97.

Helley, E.J.

1969: Field measurements of the initiation of large bed particle motion in Blue Creek near Klamath, California. U.S. Geol. Survey Prof. Paper 562-G, 19 pp.

Henderson, F.M.

1966: Open Channel Flow. Macmillan, New York, 522 pp.

Herbetson, J.G.

1969: A critical review of conventional bed load formulae. Jour. of Hydrol., 8, 1-26.

Hicks, C.R.

1966: Fundamental Concepts in the Design of Experiments. Hold, Reinhart and Winston, New York, 293 pp.

Hjulström, F.

1936: Studies of the morphological activity of rivers as illustrated by the river Fyris. Univ. Upsala (Sweden) Geol. Inst. Bull., 25, 221-527.

Hollingshead, A.B.

1968; Measurements of the bed-load discharge of Elbow River: Thesis presented to the University of Alberta, in partial fulfilment of the requirements for the degree of Master of Science.

1971: Sediment transport measurements in gravel river. A.S.C.E. Proc., 97 (HY11), 1817-1834.

Hubbell, D.W.

1964: Apparatus and techniques for measuring bed-load. <u>U.S. Geol.</u> Survey Water-Supply Paper 1748, 74 pp.

Hubbell, D.W., and Matejka, P.Q.

1959: Investigations of sediment transportation, Middle Loup River at Dunning, Nebraska. U.S. Geol. Survey Water-Supply Paper 1476, 123 pp.

Ippen, A.T., and Verma, R.P.

1953: The motion of discrete particles along the bed of a turbulent stream. Internat. Hydraulics Convention, Hinnesota, 7-20.

Jordan, P.R.

1965: Fluvial sediment of the Mississippi River at St. Louis, Missouri. U.S. Gool. Survey Water-Supply Paper 1802, 89 pp.

Kalinske, A.A.

1942: Criteria for determining sand transport by surface creep and saltation. Am. Geophys. Union Trans., 23(2), 639-643.

1947: Movement of sediment as bed load in rivers. Am. Geophys. Union Trans., 28(4), 615-620.

Keller, E.A.

1970: Bed load movement experiments, Dry Creek, California. <u>Jour. of</u> Sed. Petrology. 40(4), 1339-1344.

Kellerhals, R.

1967: Stable channels with gravel-paved beds. A.S.C.E. Proc. Waterways and Harbours Div., 93(WII), 63-84.

Kellerhals, R., and Bray, D.I.

1971a: Sampling procedures for coarse fluvial sediments. A.S.C.E. Proc., 97(HY8), 1165-1180.

1971b: Comments on "An improved method for size distribution of stream bed gravel" by Leopold. Luna B. Water Resources Research, 7(4), 1045-1047.

Kuenen, Ph.H.

1956: Experimental abrasion of pebbles. 2. Rolling by current. Jour. Geology, 64, 336-368.

Kunkle, S.H., and Comer, G.H.

1972: Suspended, bed and dissolved sediment loads in the Sleepers River, Vermont. U.S. Dept. of Agriculture, Agricultural Research Service, document ARS 41-188, 31 pp.

Lane, E.W., and Carlson, E.J.

1954: Some observations on the effect of particle shape on the movement of coarse sediments. Am. Geophys. Union Trans., 35(3), 453-462.

Laursen, E.M.

1958: The total sediment lead of streams. A.S.C.E. Proc., 84(IIY1), paper 1530, 21-36.

Leliavsky, S.

1966: An Introduction to Fluvial Hydraulics. Dover, New York, 257 pp.

Leopold, L.B.

1970: An improved method for size distribution of stream bed gravel. ... Water Resources Research, 6(4), 1357-1366.

Leopold, L.B., and "olman, M.G.

1957: River channel patterns; braided, meandering and straight. U.S., Geol. Survey Prof. Paper 282- B, 39-85.

Leopold, L.B., Wolman, M.G., and Miller, J.P.

1964: Fluvial Processes in Geomorphology. Freeman, San-Francisco, 522 pp.

Leopold, L.B., Emmett, W.W., and Myrick, R.M.

1966: Channel and hillslope processes in a semiarid area, New Mexico. U.S. Geol. Survey Prof. Paper 352-G, 60 pp.

Maddock, T. Jr.

1968: Discussion of "Similitude theory applied to correlation of flume sediment transport data" by Barr, D.T.H., and Herbertson, J.G. Water Resources Research, 4(5), 1148-1149.

1969: The behavior of straight open channels with movable beds. <u>U.S.</u> <u>Geol. Survey Prof. Paper</u> 622-A, 70 pp.

1970: Indeterminate hydraulics of alluvial chamnels. A.S.C.E. Proc., 96(HY11), 2309-2323.

Mavis, F.T., and Laushey, L.M.

1949: Formula for velocity at beginning of bed-load movement is reappraised. Civ. Engineering, 19, 38-39 and 72.

McDonald, B.C.

1969: Surficial geology of La Patrie - Sherbrooke area, Odebec, including the Eaton River watershed. Geol. Survey of Canada, Paper 67-52, 21 pp.

1972: An experimental study of the formation of transverse ribs, a bed form in shallow streams carrying coarse alluvium. Abstract of a talk given at the Symposium on Fluvial Processes, March 24, 1st session of the Third Annual Colloquium of the Geography Dept., University of Ottawa, Ontario.

McPherson, H.J.

1971: Dissolved, suspended and bed load movement patterns in Two O'clock Creek, Rocky Mountains, Canada, Summer, 1969. Jour. of Hydrol., 12; 222-233.

Meland, N., and Norrman, J.O.

1966: Transport velocities of single particles in bed-load motion. Geografiska Annaler, 48(A), 165-182.

1969: Transport velocities of individual size fractions in heterogeneous bed load. Geografiska Annaler, 51(X), 127-144.

Meyer-Peter, E., and Müller, R.

.1948: Formulas for bed-load transport. <u>Internat. Assoc. for Hydraulic Research</u>, 2nd Mtg., Stockholm, Sweden, 39-64.

Milhous, R.T.

1972: Discussion on "Sediment transport measurements in gravel river." by Hollingshead, A.B. A.S.C.E. Proc., 98(HY11), 2043-2046.

Miller, J.P.

1958: High mountain streams: effects of geology on channel characteristics and bed material. State Bureau of Mines and Mineral Resources,

New Mexico Institute of Mining and Technology, Socorro, New Mexico,

53 pp.

Ministère des Richesses Naturelles du Québec.

1967: Rivière Eaton, Donnée Météorologiques, 1965. <u>Service de Météorologie</u>, <u>Ministère des Richesses Naturelles</u>, Québec, 90 pp.

Nanson, G.C.

1972: Sediment transport measurements: Thesis presented to the University of Alberta in partial fulfilment of the requirements for the degree of Master of Science.

Neil, C.R.

1967: Mean-Velocity criterion for scour of coarse uniform bed-material.

Internat. Assoc. for Hydraulic Research, 12th Mtg., Fort Collins,
Colorado, c6<sub>1</sub>-c6<sub>9</sub>.

Novak, P.

1957: Bed load meters - development of a new type and determination of their efficiency with the aid of scale models. <u>Internat. Assoc. for Hydraulic Research, 7th Gnrl. Mtg.</u>, Lisbon, 1957, Trans., 1, A9-1 to A9-11.

O'Brien, M.P., and Rindlaub, B.D.

1934: The transportation of bed-load by streams. Am. Geophys. Union Trans., 593-603.

Østrem, G.

1972: Sediment transport in glacier streams: <u>Talk given at the Symposium on Fluvial Processes</u>, March 24, 1st session of the Third Annual colloquium of the Geography Dept., University of Ottawa, Ontario.

Richardson, E.V., Simons, D.B., and Pošakony, G.J.

1961: Sonic depth sounder for laboratory and field use. <u>U.S. Geol.</u>
<u>Survey Circular</u> 450, 7 pp.

Rubey, W.W.

1933: Equilibrium-conditions in debris-laden streams. Am. Geophys. Union Trans. 497-505.

1937: The force required to move particles on a stream bed. <u>U.S. Geol.</u>
<u>Survey Prof. Paper</u> 189-E, 121-141.

Samide, G.W.

1971: Sediment transport measurements: Thesis presented to the University of Alberta in partial fulfilment of the requirements for the degree of Master of Science in Engineering.

J. 18 . 7.3

Sayre, W.W., and Hubbell, D.W.

1965: Transport and dispersion of labeled bed material: North Loup River, Nebraska. U.S. Geol. Survey Prof. Paper 433-c, 48 pp.

Schick, A.P.

1967: Bedload trap in "Field methods for the study of slope and fluvial processes." Leopold, L.B., ed. Revue de Geomorphologie Dynamique, 17, 182-183.

Scott, K.M., and Gravlee, G.C. Jr.

1968: Flood surge on the Rubicon River, California - hydrology, hydraulics and boulder transport. <u>U.S. Geol. Survey Prof. Paper</u> 422-M, 38 pp.

Shulits, S.

1935: The Schoklitsch bed-load formula. Engineering, 139, 644-646 and 687.

Simard, G.

1970: Etude hydrogeologique du bassin de la Rivière Eaton. Service d'Hydrogeologie, Ministère des Richesses Naturelles du Québec, Québec, 28 pp.

Solov'yev, N.Y.

1966: Examination of a device for studying the movement of coarse sediment in streams. Soviet Hydrology, 1, 63-75.

Stringham, G.E., Simons, D.B., and Guy, H.P.

1969: The behavior of large particles falling in quiscent liquids.

U.S. Geol. Survey Prof. Paper 562-C, 36 pp.

Sundborg, A.

1956: The River Klaralven - a study of fluvial processes. <u>Geografiska</u> Annaler, 38, 127-316.

1967: Some aspects on fluvial sediments and fluvial morphology.

I: General views and graphic methods. Geografiska Annaler,

49(A), 333-343.

Taylor, C.H.

1972: Sediment discharge from the Eaton River basin (Quebcc) during spring runoff: Thesis presented to McGill University in partial fulfilment of the requirements for the degree of Doctor of Science.

White, C.M.

1940: The equilibrium of grains on the bed of a stream. Roy. Soc. (London) Proc., ser A, 174, 322-337.

Williams, G.P.

1967: Flume experiments on the transport of a coarse sand. <u>U.S. Geol.</u> Survey Prof. Paper 562-B, 31 pp. Willis, J.C.

1967: Discussion of "Sediment transportation mechanics: initiation of motion." A.S.C.E. Proc., 39 (HY1), 101-107.

Wolman, G.M.

1954: A method of sampling coarse river-bed material. Trans. Am. Geophys. Union, 5(6), 951-956.

Wolman, G.M., and Miller, J.P.

1960: Magnitude and frequency of forces in geomorphic processes. <u>Jour.</u> Geol., 68(1), 54-74.

Yalin, S.M.

٠.

1963: An expression for bed-load transportation. A.S.C.E. Proc., 89(HY3), 221-250.

Yang, C.T.

1971: Formation of riffles and pools. Water Resources Research, 7(6), 1567-1574.

APPENDICES

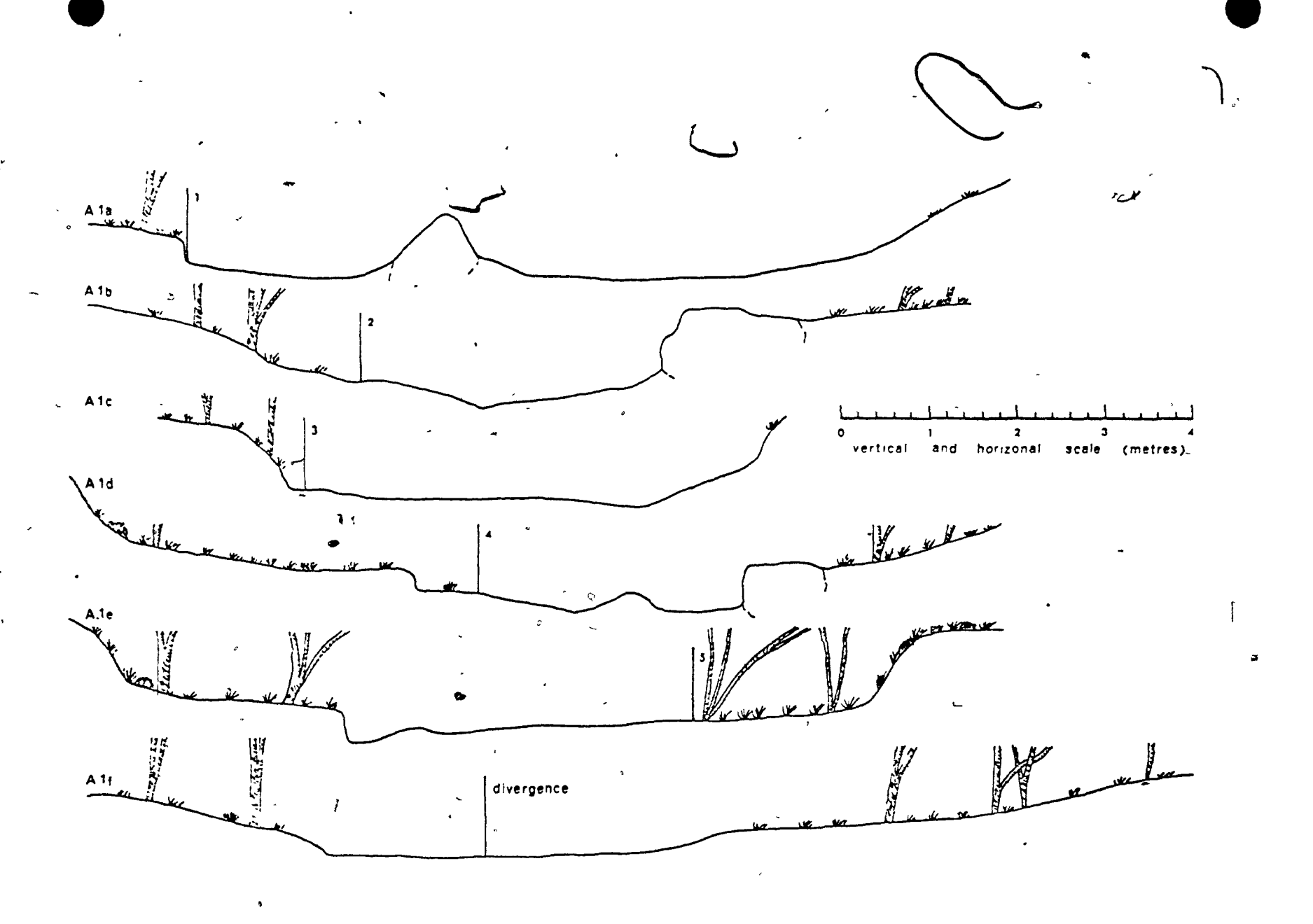


Figure A.1: Cross-sectional profiles of the upper part of the studied reach.

Ø

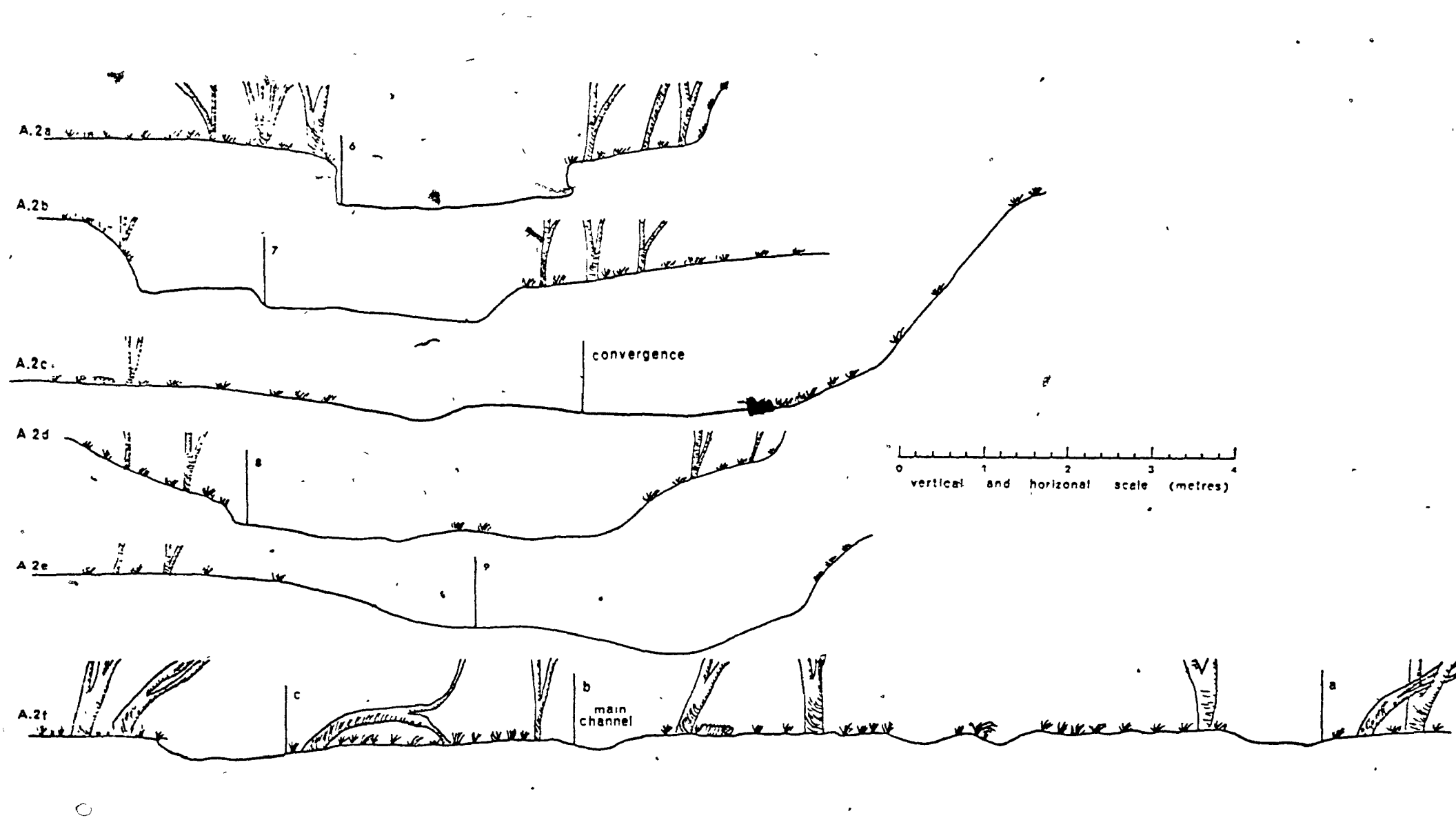


Figure A.2: Cross-sectional profiles of the lower part of the studied reach. (The horizontal and vertical scale for the lowest, braided section is four times smaller than the one for the remaining sections).

Table A.1

Particle Shape of the Div Reach, Oct, 7, 1972, Random Sampling

N	· ·	a mm	b mm	c _mm.	b/a	. c/b	bc/a <sup>2</sup>		No.	a mm	b mm	c mm	b/a	c/b	bc/a <sup>2</sup>	
_	1	155	141	31	0.9	0.21	0.42		18	210	150	69	0.71	0.46	0.47	
	<b>2</b> `	40	39	18	0.97	0.46	0.66		19	102	102	28	1.00	0.27	0.52	
	3	82	6Ò	12	0.73	0.20	0.32		20	310	230	32	0.74	0.14	0.28	
ſ	4	750	625	min 225	0.83	0.36	0.49		21	51	28	- 25	0.55	0.89	0.52	ž
	5	35	20	17	0.57	0.85	ò.52		22	143	104	99	0.73	0.95	0.60	
	6	104	63	33	0,60	0.52	0.44		23	146	80	68	0.55	0.85	0.51	
	7	51	21 -	19	0.41	0.9	0.39		24	53	36	8	0.68	0.22	0.32	_
	8	68	53	12	0.77	0.22	0.36		25	791	412	min 153	0.52	0.37	0.32	•
	9 .	50	29	14	0.58	0.48	0.40		26	255	186	82	0.73	0.44	0.48	
1	.0 -	15	8	3	0.53	0.37	0.33		27	288	208	53	0.72	0.25	0.36	
1	1	18	12	8	0.66	0.66	0.54		28	?	<8	?	X	x	x	
1	2	314	261	55	0.83	0.21	0.37		· 29	574	549	min 253	0.96	0.46	0.65	
1	.3	148	115	26	0.77	0.22	0.36	1	30	259	153	59	0.59	0.39	0.36	
1	4	130	<b>;</b> 95.	<sup>°</sup> 36	0.73	0.37	0.44	,	31	24	9	8		0.89		
1	.5	73	55	36	0.75	0.65	0.60						0.38		0.36	
1	.6	91	72	28	0.79	0.38	0.48		32	87	64	54	0.77	0.84	0.69	
1	.7	211	157	47	0.74	0.29	0.40	-	33	218	183	115	0.84	0.63	0.66	
		,	•				1		34	331	274	110	0.83	0.40	0.53	

No.	a	b rom	c man	b/a	c/b	bc/a <sup>2</sup>		No.	a mm	b mm	c mm	b/c	c/b	bc/a <sup>2</sup>
35	101	80	. 32	0.79	0.39	0.50		58	35	28	. 12	0.80	0.43	0.52
36	321	. 317	144	0.99	0.45	0.66	•	59	228	149	75	0.65	0.50	0.46
37	85	45	38	0.53	0.84	0.49		60	` 30	20	8	0.67	0.40	0.42
38	148	86	22	0.58	0.26	0.30		61	1029	426	min 153	0.41	0.36	0.24
39	25	11.8	9	0.47	0.76	0.41		62	140	103	58	0.74	0.56	0.57
<sup>-</sup> 40	83	5,5	28	0.66	0.51	0.47		63	349	305	139	0.87	0.46	0.59
41	√55	51	16	0.93	0.31	0.52		64	?	<8	?	х	х	X
42	4 343	261	min 192	0.76	0.74	0.65		65	518	313	122	0.60	0.39	0.37
43	297	289	198	0.97	0.69	0.81		66	226	166	48	0.73	0.29	0.39
44	190	136	73	0.72	0.54	0.52		67	214	159	32	0.74	0.20	0.33
45	176	32	23	0.18	0.72	0.14		68	211	178	58	0.84	0.33	0.48
46	160	132	, 58	0.83	0.44	0.55		69	149	126	38	0.85	0.30	0.47
47	93	63	38	0.68	0.60	0.53		70	103	60	23	0.58	0.38	0.36
48	153	95	68	0.62	0.72	0.53		71	147	83	<b>3</b> 8	0.56	0.46	0.37
49	30	30	9	1.00	0.30	0.55		72	115	95	15	0.83	0.16	0.33
50	444	274	163	0.62	0.54	0.49	•	73	564	338	192	0.60	0.57	0.45
. 51	98	93	21	0.95	0.23	0.45		74	169	115	42	0.68	Ö.37	0.41
52 ,	119	113	20	0.95	0.18	0.40		75	376	215	83	0.57	0.39	0.36
53	160	115	50	0.72	0.43	0.47		76	166	129	55	0.78	0.43	0.51
54	446	339	149	0.76	0.44	0.50		77	305	260	112	0.85	0.43	0.57
55	18	10 ု	2	0.56	0.20	0.24		78	101	94	24	0.93	0.26	0.47
56	119	61	. 35	0.51	0.57	0.39		79	93	85	34	0.91	0.40	0.57
. 57	195	183	52	0.94	0.28	0.50		80	115	<b>9</b> 0	47 •	0.38	0.52	0.57

	,			(	פ						•	3			_
	No.	a	ъ	c	b/a	c/b	bc/a <sup>2</sup>		No.	a	Ъ	, c	b/a	c/b	bc/a <sup>2</sup>
		mm	mm	mm					, —	mm	mm	mm			
	81	103	102	51	0.99	0.5	0.70	, .	91	302	236	89	0.78	0.38	0.48
	82	122	70	29	0.57	0.41	0.37		92	33	24	15	0.73	0.63	0.57
,	83	226	145	87	0.64	0.60	0.50		93	87	80	11	0.92	0.14	0.35
	84	14	10	5	0.71	0.50	0.50	• ->	94	47	45	12	0.96	0.27	. 0.50
	85	156	88	38	0.56	0.43	0.37		95	43	32	3	0.74	0.09	0.22
	86	152	114	55	0.75	0.48	0.52		96	63	41	16	0.65	0.39	0.41
	87	168	118	83	0.70	0.70	0.59		97	50	39	12	0.78	0.31	0.44
	88	664	363	min 125	0.55	0.34	0.32		98	21	15	7	0.71	0.47	0.49
	89	1,31	131	45	1.00	0.34	0.58	-	* 99	158	144	27	0.91	0.19	0.40
	90	· ?	· <8	?	x	х	х .		100	28	25	16	0.89	0.64	0.71

•

•

· ·

Cross-sectional location was measured to the nearest 5 cm.

The decimal places in this (11th) column refer to the cross-sectional location of the recovered particle relative to channel features as follows:

- .10 to the right of the thalweg
- .20 to the left of the thalweg
- .30 to the right of the centre of the channel

()

- .40 to the left of the centre of the channel
- .50 to the right of a longitudinal bar
- .60 to the left of a longitudinal har
- .01 refers to the right-hand side (of two) thalweg
- .02 refers to the left-hand side (of two) thalweg

example: 140.21 means 140 cm to the left of the right-hand side thalweg.

Table A.2: Transport Distance, Cross-Sectional Location, Particle and Slope Data of Recovered Labelled Bed-Material, Seale's Brook, 1972.

See pages 167-182.

					Yellow					
Rock	Weight	Distance	Sphericity	Shape	Local	Local Slope	b-axis	a-axis	c-axis	CrSec.
No.		Transported	1		Slope	Average Slope				Location
	(gr)	(m)	$\sqrt{bc/a^2}$	c/a			(mm)	(mm)	(mm)	(cm)
169	1684,30	13,02	0 • 48	0.37	0.006	1.000	110.0	177,3	65.8	175,10
165	27,41	16,22	0.48	0.37	0.001	0.167	251	40,4	14.8	20,20
168	3990,30	13,47	0.49	0.45	0,005	1.000	114.6	218.8	99.3	225,10
156	10453.40	21.42	0.69	0.63	0.001	0.200	175,9	263.0	166.2	60.40
154	58,56	22,32	0.37	0.19	0.001	0.250	48,6	67.4	12.8	120,30
160	2,84	19,42	0.37	0.20	0.001	0.200	15.6	22.0	4.3	0.30
159	64.06	20.17	0.44	0.24	0.001	0,200	46.7	59,6	14.6	10.30
155	261.84	22,27	0,53	0.38	0.001	0.250	66,9	92,2	35.1	320,30
170	4592.40	11.97	0.60	0.45	0.006	1,000	167.5	208.4	94.0	120.10
163	3613,90	17,22	0.77	0.62	0.001	0.200	166,5	175,8	109.6	60.10
149	595.14	26.02	0.52	0.34	0.001	0.250	75.9	125,4	42.3	180.30
148	2516.90	28,52	0.44	0.29	0.001	0,250	142.2	214.8	62.8	150,10
141	140.58	18,97	0.37	0.15	0.001	0.200	82,5	85.7	13,2	140.10
138	1851.80	30,47	0.57	0.36	0.001	0.250	148.0	161.0	58.4	50,20
145	8277,90	27.82	0.55	0.48	0.001	0.250	178.0	286.0	137.2	0.50
76	1.12	100,53	0.42	0.24	0.015	1.154	12.0	16.5	4.0	175.20
78	11.97	142.78	0.68	0.46	0.042	2.333	26.6	27,4	12.7	150.12

•

				3	Yellow					
Rock	Weight	Distance	Sphericity	Shape	Local	Local Slope	b-axis	a-axis	c-axis	CrSec.
No.		Transported	d		Slope	Average Slope				Location
<b></b>	(gr)	(m)	$\sqrt{bc/a^2}$	°/a			(mm)	(mm)	(mm)	(cm)
49	10.90	57,08	0,57	0.54	0.025	2,364	16.7	27.6	14.8	60.30
47	16,40	140.24	0.59	0.54	0.042	2.800	34.0	51.2	4.5	50,21
44	338.86	130.07	0.51	0.43	0.022	1.294	59,9	99.0	42.6	39.30
36	37.78	123,05	0.56	0.33	0.032	1,882	42,2	44.3	14.7	30,30
72	2.69	74.05	0.41	0.26	0.049	6,125	14.7	21.8	5.6	80.30
12	10,31	78,08	0.53	0.37	0.036	2,118	22,4	28.7	10.5	20,30
70	1.37	133,38	0.69	0.64	0.002	0.111	9,4	12.7	8.1	125.40
71	1.95	133,53	0.57	0.48	0.002	0.111	11.6	17.4	8.3	110,40
74	0,69	78,83	0.26	0.12	0.049	4.900	11.0	18.7	2.3	70,40
75	10.43	85,38	0.37	0.26	0.015	1.154	19.7	37.5	9.6	15,10
3	78,07	47,84	0.50	0.27	0.025	5,000	55.4	59.4	15.8	20.30
63	13,81	51,53	0.39	0.26	0.001	0.167	21.8	37.1	9.5	40.40
89	102.47	169,57	0.65	0.48	0.019	1.000	-46.8	52,3	25.2	100.40
90	9,25	187,12	0.45	0.30	0.019	0.950	21.8	31,5	9.3	40.40
85	26.28	221,47	0.48	0.31	0.003	0.158	31.4	42.6	13.2	125.40
97	4,60	167,12	0.50	0.39	0.009	0.450	14.2	21.9	8.6	250.10
19 .	22.09	84.73~	0.44	0.34	0.004	0.235	23.9	42.6	14.4	0.30

Yellow

Ø

								e		
Rock	Weight	Distance	Sphericity	Shape	Local	Local Slope	b-axis	a-axis	c-axis	CrSec.
No.		Transported	d		Slope	Average Slope	•		÷	Location
	(gr)	(m)	$\sqrt{bc/a^2}$	c/a		n	(mm)	(mm)	(mm)	(cm)
18	. 0.96	71,75	0.26	0.12	0.036	2,400	13.0	21.8	2.6	90.40
6	0.73	64,32	0.49	0.30	0.026	2.000	9.9	12.3	3.7	25.30
,35.	24.59	122,92	0.62	0.45	0.022	1.467	30.5	35,7	16.2	110.40
95	0.58	170.07	0.61	0.51	0.009	0.450	7,3	10.2	5.2	140.10
94	6,42	172,22	0.62	0.49	0.009	0.450	21.8	27.9	12.5	390,10
91	4.28	177,07	0.36	0.20	0.019	0.950	17.8	27,6	5.6	150.30
82	1.74	235,67	0.39	0.20	0.003	0.158	15,7	21.3	4.3	0.30
54	372,63	41,18	0.39	0.26	0.012	4.000	70.8	123,0	32.1	160.40
29	832,02	108,72	0.53	.0.34	0.032	2.286	124.2	126.0~	42.4	110.40
26	423,61	104,87	0.59	0.41	- 0.004	0.286	78.7	92,9	38.0	190.40
2.8	54.52	106.12	0.35	0.24	0.004	0.286	35.3	68,6	16.7	130.40
30	2,17	115,17	0.51	0.30	0.032	, 2.000	14.7	17.2	5.2	140.40
116	1.71	1 36,27	0.57	0.48	0.001	0.333	11.1	16.2	7.8	. 0.10
117	23.45	36,17	0.40	0.22	0.001	0.333	35.5	47.8	10.4	35.10
121	168,25	35,07	0.56	0.32	0.001	0.333	67,2	69.5	22.2	20,10
127	158,52	31,42	0.55	0.45	0.001	0.250	47.1	71.7	32.0	60,20
133	560.90 ,	31.72	0.62	0.46	0.001	0.250	81.7	99.0	45.8	0.10
	•					•				

'Yellow

Rock	Weight	Distance	Sphericity	Shape	Local	Local Slope	b-axis	a-axis	ċ-axis	CrSec.
No.		Transporte	d	٠ -	Slope	Average Slope	,		,	Location
	(gr)	(m)	$\sqrt{bc/a^2}$	c/a	4.		(mm)	(mm)	(1120)	(cm)
137	38.56	34,12	0.39	0.22	0.001	0.250	36,4	55,2	° 12.4	20.50
173	2291.20	10.67	0.59	0.43	0.006	1.000	133,4	165.6	71.6	120.20
174	1050.64	1.77	0.48	0.34	0.005	1.000	101.4	151.2	51.4	40.20
185	238,95	5,17	0.47	0.33	0.006	1.000	59,8	90.2	29.7	. 145,40
191	0,78	2,27	0.56	0.49	0.005	- 1.000	7,5	11.8	5.8	0,10
178	0.33	6,32	0.59	0.51	0,005	1,000	5,9	8,6	4.4	75,10
186 -	48,40	8,57	0.37	0.33	0.005	1.000	24.1	59.5	19.4	100,40
6 176	138.28	8,67	0.46	0,31	0,006	1.000,-	53,3	, 77.4	24.1	165020
179	16.27	6,32	0.47	0.45	0.005	1.000	18,2	37.3	16.8	0.10
182	1290.30	5.42	0.58	0.42	0,006	1.000	112.4	140,3	59.3	175,30

Red

								•		
⊃ Rock	Weight	Distance	Sphericity	Shape	Local	Local Slope	b-axis	a-axis	c-axis	CrSec.
No.		Transported	·		Slope	Average Slope				, Location
	(gr)	(m)	Vbc/a2	cj <sub>a</sub>		<del></del>	(mm)	(mm)	(ﷺ)	(cn)
57	12,13	64.79	0.57	0,41	0.001	0.091	22,3	29.1	12.0	12.30
205	9316.20	7.96	0.63	0.54	0.028	1.000	182.7	245,9	132.7	0.12
123	543,75	55,93	0.63	0.44	0.001	0.077	92.1	101.8	45.2	160.50
125	227,76	54,73	0.42	0.19	0.001	0.077	87,5	93.9	18.1	185,60
112	513,68	59,53	0.57	0.48	0.001	0.077	70.8	103.3	49.9	150.10
104	322,10	61.83	0.65	0.45	0.000	0.000 ~	74.9	79.4	35.6	0.30
110	37.02	62,83	0.39	0.16	0.000	0.000	53,Ŝ	57.6	9.4	-0.10
103 .	3.04	67,88	0.44	0.34	0.012	1.000	12.4	22.0	7.4	20.10
104	0.48	68,28	0.44	0.33	0.012	1.000	7,6	13.3	4.4	20.20
106 .	0.18	86.28	0.44	0.23	0.026	1.733	7.1	8.7 .	2.0	90.10
107	0.70	100,39	0.37	0.17	0.004	0.200	11.3	14.0	2.4	20.20
118	104.07	58,08	0.41	0.28	0.001 -	0.077	44,8	74.9	20.8	0.10
119	13,21	57,83	0.37	0.20	0.001	0.077	27.7	41.0	8.3	135.10
120	38,56	57,33	0.35	0.15	0.001	0.077	47.2	60.4	9.3	160.20
126	34.64	54,03	0.33	0.16	0.001	0.077	39.4	·58 <sub>*</sub> 5	9.5	170.20
132	466,42	54,58	0.24	0.13	0.001	0.077	78.6	172.0	21.9	100.60
124	1524.20	55,18	0.61	0.49	0.001	0.077	110.4	1,44.7	71.6	60.50

D	_	
л	e	а

					vea					
Rock	Weight	Distance	Sphericity	Shape	Local	Local Slope	b-axis	a-axis	c-axis	CrSec.
No.		Transported	3		Slope	Average Slope				Location
`	(gr)	(m)	$\sqrt{bc/a^2}$	c/a			(mm)	(===)	(mn)	(cm)
5	244,60	71,83	0.74	0.56	0.025	2.083	63,3	64.6	36.2	35,30
62	0.36	72,94	0.61	0.40	0.001	0.077	7,4	8.0	3.2	85.30
60	17.86	68,84	0.36	0.16	0.001	0.083	36,5	45.7	7.2	10.40
84	23,50	244,33	0.52	0.32	0.003	0.143	35.1	42.2	13.7	180.40
8.5	6.70	226,48	0.66	0.55	0.021	1.000	16.4	21.0	11.5	0.30
87	0.49	226,28	`0.45	0.29	0.021	1.000	8,6	12.2	3.5	80.30
100	5.68	197,33	0.67	0.51	0.019	0.905	18,4	20,8	10.6	30,10
98	2.79	188,43	0.57	<b>9.44</b>	0.009	0.429	13,3	18.2	8.0	230.10
96	2.62	191,03	0.65	0.45	0.009	0.429	15,9	17.0	7.6	29ó.10
8	10.41	100,24	0.48	0.34	0.036	1.875	23.1	33,6	11.3	50.40
93	0:37	194,68	0.33 %	0.20	0.009	0.429	6,7	11.7	2.3	260.10
65	179.17	74,34	0.48	0.31	0.001	0.077	59.7	80.5	25.2	0.30
68	1.79	82,82	0.55	0.51	0.004	0.363	9.6	16,4	8.4	140.30
67	26,27	79.89	0.44	0.27	0.004	0.333	34,5	48.0	12.9	30.30
34	8.41	139,33	0.54	0.42	0.032	1.778	18.5	27.0	11.4	30.30
83	4.09	246,93	0.40	0.22	0.003	0.150	18.8	25.9	5.6	180.40
32	2.55	137.98	0.22	0.12	0.032	1.684	13.0	32.3	3.9	90.30

•		•
ĸ	ø	d

Rock	Weight	Distance	Sphericity	Shape	Local	Local Slope	b-axis	a-axis	c-axis	CrSec.
No.		<sub>e</sub> Transporte		7	Slope	Average Slope				Location
	(gr)	(m)	$\sqrt{bc/a^2}$	c/a			(mm)	(mm)	(==)	(cm)
215	1094.98	0.38	0.35	· 0.•23	0.028	1.000	101.0	192.8	44.5	125.10
210	904.12	3,13	0.55	0.38	0.028	1.000	109.6	140.9	53.9	105.22
197	8.21	42.83	?	?	0.001	0.059	7	7	7	60.10
214	164,71	0.43	0.39	0.25	0.028	1.000	62,3	104.7	26.2	110.10
213	0.73	0,68	0,40	0.20	0.028	1.000	10.0	12.7	2.6	120.10
196	19,36	63,39	0.49	0.32	0.000	0.000	31.2	41.3	13.3	0.30
201	17.91	12,18	0.53	0.33	0.028	1.000	30.6	35,6	11.8	175.20
200	579,65	13,08	0.35	0.22	0.028	1,000	77.9	143.4	31.5	75.20
22	4.53	126,48	0.40	0.26	0.004	0.235	15.3	24.2	6.4	10.40
23	1.57	126.98	0.30	0.12	0.004	0.235	15,6	21.8	2.6	50.30
11	0.29	100,49	0.50	ố.35	0.035	1.895	6.0	8,4	2.9	95.30
45	6.59	153,93	0.33	0.12	0.022	1,222	30.2	33,5	4.0	0.30
37	154,76	143,83	0.26	0.23	0.032	1.778	35,3	122.1	28.3	0.30
38	0.96	143,88	0.47	0.30	0.032	-1.778	9.8	13,5	4.1	45,30
1	1.91	76,35	0.33	0.15	0.268	14.889	17.4	23,2	3.4	155.30
2	129,61	69,10	0,36	0.23	0.012	1.000	53.8	92,6	20.9	10.40
4	1.48	68,85	0.48	` 0,37	0.012	1.000	10.2	16,5	6.1	0.30

Red

Rock	Weight	Distance	Sphericity	Shape	Local	Local Slope	b-axis	a-axis	c-axis	CrSec.
No.		Transporte	d		Slope	Average Slope				Location
	(gr)	(m)	$\sqrt{bc/a^2}$	c/a	•		(mm)	(mm)	(ma)	(c=)
			<b>A</b> ,							
167	10.24	36,63	0.35	0,29	0.001	0.053	15.4	36.4	10.5	15.20
171	1320.90	33,43	0.37	0.23	0.005	0.300	126.5	201.3	46.5	290.10
158 -	957,48	42,85	0.42	0.29	0.001	0.059	101.0	164,6	48.3	90.30
161	165,94	41,23	0.50	0.25	0.001	0.059	76.6	5 , 7ٌ۲	19.1	60.30
153	170.35	53,13	0.70	0.63	0.001	0.077	47,8	61.4	38.8	- 60.40
164 -	43,55	38,83	0.40	0.27	0,001	0.056	34.9	57.0	. 15.6	75,10
146	0,53	49,58	0.62	0.50	0.001	0.067	8.1	10.5	5.3	170.20
139	9.20	51,38	0.28	0.12	0.001	0.071	26,3	40.8	4.9	60.20
143	. 3,27	50,73	0.52	0,34	0.001	0.071	15.7	20.0	6.8	55.10
142	32.93	50,83	0.30	0.11	0.001	0.071	49.0	61.9	6.8	60.10
140	2158.20	51,59	0.49	0.31	0.001	0.071	151,1	195.8	61.0	150.10
144	296,42	50,22	0.59	0.38	0.001	0.071	73,7	79.5	30.3	185.10
151 ,	3880,20	49,37	0.62	0.58	0.001	0.067	129.9	197.9	113.8	120.10
207 <b>-B</b>	154,24	6,45	0.35	0.18	0.028	1.000	64.7	98.7	18.0	35.22
206	113.70	8,07	0.75	0,59	0.028	1.000	51,9	53,6	31.7	0.22
209	454,36	2,92	0.71	0.48	0.028	1.000	79.3	92.9	44.7	80.22
215	1594,20	0.29	0,64	0.43	0.028	1.000	133.2	135.1	58 <sub>9</sub> 0	0.30

•

.

•

•

Rock,	Weight	Distance Transporte	-	Shape	Local Slope	Local Slope Average Slope	b-axis	a-axis	e-axis	CrSec. Location (cm)
	(gr)	(m)	$\sqrt{bc/a^2}$	c/a			(mm)	(mm)	(mm)	
129	5817.20	51.52	0.70	0.67	0.001	0.071	160.8	186.8	124.7	30.10
130 (	2307.20	52,33	0.56	0.42	0.001	0.071	128.0	173.8	72.7	130.10
219	1805,60	4,18	0.48	0.35	0.028	1.000	123,6	184.0	63.6	0.10
195 -	656,52	25.,03	0.32	0.14	0.005	0.240	112.6	160.6	22.4	0.10
187	1.33	27.03	0.26	0.11	0.005	0.250	15.0	22,8	2.4	40.40
188	209,18	25,48	0.30	0.19	-0.005	0.250	50.5	108.2	20.4	0.10
175	79,94 .	31,33	0.46	0.26	0.005	0.286	57.6	71.4	18.8	65.10
174	288.32	32,13	0.52	0.37	0.005	0.286	67.0	92.1	33.7	70.20
181	5,92	27.53	0.48	0.37	0.006	0.250	18.2	28.8	10.6	120,40
183	4.79	27,18	0.33	0.15	0.028	1.167	21.7	30.4	4.5	105.30
177	3049.30	28,58	0.46	0.30	0.005	0.250	154.9	225.3	67.1	70.10

· ·

Green

Rock	Weight	Distance	Sphericity	Shape	Local	Local Slope	b-axis	a-axis	c-axis	CrSec.
No.	•	Transported	i		Slope	Average Slope	e			Location
	(gr)	(m)	$\sqrt{\frac{bc}{a^2}}$	c/a			(ww̄)	(mm)	(ma)	(cm)
232	3042.30	4,92	0.47	0.29	0.004	1,000	157.4	204.8	59.5	0.10
166	291.80	64.12	0,55	0.38	0.006	0.261	70.9	91.3	34.5	155.10
162	14.88	67.47	0.47	C.25	0.001	0.045	28,4	32.7	8.1	0.10
157	2696.30	70.07	0.61	0.50	0.001	0.045	128.7	175.8	87.3	0.10
203	8550.70	35.91	0.57	0.46	0.028	1.000	202.8	283.3	129.9	15.20
152	154.88	75.77	0.26	0.22	0.001	0.005	42.8	131.8	29.2	100.30
150	173.06	76,92	0.50	0.37	0.001	0.005	55,2	81.0	30.3	60.10
202	546,38	37.37	0.45	0,29	- 0.028	1.037	83,6	122.7	35.8	95.20
208	1.41	31,27	0.44	0.34	0.028	1.333	8.8	15.7	5.3	0.11
207	>104,48	34.37	0.39	0.23	0.028	1.000	52,3	81.1	18.9	20.21
211	6.11	28,92	0,32	0.14	0.028	1,273	23,3	33.9	4.6	135.10
217	1.04	44.57	0,69	0.49	0.028	1.037	11.3	11.6 %	5.7	25.12
218	0.37	26.12	0.40	0.38	0.028	2,333	4,4	10.4	3.9	140.30
204	3056,70	36.17	0.81	0.74	0.028	1.120	134.2	150.6	111.6	5.20
198	471.12	42,72	0.46	0.34	0.028	1.037	75.4	120.0	40.2	220.20
199	1654,50	41.02	0.45	0.31	0.028	1.000	116.7	183.3	56.8	130.20
79	15,46	184,49	0.62	0.46	0.022	1.048	24,7	29.2	13.3	10.22

Rock No.	Weight	Distance Transported	•	Shape Local Slope		Local Slope Average Slope	b-axis	a-axis	c-axis	CrSec.
	(gr)	(m)	$\sqrt{bc/a^2}$	c/a	•		(mm)	(mm)	(ma)	Location (cm)
77	1.22	184.92	0.71	0,59	0,022	1,100	9,4	10.8	6.4	20,50
25	41,62	154.57	0.24	0.09	0.004	0,211	57,4	82.0	7.7	65.30
16	8,57	148,77	0.35	0.19	0.004	0,250	24,5	40.8	7.8	130.40
17	4.87	149.62	9.71	0.59	0.004	0.211	15.7	18.5	10.9	40.40
46	0.73	185.02	0.42	0.28	0.022	1,158	9.0	13.6	3.8	140.30
51	5.04	95,62	0.58	0,46	0.012	``	15.1	20.3	9.4	9.30
13	1.05	142,22	0.32	0.19	0.004	0.250	9.7	17.8	3.3	25.30
14	7,96	145,12	0,65	0.53	0.004	0.250	18.2	22.7	12.1	90.40
15	126.02	146,47	0,75	0.58	0.004	0.250	49,8	51.8	30.0	90.30
43 `	10.48	176.42	0.20	0.08	0.022	1,100	30.0	54.2	4.3	85.40
43	0 , 8,6	175,52	0.49	0.36	0.022	1.100	9,1	13.8	5.0	0.10
41	6,85	175,47	0.49	0.31	0.022	1.150	20,9	27.4	8.5	5.40
39	7.05	170,92	0.71	0.56	0.032	2,286	18.9	20.9	11.8	45.30
÷0	1.19	172.82.	Ò.44	0.27	0.032	2.286	10.0	14.0	3.8	80.30
79	1.98	122.54	0.77	0,69	0.049	3.500	9.6	11.3	7.8	120.40
8	6,44	93.40	0.37	0.36	0.001	0.063	12.0	30.7	11.2	60.40
	1.32	95.00	022	0.10	0.001	0.063	12.5	23.2	2.4	90.30

Green

					Green			_		
Rock No.	Weight	Distance	•	Shape	Local	Local Slope	b-axis	a-axis_	c-axis	CrSec.
		Transported	d		Slope	Average Slope	₿ .			Location
	(gr)	(m)	$\sqrt{bc/a^2}$	c/_			(mm)	(mm)	(mm.)	(cm)
61	35,92	99.89	0,45	0.28	0.001	0,063	39.2			. /
88	1.17	250,07	0.28	0.10	0.021	0,955	18,4	, 53.5 22.1	15.2	80.40
9	4,29	127.08	0,62	0.61	0.036	1.714	13,2	20.7	2.2	30.30
102	1,07	211.08	0.45	0.24	0.042	1,909	10.7	12.9	12.6	110.30
101	1,40	219,97	0.48	0,32	0.009	0.409	12.0	17.0	5,4	260.10
99	0.56	211.28	0.33	0.20	0.042	1.909	7.9	14.7	2;9	190.10
20	5,06	151.82	0,73	10,55	<b>0.004</b>	0.211	18.2	19.0	10.5	80.40
7	3,10	126,48	0,57	0.38	0.036	1.714	15.4	18.2	7.0	50.30
81	13.28	281.92	0.72	0.69	0.003	0.143	19,2	25.3	17.5 e	•
80	2,31	283.72	0.20	0.06	0.003	0,143	20.0	. 31,5	1.9	0.30
31 64	0,71	160.17	0,51	0.31	0.027	1.421	10.4	12.4	3,9	₹10.40
	1,60	101.19	0.41	0.30	0.004	0.250	10.0	17.8	5.4	5
69	8,13	111.39	0.24	0.13	0.004	0.250	204.9	44.5	5.7	60.40 90.30
792	1.29	219.87	0,56	0,43	0.009	0.409	10,3	14.1	•	
52	1507.20	90.50	0.55	0.36	0.000		130.0	150.1	56.6	345.10
56	46.67	92.80	0,42	0.30	0.000	0.000,	33.0	55,2	16.7	30.30 60.30
55	7.66	92.70 -	- 0.42	0.21	0.000	0.000	29,1	34.5	7.3	70.30

Green

, Rock	Weight	Distance	Sphericity	Shape	Local	Local Slope	b-axis	a-axis	c-axis	CrSec.
%o.		Transported	1		Slope	Average Slope	£.			Location
<u> (-</u>	(gr)	(m)	$\sqrt{bc/a^2}$	c/a	3		(mm)	(mm)	(m)	(c m)
228 ,	9589.10	7.76	0.84	0.78	0.004	1.000	186.3	204.8	159.3	0.10
225	14,80	17,12	0,39	0,21	0.004	1.000	25.7	35,0	7.4	0.10
223	2.18	17.47	0.39	0.16	0.004	1.000	23.5	24.7	3.9	200.12
221	216,30	21.07	0.69	0.58	0.004	1.000	59,9	73.5	42.6	120.10
226	164.32	15.87	0,58	0.36	0.004	1.000	67.4	72.0	26.2	140.10
232 -B	111,68	0.97	0.54	0,35	, 0.004	1.000	54.2	65.6	23.0	275.20
231 -B	306,87	2.32	0.28	0.15	0.004	1.000	81.3	147.5	22.8	320.20
222	456,30	18.72	0.41	0.22	0.004	1.000	100.2	132.9	29.3	65.10
134	2,74	80,42	0.63	0.44	0.001	0.053	14.5	16.0	7.0	140.20
129	181,81	80,27	` 0,33	0.15	0.001	0.053	77.3	108.6	16.0	30.10
114	93,30	86,02	0.54	0.36	0.001	0.053	52.1	64.3	22.9	180.20
113	97.29	86,32	0.24	0.24	0.001	0.053	25.5	101.3	24.4	180.20
115	1,12	87,22	0,35	0.15	0.001	0.053	14.2	17.1	2.6	115.10
105	1,50	111.72	0,36	0.16	Ŏ.056	1,368	15.0	18.3	3.0	70.10
135	0,24	84,40	0,35	0.18	0.001	0.053	7.0	10.2	1.8	105.60
122	17.77	83.42	0.39	0.15	0.001	0.053	39.2	40.4	5.9	130.50
131	1,57	82.12	0.56	0,33	0.001	0.053	14.6	15.5	5.1	100.60

• `		•			Green			-		
Rock	Weight -	Distance	Sphericity	Shape	Local	Local Slope	b-axis	a-axis	c-axis	CrSec.
No.		Transporte	d		Slope	Average Slope	1	•		Location
	(gr)	(m)	$\sqrt{bc/a^2}$	c/a			(mm) (_	(mm)	(mm)	(cm)
229 .	2354,20	7,33	0.44	0.22	0.004	1.000	172,6	199.3	43.2	50.22
231	1185,95	2.02	0.42	0.23	0.004	1.000	147.0	188.0	43.0	320.20
227	2231.00	13,48	0,51	0.33	0.004	1.000	.139.7	173.9	56.8	65.30
180	1.68	54,97	0,35	0.16	0.006	0,231	15,5	21.6	3.4	0.10
189	62,69	21.87	0,32	0.20	0.004	1.000	40.6	83.8	16.9	0.10

0.004

1.000

0.25

0,39

4:

42,95

15.0 215.10

Blue Local Weight Distance Sphericity Shape Local Slope Rock

No.		Transported			Slope	Average Slop	pe	•	Location	
	(gr)	(m)	$\sqrt{bc/a^2}$	c/a			(mm)	(mm) <sup>- 1</sup>	(mm)	(cm)
242	5715.10	1,42	0,50	0.33	0.003	1.000	196,0	250.8	83.7	25.20
239	8182,90	15.62	0,47	0.40	0.047	1.237	162,6	291.9	119.6	50.11
237	4179,40	39.60	0.37	0.30	0.034	0.919	121.5	249.4	74.9	130.12
235	0,97	39.35	0.24	0.10	0.034	0.919	11.5	18.0	1.9	0.11
234	136.01	65.55	0,56	0.39	0.025	0.714	54.0	67.5	26.4	320.20
241	12463,80	11.57	0.60	0.51	0.047	1.306	220,2	307.3	156.8	120.11
240	2692,30	13.32	0,58	0.41	0.047	1.306	⊸ 150 <b>.</b> 0	180.2	74.8	0.11
235	85,74	49,, 50	0.37	0.18	0.034	.0.919	59.6	75.3	13.6	0.11
147	3,69	157.75	0.56	0.47	0.001	0.030	13.5	20.4	9.6	0.50
212	139,11	109.15	0.57	0.40	0.027	0.711	52.0	65.0	26.4	75.10
21	0,54	232,65	0.57	0.47	0.004	0,143	7.0	10.1	4.8	140.40
24	4.88	234,95	0,35	0.27	0.004	0.143	16.2	34.5	9.6	80.30
50	1.40	1,77.75	0.37	0.37	0.001	0.034	7.0	17.5	6.5	40.30
48	0,85	253.15	0.24	0,11	0.032	0.344	12.6	20.8	2.4	110.40
33	1.06	245,95	0,22	80,0	0.004	2.000	13,8	19.3	1.6	85.30
10	1,03	207,41	0,73	0.60	0.026	0,897	8,5	9.4	5.7	80.30
66	1.59	194.81	0.39	0.31	0.001	0.037	9,8	19.8	6.2	90.40

·					Blue					
Rock	Weight	Distance	Sphericity	Shape	Local	Local Slope	b-axis	a-axis	° c-axis	CrSec.
No.		Transporte	đ		Slope	Average Slope	B			Location
	(gr)	(m)	$\sqrt{bc/a^2}$	c/a			(mm)	(mm)	(mm)	(cm)
27	0,83	236,15	0.42	0.34	0.004	0,143	7,1	13.5	4.7	50,40.
53	0.35	169,96	0.55	0.39	0.001	0.032	7.0	8.9	3.5	0.30
230	1799,20	83,49	0.59	0.44	0.027	0.730	127.5	160.1 3	71.5	210.20
220	0.85	101.00	0.28	0.24	0.027	0.844	5.4	15.5	3.8	270.40
224	6,19	98.25	0.41	0.25	0.027	0.794	17,9	26.0	6.5	30.12
136	16,24	165,15	0.61	0.60	0.001	0.031	17.2	27.1	16.5	90.60
108	29.03	222,75	0,53	0.38	0.036	1.241	30.7	41.4	15.8	0.10
111	4,06	170.50	0,58	0.36	0.001	0.032	20.5	21.5	7.9	120.40
172	47,94	141.10	0,33	0.15	0.028	0.778	50,3	67.5	10.4	0.10
195	0.34	143.30	0,56	0.35	0.006	0,167	7,4	8.2	2.9	200.10
184	70,67	134.85	0,57	0.48	0.028	0.757	36.2	<u>/</u> 53.7	25.9	180.30
233	~ 539,18	69,40	0.41	0.26	0.102	2.757	90 20	130.8	34.1	110.10

Raw Data and Particle Size Distribution of the Surface of the Bed and of Underlying Material

8			Volumetric Sample				Surface Sample				
Size	Dor	midpoint	Weight	Inc	l. Sand	Excl	. Sand	N	$ND^2$	% of	Cumul. %
<u>(mm)</u>	(mm)	<u>(þ)</u>	(gm)	<u> 7.</u>	comul. %	<u> 7.</u>	comul. %	(No.)		total ND2	of total
(sand)	(max)	(min)	(min)				ţ	,			
<2	1.0	0	1333.00	5.3	5.3	-	-	<<100	<<100	<0.03	<0.03
2-4	2.9	-1.5	1912.60	7.5	. 12.8	8.0	8.0	147	1235	0.38	0.41
4-8	5.6	-2.5	2418.36	9.5	22.3	10.1	18.1	96	3060	0.82	1.23
8-16	11.3	-3.5	2607.24	10.3	32.6	10.8	28.9	132	16880	4.50	5.73
16-22.6	19.0	-4.25	387.94	1.5	34.1	1.6	30.5	50	18050	4.81	10.54
22.6-32	26.9	-4.75	2966.09	11.7	45.8	12.3	42.8	25	18075	4.83	15.37
32-45	38.1	-5.25	1749.53	6.9	52.7	7.3	50.1	15	21750	5,80	21.17
45-64	53.8	-5.75	2772.89	10.9	63.6	11.5	61.6	, 16	46450	12.38	33455
64-90	76.1	-6.25	3261.54	12.9	76.5	13.6	75.2	7	40600	10.83	44.38
90-128	107.7	-6.75	3546.56	14.0	90.5	14.8	90.0	, 10	116000	30.92	75.30
128-180	152.2	-7.25	2414.10	9,5	100.0	10.0	100.0	2	46400	12.35	87.65
180-256	215.3	<del>-</del> 7.75	-					. 1	46400	12.35	100.00
Total	•		24036.81	100.0		100.0			<b>375000</b>	100.00	_